

Aus der Klinik für Hals-Nasen-Ohrenheilkunde  
(Prof. Dr. med. N. Strenzke)  
der Medizinischen Fakultät der Universität Göttingen

**Behavioral and electrophysiological  
assessment of hearing function in mice with  
deficient sound encoding at inner hair cell  
ribbon synapse**

INAUGURAL-DISSERTATION

zur Erlangung des Doktorgrades  
der Humanmedizin  
der Medizinischen Fakultät der  
Georg August Universität zu Göttingen

vorgelegt von

Iman Bahader

aus

Kairo, Ägypten

Göttingen 2021

Dekan: Prof. Dr. med. W. Brück

### **Betreuungsausschuss**

Betreuerin: Prof. Dr. med. N. Strenzke

Ko-Betreuer: Prof. Dr. rer. nat. M. Müller

### **Prüfungskommission**

Referentin: Prof. Dr. med. N. Strenzke

Ko-Referent: .....

Drittreferent/in: .....

Datum der mündlichen Prüfung: .....

Hiermit erkläre ich, die Dissertation mit dem Titel "Behavioral and electrophysiological assessment of hearing function in mice with deficient sound encoding at inner hair cell ribbon synapse" eigenständig angefertigt und keine anderen als die von mir angegebenen Quellen und Hilfsmittel verwendet zu haben.

Göttingen, den ..... ..

## Contents

<b>List of tables .....</b>	<b>VIII</b>
1 Introduction .....	1
1.1 The auditory system .....	1
1.2 Peripheral auditory system .....	1
1.3 The sensory component .....	2
1.3.1 The endolymphatic potential (EP) .....	3
1.3.2 Sound transduction .....	3
1.3.3 Outer hair cells.....	3
1.3.4 Inner hair cells .....	4
1.4 The synaptic component.....	4
1.4.1 The synaptic vesicle cycle .....	5
1.4.2 Cochlear IHC ribbon synapses .....	6
1.5 Synaptic proteins studied in this thesis.....	7
1.5.1 Ribeye protein .....	7
1.5.2 Ca <sup>2+</sup> dependent activator protein for secretion (CAPS).....	8
1.5.3 Otoferlin .....	9
1.6 Auditory nerve fibers.....	10
1.7 Central auditory pathways and connections .....	11
1.7.1 Cochlear nucleus.....	11
1.7.2 Superior olivary complex .....	12
1.7.3 Inferior colliculus .....	12
1.8 Hearing loss and auditory neuropathy .....	12
1.8.1 Prelingual hearing loss .....	12
1.8.2 Auditory neuropathy (AN) and auditory synaptopathy (AS) .....	13
1.8.3 Hearing rehabilitation and gene therapy.....	13

2	Materials and methods.....	15
2.1	Study approval and animals.....	15
2.2	Electrophysiology .....	15
2.2.1	Auditory brainstem response (ABR) recordings .....	15
2.2.2	Auditory steady state response (ASSR).....	16
2.2.3	Distortion product otoacoustic emissions (DPOAEs) .....	17
2.3	Behavioral auditory experiments.....	17
2.3.1	Acoustic Startle Reflex setup .....	17
2.3.2	Shuttle box setup .....	18
2.3.3	Intellicage setup.....	19
3	Results .....	24
3.1	Shuttle box results .....	24
3.2	Intellicage results.....	26
3.2.1	Frequency discrimination experiment .....	26
3.2.2	First Ribeye threshold experiment.....	28
3.2.3	Second Ribeye threshold experiment .....	30
3.2.4	Third threshold experiment .....	37
3.3	<i>Otof<sup>QX</sup></i> and <i>Otof<sup>2M</sup></i> mice: electrophysiological and behavioral assessment.....	41
3.3.1	<i>Otof<sup>QX</sup></i> ABR .....	41
3.3.2	<i>Otof<sup>2M</sup></i> ABR .....	42
3.3.3	<i>Otof<sup>2M</sup></i> behavioral auditory assessment.....	44
3.4	Viral rescue in <i>Otof<sup>-/-</sup></i> mice .....	47
3.4.1	<i>Otof<sup>-/-</sup></i> rescue assessed by ABR.....	47
3.4.2	<i>Otof<sup>-/-</sup></i> rescue assessed by behavioral testing .....	54
3.5	Auditory phenotype of <i>CAPS</i> mutant mice .....	56
3.5.1	<i>CAPS</i> ABR .....	57
3.5.2	<i>CAPS</i> DPOAE .....	58
3.5.3	<i>CAPS</i> auditory steady state responses (ASSR) .....	59

4	Discussion.....	60
4.1	Auditory phenotype of Ribeye KO mice.....	61
4.2	Auditory phenotype of <i>Otof<sup>QX</sup></i> mice and <i>Otof<sup>2M</sup></i> mutant mice .....	62
4.2.1	Electrophysiological auditory assessment .....	62
4.2.2	<i>Otof<sup>2M</sup></i> behavioral auditory assessment.....	63
4.3	Partial <i>Otof<sup>-/-</sup></i> rescue .....	63
4.4	Auditory phenotype of <i>CAPS</i> mutant mice .....	65
4.5	ABR waveform morphologies in mouse models of auditory synaptopathy...	66
4.6	Behavioural assessment of hearing function in mice .....	66
5	Summary.....	70
6	References .....	72

<b>List of figures</b>	
Figure 1: Anatomy of the ear .....	1
Figure 2: The organ of Corti .....	2
Figure 3: The synaptic vesicle cycle at CNS synapses .....	5
Figure 4: Schematic drawing of an inner hair cell ribbon synapse.....	7
Figure 5: Startle wire mesh cage with the accelerometers connected to its lower border. ..	18
Figure 6: Shuttle box setup placed in soundproof chamber.....	19
Figure 7: Intellicage setup.....	20
Figure 8: Examples of good and poor performance in the shuttle box.....	26
Figure 9: <i>Spnb</i> WT mouse performance in frequency discrimination experiment.....	28
Figure 10: First threshold experiment in Ribeye mice: thresholds in quiet.....	29
Figure 11: Photo of the modified Intellicage setup for testing thresholds in noise .....	31
Figure 12: Second threshold experiment (in quiet) in Ribeye KO mice. ....	32
Figure 13: Daily monitoring of the performance of a Ribeye KO mouse. ....	33
Figure 14: Second threshold experiment in Ribeye KO mice: 45 dB background noise ....	34
Figure 15: Second threshold experiment in Ribeye KO mice: 60 dB background noise. ....	35
Figure 16: Second threshold experiment in Ribeye KO mice: after cessation of background noise.....	36
Figure 17: Average fraction of visits without nose-poke in third threshold experiment (in quiet). ....	38
Figure 18: Average fraction of visits without nose-poke in third threshold experiment (in noise).....	38
Figure 19: Summary of results for the three Intellicage threshold experiments.....	40
Figure 20: <i>Otof<sup>QX</sup></i> mice auditory phenotype.....	41
Figure 21: <i>Otof<sup>2M</sup></i> mice auditory phenotype.....	42
Figure 22: <i>Otof<sup>2M</sup></i> ABRs to 1, 20, and 100 Hz click stimulation .....	43
Figure 23: Examples of a) <i>Otof<sup>2M</sup></i> WT and b) mutant performance on daily monitoring during training in the Intellicage.....	45
Figure 24: Example of <i>Otof<sup>2M</sup></i> WT and mutant mouse performance in a gap detection experiment. ....	46
Figure 25: <i>Otof<sup>2M</sup></i> mutants in gap detection experiment.....	46
Figure 26: <i>Otof<sup>-/-</sup></i> rescue: averaged waveforms of ABRs .....	48
Figure 27: <i>Otof<sup>-/-</sup></i> rescue mice: comparison to WT .....	49
Figure 28: <i>Otof<sup>-/-</sup></i> rescue: ABR amplitude growth functions .....	49
Figure 29: <i>Otof<sup>-/-</sup></i> rescue: suprathreshold growth of ABR amplitudes. ....	50

Figure 30: <i>Otof</i> <sup>-/-</sup> rescue: duration of ABR rescue.....	51
Figure 31: Grand averages of ABR waveforms evoked by 80 dB click 20 Hz from WT mice, <i>Otof2M</i> mutant, <i>Otit/C57</i> and <i>Otof</i> <sup>-/-</sup> rescue mice. ....	52
Figure 32: Comparison of ABR wave amplitudes in different mutant mouse strains.....	53
Figure 33: Representative example of startle response recordings from an <i>Otof</i> <sup>-/-</sup> rescue mouse.....	54
Figure 34: <i>Otof</i> <sup>-/-</sup> rescue: sound detection in the Intellicage .....	55
Figure 35: Comparison between WT (black) and <i>Otof</i> <sup>-/-</sup> rescue mice (red). ....	56
Figure 36: <i>CAPS</i> mice have normal ABRs:.....	57
Figure 37: DPOAE elicited in <i>CAPS</i> mutant mice and WT littermates. ....	58
Figure 38: ASSR in <i>CAPS</i> mice .....	59

## List of tables

Table 1: Summarized results of mice trained in shuttle box.....	24
Table 2: Conditioning paradigm in frequency discrimination experiment.....	27
Table 3: Conditioning paradigm in first behavioral threshold experiment.....	29
Table 4: Conditioning paradigm in second behavioral threshold experiment (in quiet). ....	31
Table 5: Conditioning paradigm in second behavioral threshold experiment (in noise). ....	33
Table 6: Comparison between first, second and third threshold experiment.....	40
Table 7: Conditioning paradigm during the gap detection experiment. ....	44
Table 8: Comparison between <i>Otof</i> <sup>-/-</sup> rescue with age and sex matched WT mice. ....	55

## List of abbreviations

AAV	adeno-associated virus
ABR	auditory brainstem response
ASSR	auditory steady state response
ANF	auditory nerve fiber
AN	auditory neuropathy
AZ	active zone
CAPS	Ca <sup>2+</sup> dependent activator protein for secretion
Cav1.3	Voltage-gated calcium channel 1.3
DCV	dense core vesicle
DFNA	autosomal-dominant nonsyndromic deafness
DFNB	autosomal-recessive nonsyndromic deafness
DPOAE	distortion product otoacoustic emission
EP	endolymphatic potential
IHC	inner hair cell
KO	knockout
MF	modulation frequency
Munc 13	mammalian uncoordinated 13
OHC	outer hair cell
RRP	readily releasable pool
RWM	round window membrane
SCC	semicircular canals
SGN	spiral ganglion neuron
SNARE	soluble N-ethylmaleimide-sensitive factor attachment receptor
TEOAE	transient evoked otoacoustic emission
Vglut3	vesicular glutamate transporter 3
WT	wild type

# 1 Introduction

## 1.1 The auditory system

Perception of any acoustic stimulus requires sound information to travel from the peripheral to the central centers of the auditory pathway. The peripheral auditory system consists of three main parts: the sensory part including the organ of Corti with the hair cells, the synaptic part and the neuronal part. The spiral ganglion neuron can be considered the margin between the peripheral and central auditory system (Nayagam et al. 2011).

## 1.2 Peripheral auditory system

The human ear is anatomically constituted of three main parts: external, middle and inner ear. Ear pinna, outer ear canal and the tympanic membrane constitute the external ear. The middle ear is a cavity between the tympanic membrane and the inner ear, that is occupied by three tiny ossicles; malleus, incus and stapes. The temporal bone contains the cochlea for sound encoding and the vestibular system for balance sensation. The semicircular canals (SCCs) and the macula are the main components of the vestibular system. The cochlea is connected to the three SCCs via the vestibule. The cochlea is formed of a bony labyrinth filled with perilymph and lined by membranous labyrinth filled with endolymph. Within the cochlea exists the receptive sensory component responsible for hearing, the organ of Corti. The main function of the cochlea is to receive sound waves and convert them into electrical signals that are then conveyed to the brain along the auditory pathway. Sound information is processed at various levels in the brainstem until its perception at cerebral cortex.

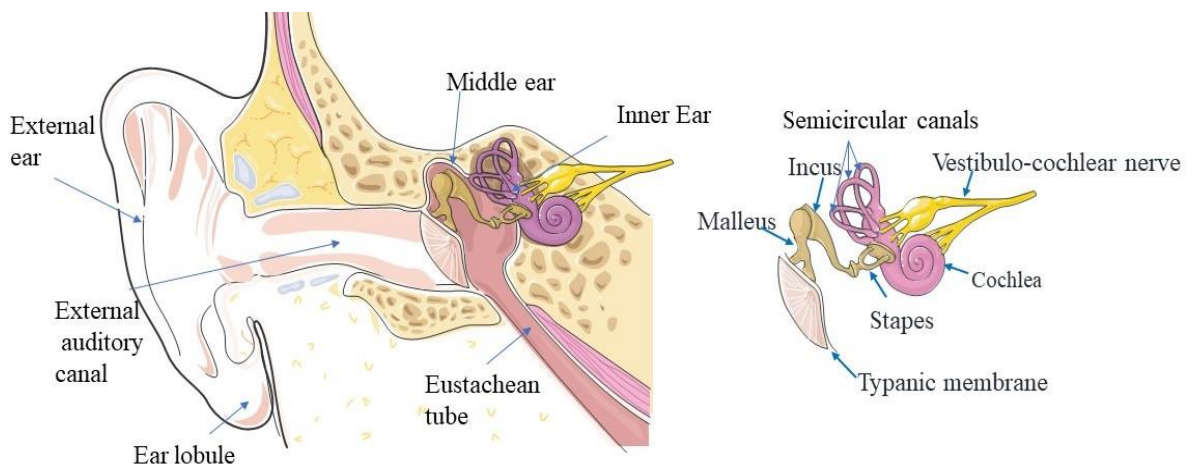


**Figure 1: Anatomy of the ear**

(Original figure done using toolboxes provided at <http://smart.servier.com/>, CC BY-SA 3.0)

Sound waves are a series of air pressure changes of alternating compression and rarefaction that vary in intensity and frequency over time. The pinna and external auditory canal collect sound waves and transfer them toward the middle ear. The resulting tympanic membrane vibration passes through malleus, incus and stapes to the oval window (on medial wall of the middle ear) then to the fluid filled cochlea. Sound pressure undergoes hydraulic amplification because of the larger surface area of tympanic membrane in comparison to the stapes footplate and by the lever like action of the ossicular system (Pickles 2015). Those two mechanisms lead to impedance matching that transmits air-borne sound waves into the fluid filled cochlea.

The cochlea is divided into three compartments (scalae) rotating around a bony axis (modiolus). Those three scalae are scala vestibuli, media (cochlear duct) and tympani. Scala vestibuli is separated from cochlear duct by Reissner's (vestibular) membrane. The basilar membrane supports the organ of Corti and separates the scala media and tympani. The perilymph in scala vestibuli and scala tympani is connected at the cochlear apex via a small opening called the helicotrema. Perilymph fluid is rich in  $\text{Na}^+$  and contains little  $\text{K}^+$ , whereas endolymph, filling the scala media, has a high  $\text{K}^+$  and low  $\text{Na}^+$  concentration.

### 1.3 The sensory component

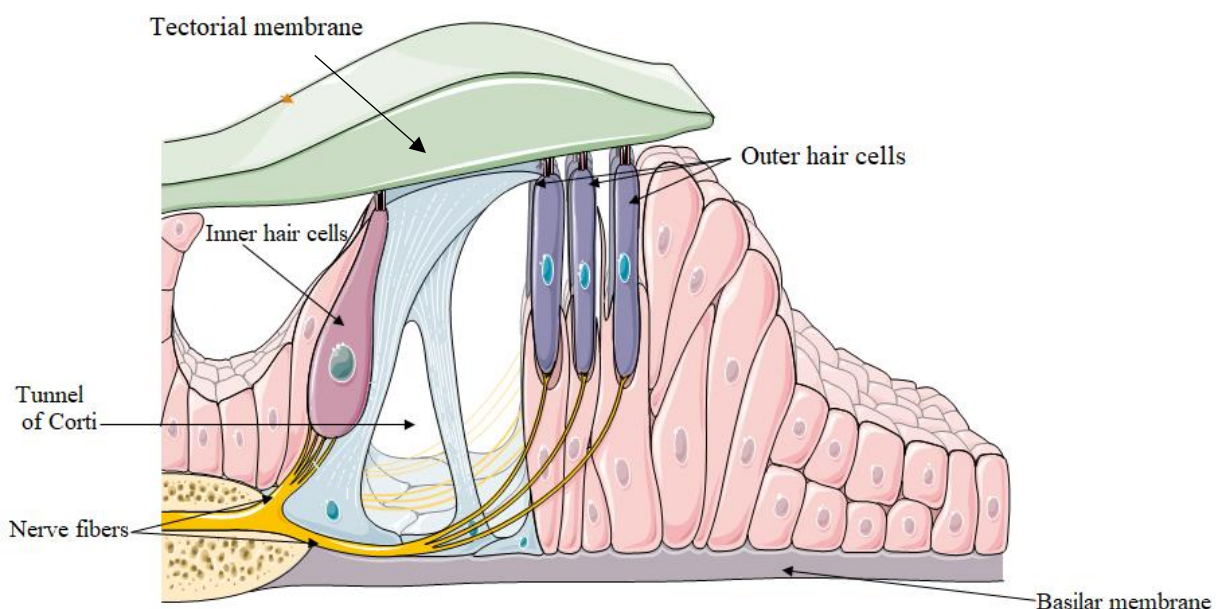


**Figure 2: The organ of Corti**

(Original figure done using toolboxes provided at [smart.servier.com/](https://smart.servier.com/), CC BY-SA 3.0)

The sensory component is also known as the organ of Corti that is composed of the inner hair cells (IHCs), outer hair cells (OHCs), basilar membrane, tectorial membrane, spiral ganglions and the cochlear nerve and different types of supporting cells. Both outer hair cells and inner hair cells are covered on their apical surface by approximately 100 tiny hair like projections called stereocilia. Stereocilia are facing the tectorial membrane of the organ of Corti and are connected together by filamentous protein at their apex (tip links). Tip links are connected to the mechano-transduction channel and have a role in their traffic regulation (Schwander et al. 2010).

### 1.3.1 The endolymphatic potential (EP)

Cochlear endolymph is produced by stria vascularis in the cochlea. It is an extracellular fluid whose main cation is potassium ( $K^+$ ). It creates a positive potential which exceeds that of the perilymph by 80 to 90 mV. Intermediate cells (melanocytes) in the Stria vascularis are critical for the generation of EP and  $K^+$  transport (Takeuchi et al. 2000).

### 1.3.2 Sound transduction

The basilar membrane has variable resonant frequencies from base to the apex of the cochlea. The auditory system thus accomplishes a sort of Fourier transformation of the incoming sound waves. The coordinated movement of the basilar membrane and tectorial membrane together with stereocilia covering the inner and outer hair cells control the opening and closure of selective cation mechanosensitive transduction channels. Opening of those channels promotes  $K^+$  influx leading to depolarized membrane potential changes (Schwander et al. 2010). Outer hair cells amplify each sound frequency in a non-linear fashion (Peng et al. 2011) after sound has been spectrally decomposed by basilar membrane.

### 1.3.3 Outer hair cells

They are receptive cells present in the cochlea that mechanically amplify the low-level sound waves allowing mammals to hear low magnitude sounds with high sensitivity. They are arranged into three rows and they are approximately 12,000 hair cells in humans (Dallos 1992). They are mainly innervated by efferent nerve fibers from the medial olivary complex, which regulate their sensitivity.

Outer hair cells express prestin which is a motor protein supporting the electromotility process which promotes the amplification of the low-level sounds. Prestin contracts and elongates corresponding to the depolarization or hyperpolarization status of the outer hair cells. Those voltage dependent conformational changes, actively amplify the

sound-induced vibrations of the basilar membrane (Dallos and Fakler 2002). This process sharpens the sensitivity of the inner ear for low sound intensities and enables high frequency selectivity (Ashmore et al. 2010). OHC function is usually assessed by non-invasive recordings of otoacoustic emissions, which record sounds produced by active cochlear amplification, or by cochlear microphonic recording during electrocochleography, capturing their electric response

#### 1.3.4 Inner hair cells

They are primary auditory sensory receptive cells present in the cochlea. Their main role is to receive the acoustic information and convert it into neuronal electrical impulses, which are then propagated through the auditory nerve through the brainstem to the auditory cortex. They are arranged in a single row. Approximately 3500 hair cells exist in the human cochlea, Each IHC forms about 8 to 20 afferent ribbon synapses with afferent nerve fibers (ANF) (Dallos 1992).

The EP and the high potassium ion concentration play an important role in sound transduction carried by hair cells. Cilia covering the hair cells are in contact with endolymph and bear mechano-transduction channels. The process of sound transduction begins when this transducer channels open promoting influx of  $K^+$  ion into hair cells.  $K^+$  entry into the hair cells is driven by the electrical gradient changes across membrane of the cilia covering the hair cells, which resulted from the sum of the EP and resting membrane potential.

$K^+$  influx together with smaller amounts of  $Ca^{2+}$ , initiate hair cell depolarization which opens voltage dependent  $Ca^{2+}$ -channels ( $Ca_v1.3$ ).  $Ca^{2+}$  entry facilitates the release of vesicles filled with glutamate at the ribbon synapse through  $Ca^{2+}$ -dependent exocytosis (Fettiplace and Hackney 2006). Glutamate then binds to postsynaptic AMPA receptors initiating action potential and spiking in the afferent fibers. The released neurotransmitters at the synaptic junction (active zone) of the inner hair cells trigger the generation of action potentials in ANF (Wichmann and Moser 2015).

### 1.4 The synaptic component

The synapse is defined as the intercellular junction between the presynaptic neuronal terminal and postsynaptic terminal. Information arrives to the presynaptic terminal as a travelling action potential depolarizing the neuron and thereby triggering the opening of synaptic voltage gated calcium channels. The resulting calcium influx triggers exocytosis of

synaptic vesicles and release of neurotransmitter with subsequent activation of the postsynaptic terminal (Sudhof 2012).

### 1.4.1 The synaptic vesicle cycle

Neurochemical synaptic communication depends on controlled release of neurotransmitters into the synaptic cleft. The genesis and renewal of those vesicles in the active zones (AZs) constitute the vesicle cycle which is fundamental for the fidelity and precision of synaptic transmission (Sudhof 2004).

Synaptic vesicle fusion competence depends crucially on tethering, docking and priming processes. First, tethering occurs when the synaptic vesicles (SVs) are loosely attached to the membrane of the presynaptic active zone. Then docking follows when SVs are closely attached to the membrane. Priming of the vesicles allows them to become competent for the  $\text{Ca}^{2+}$  dependent exocytosis. For complete SVs fusion competence to be fulfilled, protein tethers of variable numbers and length are involved in the process. After fusion, different endocytosis pathways allow renewal of the vesicle pool to insure continuous abundance.

After SVs being loaded with neurotransmitters, they are stowed and initiated at the plasma membrane. Following the calcium influx, vesicles merge and are then recycled by different endocytosis pathways.

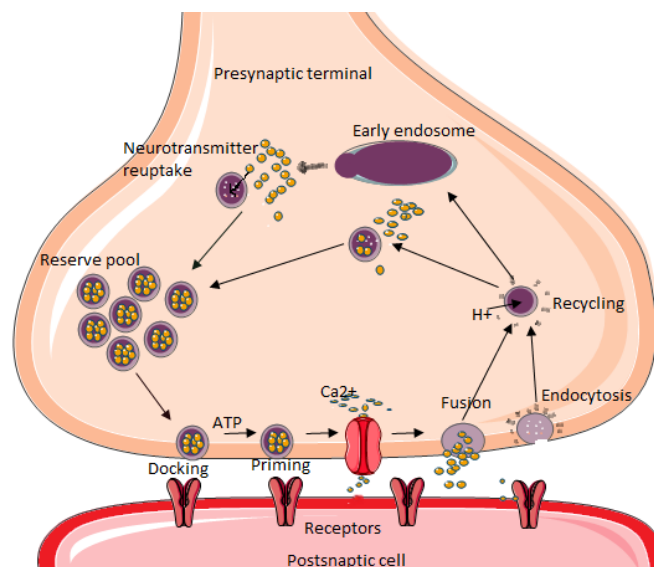


**Figure 3: The synaptic vesicle cycle at CNS synapses**

(Original figure done using toolboxes provided at [smart.servier.com/](http://smart.servier.com/), CC BY-SA 3.0)

### 1.4.2 Cochlear IHC ribbon synapses

Transmission of acoustic information from its physical state to perception is carried out by chemical synapses, which transform the hair cells receptor potential into SGN action potential firing. IHC synaptic transmission depends highly on precisely timed release of the neurotransmitter filled synaptic vesicles at the active zones (AZs). IHCs ribbon synapses are highly specialized synapses for this purpose being capable of indefatigable sound encoding at rates of hundred Hertz (Hz) with very high temporal accuracy (Moser and Starr 2016). This highly precise function requires a rapid vesicle replenishment mechanism, which is also fundamental for sustained stimulation.

Each neuron of the SGN is connected to only one inner hair cell ribbon synapse unlike conventional CNS synapses, which typically have numerous active zones. Each IHC ribbon synapse shows a characteristic electron dense projection (“ribbon”) at the AZ which is composed of the protein ribeye. The ribbon is thought to help recruitment of a greater number of vesicles to be fully ready for release upon stimulation. Synaptic ribbons are thought to provide more availability of SVs by tethering them close to the AZs (Moser et al. 2019). The tethering of the SVs to the ribbon allow the availability of a large vesicle pool that exceeds the docked pool (required for fast release) by almost five folds (Sterling and Matthews 2005).

This highly specialized function of the IHC ribbon synapse requires unique proteins at the active zone. In contrast to conventional synapses, mature IHC ribbon synapses are devoid of the neuronal SNARE proteins synaptotagmin 1-3, synaptobrevin 1-3, synaptophysin and synapsin (Safieddine and Wenthold 1999; Nouvian et al. 2011), and complexins (Strenzke 2009), Munc13-1 and tomosyn (Uthalah and Hudspeth 2010). The efforts to identify the proteins in IHC ribbon synapses are ongoing. Identified proteins in the IHCs presynaptic active zone include otoferlin (Roux et al. 2006), piccolo (Regus-Leidig et al. 2014), synaptotagmin 7, synuclein, syntaphilin and synaptojanin (Uthalah and Hudspeth 2010).

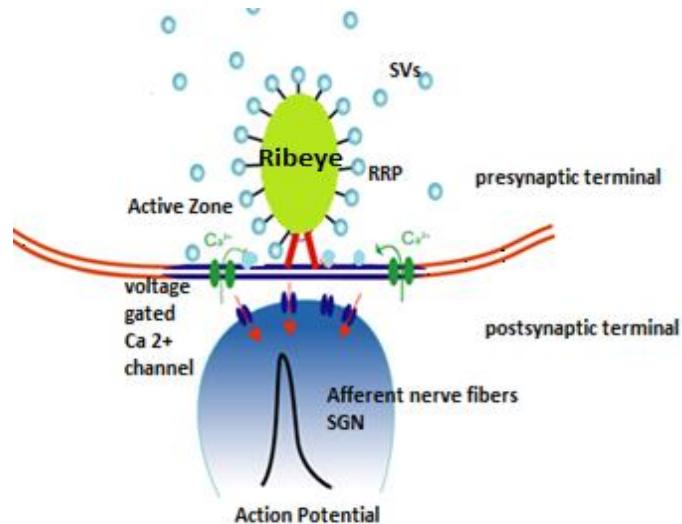


**Figure 4: Schematic drawing of an inner hair cell ribbon synapse**

Therefore, the most prominent difference between IHCs ribbon synapse and the CNS synapses is the synaptic ribbon with its characteristic protein ribeye, and the important IHC specific protein otoferlin. Those are the two proteins I focused on in my thesis.

## 1.5 Synaptic proteins studied in this thesis

### 1.5.1 Ribeye protein

Ribeye is a unique protein expressed at the ribbon synapse. It is essentially required for ribbon formation in presynaptic terminal. It was discovered for the first time in the retina, hence the name (Schmitz et al. 2000). Mice lacking Ribeye protein showed a significant reduction in the amplitude of ABR wave I, but only a slight increase in ABR and auditory nerve fiber thresholds (Becker et al. 2018; Jean et al. 2018). The loss of synaptic ribbons in Ribeye KO mice was compensated by several strategies, for instance, the formation of several smaller active zones per synapse, and an alteration of clustering of synaptic Ca<sub>v</sub>1.3-channels into smaller and multiple spots like aggregates causing a wider spread of the presynaptic calcium signal. Ribeye deficiency also causes a shift of depolarized calcium channels activation potentials towards stronger depolarization suggesting that Ribeye play a role in the regulation of presynaptic calcium current (Jean et al. 2018). In vivo, postsynaptic recordings from spiral ganglion neurons showed a reduction in synaptic transmission affecting both peak and sustained firing rates (Moser et al. 2019).

### 1.5.2 $\text{Ca}^{2+}$ dependent activator protein for secretion (CAPS)

Another important protein, which is present at conventional CNS synapses, is the CAPS protein. A newly generated mutant mice line lacking Exon 2 in *CAPS1* was shown to have reduced startle reflex upon acoustic stimulation. They were thus referred from Jeong Seop Rhee's laboratory to our auditory physiology group in order to undergo auditory assessment.

Neuropeptides are fundamental components involved in brain development and plasticity. Dense core vesicles are packed with neuropeptides in the cytosol of the presynaptic neuronal terminal. At rest, the DCV are more dynamic in the cytosol, and upon stimulation, they become more stabilized near synapses to be ready for release. CAPS proteins are thought to be involved in mediating membrane fusion competence of the DCV to the presynaptic terminal by promoting its fusion with subsequent release of neuropeptide into the extra-synaptic sites. The CAPS protein is found in most synapses but not in all of them. Synapses with higher CAPS expression exhibit a higher DCV release probability. At conventional CNS synapses, CAPS and mammalian uncoordinated 13 (Munc13) protein families are important regulators for the priming process.

The CAPS protein family is composed of CAPS1 and CAPS2. CAPS1 is the dominant of the two isoforms (Sadakata et al. 2006). CAPS proteins are located at the presynaptic terminal, their genetic deletion causes a severe reduction in the synaptic readily releasable vesicle pool (RRP) with severe affection of both spontaneous and evoked neurotransmission (Jockusch 2007). CAPS protein has an N-terminus with a C2 domain and a PH domain (Martin 2015) and its C terminal domain is composed of a SNARE-interacting MUN domain. CAPS1 plays a role in DCV exocytosis since it is localized in its membrane. Mice lacking CAPS1 and CAPS2 in hippocampal neurons display a severe reduction in synaptic transmission (Jockusch 2007) and die before the onset of hearing function.

At inner hair cell ribbon synapses, exocytosis is SNARE-independent as they seem not to be expressed in the cochlear hair cells (Nouvian et al. 2011). Vogl and colleagues (2015) studied the role of CAPS in IHCs. Immunohistochemistry revealed no visible staining, arguing against CAPS expression. ABRs from CAPS1<sup>+/-</sup> CAPS2<sup>-/-</sup> double mutant mice showed normal thresholds, latencies and amplitudes, and patch-clamp recordings showed normal vesicle exocytosis. These findings argued against a role of CAPS protein at cochlear IHC synapse (Vogl et al. 2015). However, since the complete genetic deletion of

CAPS1 results in perinatal lethality, only heterozygous mice could be tested which might still express CAPS protein to support its function in IHCs.

An exon 2 deletion in CAPS1 was identified in a female patient with bipolar disorder (Sitbon et al., unpublished results). Dennis Nestvogel (AG Rhee) found abnormal pulse train adaptation in cultured hippocampal neurons carrying a similar mutation. Together with Fritz Benseler and his team generated a mouse model of such a mutation carrying genetic deletion of exon 2 in CAPS1 by using the CRISPR/CAS9 system (Nestvogel 2017). The generated homozygous mutant mice lacking Exon2 were viable, but they showed reduced startle reflexes in response to acoustic stimuli (Prof. Rhee, personal communication), which might be due to a sensory or a motor deficit. We thus assessed peripheral auditory function in CAPS1 Exon2 deletion mice.

### 1.5.3 Otoferlin

Otoferlin is expressed in the mammalian IHCs, OHCs, vestibular hair cells, ANFs and in the brain (Schug et al. 2006). It is a multi C2 domain protein, which belongs to the Ferlin family. Yasunaga and colleagues first identified otoferlin and its role in the vesicle membrane fusion at IHC ribbon synapse (Yasunaga et al. 1999). Vesicle exocytosis at IHC ribbon synapse was found to be completely abolished in otoferlin knockout mice (Roux et al. 2006). Otoferlin regulates the tethering of membrane proximal SVs at the presynaptic terminal and is involved in vesicle replenishment mechanisms in IHC ribbon synapse (Pangršič et al. 2010; Pangršič et al. 2012, Strenzke et al. 2016). Otoferlin is expressed in OHCs from embryonic day 18 (E18) until the fifth postnatal day (P5). In IHCs, otoferlin remains to be expressed (Roux et al. 2006). Mice lacking otoferlin show no ABR waves although they show preserved cochlear amplification as assessed by DPOAE. Calcium triggered exocytosis is almost totally abolished in mice lacking otoferlin (Roux et al. 2006).

Most human patients with otoferlin mutations are profoundly deaf. However, some human *Otof* gene mutations result in a mild elevation of hearing thresholds with disproportionally poor speech discrimination. A temperature sensitive auditory phenotype has been reported in some patients who exhibited picture of moderate auditory synaptopathy where their hearing threshold deteriorated when their body temperatures increased (Marlin 2010).

Mice homozygous for one such mutation *Otof*<sup>I515T/I515T</sup> have moderate hearing threshold elevation with enhanced adaptation upon prolonged repetitive stimulation. *Otof*<sup>I515T/I515T</sup> mutant mice showed a decrease by 65% in otoferlin membrane-bound levels,

they exhibited a reduction in the  $\text{Ca}^{2+}$  triggered vesicle exocytosis with prolonged repetitive stimulation with enlargement of synaptic vesicles at the presynaptic terminal. This supports the fundamental role of otoferlin in vesicle exocytosis and replenishment at IHCs ribbon synapse (Strenzke et al. 2016).

The Q829X mutation in the *Otof* gene (p.Gln829X) is the third most common genetic cause of congenital deafness in the Spanish population (Rodríguez-Ballesteros 2008). Patients with such deficit show an auditory synaptopathy: absence of ABR waves with preservation of the transient evoked otoacoustic emission (TEOAE) indicating normal outer hair cells' cochlear amplification function. However, TEOAEs can be lost afterwards. Those patients exhibited a good outcome upon cochlear implantation (Rodríguez-Ballesteros et al. 2003). I studied a new mouse line with the same stop mutation in Q829X, which was introduced using CRISPR/Cas9 by PD Dr. Ellen Reisinger.

*Otof2M* mutant mice were generated as an additional unplanned result of the generation of *OtofQX* genetic mutant mouse line when non-specific deletion of three bases exhibited a mutation: the original amino acids lysine (K) and leucine (L) were replaced by a methionine (M). Such mutation might affect the FerA domain of otoferlin which is a phospholipid- and Calcium-binding domain. Its function is yet unknown and there are no published mouse models with mutations in this domain.

During my MD thesis, I contributed to the characterization of the auditory phenotype of a mouse model for a human relevant point mutation; Q829X mutation in the *Otof* gene. In addition, I assessed the auditory electrophysiological and behavioral phenotype of *Otof2M* mutant mice. In addition, I was involved in auditory electrophysiological and behavioral assessment of *Otof*<sup>-/-</sup> mice after genetic rescue with overloaded viral vectors carrying full-length otoferlin.

## 1.6 Auditory nerve fibers

ANFs (also called spiral ganglion neurons SGNs) are bipolar neurons with their soma inside the cochlea and their axons projecting to the cochlear nucleus in the lower brainstem (Nayagam et al. 2011). As the IHCs receptor potential follows the oscillations resulting from the sound pressure changes (Palmer and Russell 1986), the ANF firing follows precisely those oscillations and its spikes are phase locked to the stimulus.

There is great heterogeneity in the recorded responses from type 1 afferent fibers of SGN (Liberman 1978). ANFs are classified according to their spontaneous firing rates and

thresholds into high spontaneous rate/low threshold fibers, intermediate fibers and low spontaneous rate/high threshold fibers (Liberman 1978). Low spontaneous rate/high threshold fibers are thought to be responsible for sound perception in background noise and a selective loss of those fibers likely results in poor speech discrimination in noisy environments (Furman et al. 2013).

## 1.7 Central auditory pathways and connections

The tonotopic representation of the acoustic spectrum of the signal is achieved and maintained through the whole auditory system. The process of sound localization is carried out in a frequency-based manner with the aid of two main cues; inter-aural time difference (ITD) and inter-aural level difference (ILD). ITDs are more important at low frequencies where phase locking is possible. For high frequencies where phase locking is not possible, mostly ILDs are used. ITDs require great temporal precision of coding, for which fast and strong synaptic transmission is a prerequisite.

The afferent auditory fibers enter the brainstem then the neurons project from the ventral cochlear nucleus (VCN) to the medial and lateral superior olivary complex at the same and opposite side. Then fibers propagate to the lateral lemniscus on the ipsilateral and contralateral sides, then the fibers propagate to the inferior colliculus in the midbrain to the medial geniculate nucleus in the thalamus then to the primary auditory area and auditory association area in cerebral cortex (Møller et al. 1981). The important connection stations in the auditory system are discussed in the next section.

### 1.7.1 Cochlear nucleus

The cochlear nucleus is composed of two major divisions, which are the dorsal cochlear nucleus (DCN) and VCN. The VCN is subdivided into the antero-ventral cochlear nucleus and the postero-ventral cochlear nucleus (Godfrey et al. 2016). These nuclei receive the axons from type 1 bipolar neuron of the spiral ganglion. In these nuclei, cochlear frequency tonotopy is preserved and a very fine analysis of the electrical impulses of the auditory nerve fibers is carried out in order to decode the properties of the acoustic stimulus regarding the intensity, frequency and duration.

The main types of cells in the cochlear nucleus are globular bushy cells, spherical bushy cells, T stellate cells and Octopus cells (Cao and Oertel 2010). Each of these cells receives input signals from different numbers of ANFs and promotes the encoding of different features of the incoming sound (Cao and Oertel 2010).

### 1.7.2 Superior olivary complex

It constitutes the second major relay at the brainstem onto which the projections of neurons of the cochlear nuclei from both sides converge. It consists of several nuclei, where the tonotopy of the cochlear nuclei is preserved. It forms an intense neural network with many ascending and descending projections, allowing feedback on hair cells. It is the first relay where the binaural inputs of the two cochleae converge. It constitutes the first level where the computation of the inter-aural time and level differences necessary for the spatial location of sound sources takes place (Spitzer and Semple 1995). The medial olivocochlear reflex pathway regulates OHC sensitivity via the medial olivocochlear efferents, whereas the lateral olivocochlear reflex pathway regulates SGN excitability via the lateral olivocochlear efferents.

### 1.7.3 Inferior colliculus

The inferior colliculus plays a major role in the process of sound decoding. It is located in mid brain and receives highly heterogenic projections providing interconnections between auditory and other non-auditory pathways. There is evidence that IC receives input signals from visual, motor, somatosensory and cognitive pathways (Gruters and Groh 2012). The IC is thought to contribute to Wave IV and V of the ABR however there is no clear one to one correlation (Land et al. 2016). The IC plays an important role in spatial location of moving sound sources and is involved in analysis of complex sounds.

Signals propagate from the IC to the medial geniculate bundle in the thalamus. From there they are transmitted to the primary auditory area and auditory association area in the cortex, resulting in sound perception.

## 1.8 Hearing loss and auditory neuropathy

Hearing loss is considered one of the most prevalent disabilities in human population. It is stated by World Health Organization that more than 5 percent of the whole world population are suffering from hearing impairment. By year 2050, one in every ten people might be suffering from disabling hearing loss.

### 1.8.1 Prelingual hearing loss

Prelingual hearing loss means impairment of hearing before the development and production of speech. There are several related precipitating factors, which can be genetically determined or acquired due to environmental factors. Acquired hearing loss can

occur as a complication of hypoxia, hyperbilirubinemia at birth or certain infectious agents (TORCH, meningitis), ototoxic drugs (e.g., aminoglycosides).

About 70% of genetic causes are non-syndromic, meaning that no clinical deficit other than hearing loss is identified (Matsunaga 2009). There are four types of genetically inherited hearing loss: type A i.e., autosomal dominant inheritance (deafness type A = DFNA; ~ 10-15%), while type B i.e., autosomal recessive inheritance (deafness type B = DFNB; ~ 75%). Non-syndromic deafness is rarely found to be linked to the X-chromosome (DFN) or mitochondrial (1-2%) (Shearer et al. 1993).

### 1.8.2 Auditory neuropathy (AN) and auditory synaptopathy (AS)

AN was first described by Starr as hearing impairment which is characterized by absent or abnormal ABR and stapedial reflexes with normal otoacoustic emissions (Starr 1996). Both environmental and genetic causes can result in AN/AS. Patients with AN/AS can present with mild to profound hearing impairment, which in cases of genetic origin is usually bilateral. Hearing thresholds can range from normal thresholds to profound deafness.

In such cases with preserved hearing, speech perception especially in noise is poorer than expected from the pure tone audiogram. The deficit can affect inner hair cell and their synapse (AS) or the spiral ganglion neurons (AN) (Moser and Starr 2016). The distinction between AS and AN mostly relies on genetic testing which is not yet universally performed. AN/AS constitutes less than 1% in patients with hearing loss up to < 10% (Rance 2005; Moser and Starr 2016; de Siati et al. 2020).

### 1.8.3 Hearing rehabilitation and gene therapy

According to the degree of hearing loss and speech perception, several strategies are considered for rehabilitation of hearing-impaired humans. When hearing deficit is mild to severe, patients can benefit from sound amplification by hearing aids and assisting listening devices to a variable extent. Cochlear implants are widely used in case of profound hearing impairment and total deafness and are quite successful in restoring speech in quiet. Cochlear implants stimulate ANFs electrically by passing defective or missing IHC. However, patients with cochlear implant usually suffer from poor speech perception in noisy environment, experience music not like normal listener and encounter difficulty in perceiving vocal emotions. Gene therapy is a recently developing technique that promises to restore the physiological natural way of hearing (Al-Moyed et al. 2019). *Otof*-mutation related hearing deficits are a suitable target for gene therapy as it accounts for up to 5-8% of the autosomal

recessive non syndromic hearing impairment in western populations (Rodríguez-Ballesteros et al. 2008) and leaves the organ of Corti mostly intact.

The adeno-associated viral vectors (AAV) are broadly used in genetic therapeutic interventions due to their favorable safety profile. The packaging size of the adeno-associated viral vectors is less than 4.7 kb (Grieger and Samulski 2005). However, *Otof* coding sequence is larger (approximately 6 kb). Dual-AAV approaches have been used recently to overcome the limited cargo capacity of a single viral vector especially for the delivery of large protein, successfully achieving partial hearing restoration in *Otof* KO mice (Akil et al. 2019; Al-Moyed et al. 2019). However, concerns regarding the safety and the long-term efficacy of the virus treatment in addition to the complexity of this approach might complicate the clinical translation and regulatory process for approval as therapeutics.

I contributed in *Otof*<sup>-/-</sup> rescue project that proposes a more simplified strategy for delivery of *Otof* coding sequence into mouse hair cells using a single AAV. My role was the electrophysiological and behavioral assessment of hearing function in *Otof*<sup>-/-</sup> mice whose cochlea had been injected with overloaded AVVs carrying full-length otoferlin. The *Otof* sequence coding for full-length otoferlin was packed into several natural AAV serotypes as well as in more recently developed synthetic versions like PHP.B and PHP.eB.

## **2 Materials and methods**

### **2.1 Study approval and animals**

Animal handling and experiments fulfilled national animal care guidelines and were approved (under protocol number 33.19-42502-04-15/1998, -16/2080 and -14/1391) by the board for animal welfare of the University of Göttingen and the animal welfare office of the state of Lower Saxony, Germany.

All mice were kept in social groups in individually ventilated cage (IVC) holders in a specific pathogen-free facility having free access to food and water of 12-h/12-h light/dark cycles. All mice were genotyped using PCR before and after the experiment. Male and female mice were used. Mice used will be mentioned separately in each section.

### **2.2 Electrophysiology**

The electrophysiology experiments were performed as described essentially in (Pauli-Magnus et al. 2007). Tucker-Davis-Technologies (TDT) system II and III were used for sound stimulus formation, delivery and data acquisition (Tucker-Davis-Technologies, Ft Lauderdale, FL, USA). Bio-Sig32 software (TDT) was used to record ABR routines. Analysis of ABR data was carried out using MATLAB (The Mathworks, Natick, MA, USA), Excel, and ABR waveforms were presented using Igor Pro software (Wavemetrics, Eugene, OR, USA).

Sound pressure levels were provided in decibel SPL RMS (tonal stimuli) or decibel SPL peak equivalent (PE, clicks) and were calibrated using a ¼-inch Brüel and Kjaer microphone (D 4039, Brüel & Kjaer GmbH, Bremen, Germany).

#### **2.2.1 Auditory brainstem response (ABR) recordings**

ABR was done as described in (Pauli-Magnus et al. 2007). All experiments were performed under ketamine/xylazine administrated through intraperitoneal injection. Mice were placed on a heat blanket to maintain body temperature at 37°C. The acoustic stimulus for the tone burst ABR was a 12-ms tone-burst (cos2 rise/fall with a gate time of 1 ms; 10 ms plateau) presented at a stimulation rate of 40 Hz and frequencies of 4, 8, 12, 16, 24 and 32 kHz. Clicks (duration of 0.03 ms) were applied at a rate of 20 and 100 Hz. All stimuli were presented ipsilaterally in the free field using JBL 2402 speaker (JBL GmbH & co, Neuhofen, Germany).

ABRs were measured by recording the potential difference between subcutaneous needle electrodes placed at the vertex and the mastoid process. A ground electrode was inserted on the back near the mouse tail. The difference in potential between both electrodes was amplified 50,000 times by a custom amplifier (JHM NeuroAmp 401) or 20 times by a medusa amplifier (TDT), filtered (0.4 kHz high-pass, 4 kHz low-pass) and averaged (1300 sweeps) to obtain two mean traces with each intensity. Sweeps contaminated by noise (mostly EEG activity) were rejected through the artifact rejection property in BioSig32 software.

Click ABR were measured in 10 dB descending steps starting from 100 dB SPL until no ABR waves were observed. Hearing threshold was visually inspected and manually estimated as the lowest stimulus intensity which evoked a reproducible response waveform in both traces. Tone burst thresholds were recorded in 10 dB SPL steps and confirmed by an independent observer.

ABR peaks were manually assigned according to their normal latency values. The amplitude of each ABR wave was calculated as the difference between the highest point of a wave and the subsequent local minimum. The summed ABR wave I–V amplitude was calculated by adding up the individual amplitude values of ABR waves I–V.

### 2.2.2 Auditory steady state response (ASSR)

ASSR were recorded essentially as described in (Pauli-Magnus et al. 2007), using custom-written MATLAB software (designed by Gerhard Hoch) and TDT System 3 hardware. Stimuli were continuous sine wave carrier tones of 12 kHz, which were amplitude modulated at a modulation depth of 100% with different modulation frequencies (MF) and presented at 80 dB SPL.

The electric potentials between mastoid and vertex were amplified (TDT Medusa), digitized and then filtered digitally (50 Hz Notch and 60 Hz high pass). No artifact rejection was employed. The complete MF range from 110 to 893 were scanned in 28 Hz steps (4 s for each MF). For offline analysis using custom-written MATLAB software (Gerhard Hoch and Nicola Strenzke), the signal was converted into the frequency domain by fast Fourier transform (FFT) with a resolution of 0.016 Hz to determine the amplitude of the ASSR at the MF and the background noise (averaged in sweeps of 0.2 seconds in total of 7.5 minutes).

### 2.2.3 Distortion product otoacoustic emissions (DPOAEs)

For generation of two continuous sine wave stimuli ( $f_1$ ,  $f_2$ ) for the DPOAE measurement, Tucker-Davis system III and ED1/EC1 speaker system (Tucker-Davis) were used. A custom-made ear probe was used for the delivery of the two primary tones into the ear canal and for recording the DPOAE via a miniature microphone (MKE-2, Sennheiser, Hannover, Germany). The latter was amplified via an external sound card signal (Terratec DMX 6Fire USB) and digitalized using TDT III. The data was acquired and analyzed by custom-written MATLAB software.

## 2.3 Behavioral auditory experiments

Behavioral procedures used for assessment of hearing in mice can be divided into main types: methods that make use of an already existing reflex in response to acoustic stimuli for example as startle reflex, so they can be termed reflexive or unconditional methods. On the other hand, methods which require training of animals to produce a specific repeatable response upon auditory stimulation and are termed conditioning procedures. Conditioning procedures are more reliable, sensitive and have higher precision than reflexive procedures but they require lengthy training sessions (Heffner et al. 2006).

I used the acoustic startle reflex as a reflexive procedure and the shuttle box and Intellicage as operant conditioning procedures for subjective hearing testing. While the shuttle box relies on the use of negative reinforcement (punishment by electric foot shocks), the Intellicage setup involves the use of water reward as positive reinforcement and only mild punishment by air puffs as negative reinforcement.

### 2.3.1 Acoustic Startle Reflex setup

The startle setup is a custom-made setup, designed by Gerhard Hoch. The tested mouse is transferred into a small cage (13 x 13 x 6 cm) which is made of wire mesh to minimize resonance. The Stimulus is delivered from a loudspeaker (Avisoft scan speak) placed seven cm above the cage. Deflections of the cage are recorded via an accelerometer that produce a voltage when the mouse cage move.

The cage is placed during measurement in a sound attenuating chamber. The examiner can observe the tested mouse via USB camera and the experiment is set to begin when the tested mouse stops its exploration behavior (usually takes approximately 5 min). The cage is carefully cleaned between sessions to remove the odors.

The experiment is controlled through a custom-written Matlab program (The MathWorks, Inc., Natick, Massachusetts, USA) which control the experimental parameters as type, intensity, duration, and frequency of stimuli and the inter-stimulus interval (ISI) which usually varied between 10 and 20 seconds. White noise, 12 kHz tone burst and click 20 Hz at different intensities (70 to 110 dB SPL) were used to elucidate acoustic startle response. A voltage threshold corresponding to cage acceleration (mouse motion) is set to be 0.1-0.2 V and is checked every five seconds and the stimulus is not delivered when voltage exceed that threshold.



**Figure 5: Startle wire mesh cage with the accelerometers connected to its lower border.**

### 2.3.2 Shuttle box setup

Shuttle box used as an operant conditioning method for behavioral assessment of auditory functions in mice. It is a foot shock-motivated go/no-go paradigm. I first trained the mice on a simple tone detection task, aiming to proceed to a threshold task. I also tried to train the mice to discriminate between two pure tones of different frequencies.

The custom-designed shuttle-box setup was used as described in (Kurt and Ehret 2010) and is composed of two compartments ( $16 \times 20 \times 23$  cm) with a hurdle 2.5 cm high separating them. The stimulus is delivered via a loudspeaker (Avisoft scan speak) and it is placed above the setup in a soundproof chamber. The stimulus parameters were as the following: 4 seconds reinforcement window, 16-21 seconds intertrial interval, 300 seconds adaptation time, 20 dB attenuation for the maximum loudspeaker gain yielding  $\sim 80$  dB.

Several stimuli were tried in tone detection experiment: click-train, 12 kHz, 9 kHz and 6 kHz. Electrical foot shocks of 50–200  $\mu$ A applied via the floor grid served as punishment. The current level of the shock was adjusted individually to produce a mild

escape response for the mice. Mice learned to avoid the foot shock by crossing the hurdle within 4 s after acoustic stimulus onset.



**Figure 6: Shuttle box setup placed in soundproof chamber.**

At the beginning of my early attempts to achieve mouse training in the shuttle box, the mice were subjected to one daily session each of 70 trials (60 hit trials and 10 catch trials). I noticed that mice usually have good performance at the early beginning (high hit rates) then it declines as mice usually become more stressed with longer sessions so, I divided each long session into two daily shorter sessions each of 40 trials (33 hit trials and seven catch trials) with 5 to 15 minutes pauses in between.

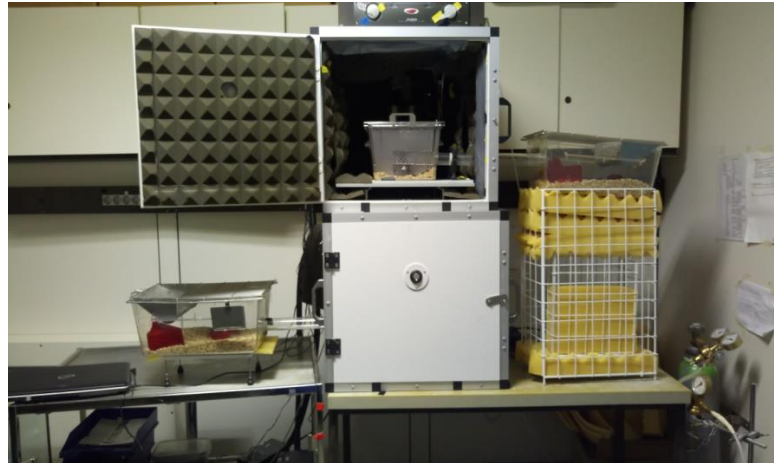
Either one of the following responses were obtained: hurdle crossing within four seconds after sound onset is considered a hit. Acoustic stimuli are stopped immediately upon hurdle crossing and no punishment is delivered. A miss is counted when the animal did not cross the hurdle within 4 s after sound onset. In that case, the stimulus is continuously displayed for another four seconds and at the same time foot shocks are delivered to stimulate the animal to cross the hurdle. A false alarm was noted when mouse crossed the hurdle while no sound was delivered (catch trial).

### 2.3.3 Intellicage setup

Operant conditioning in the “Audiobox” (Auditory Box Intellicage System, TSE Systems GmbH, figure 7) was carried out as described in (de Hoz and Nelken 2014). The setup consisted of a home cage, in which the mice have unlimited access to food. In order to drink water, the mice have to walk into a sound-shielded box containing loudspeakers and the “corner”. The presence of each mouse in the corner is automatically detected by a heat

sensor and a subcutaneously injected transponder. In order to drink, mice have to poke their nose into a small opening, breaking a light beam. Behind the opening is a moving door, allowing water access. The laptop computer then automatically controls sound playback, water access and air puff punishment according to the settings made by the experimenter for each mouse.

a)



b)



**Figure 7: Intellicage setup**

a) two sound-shielded boxes each connected to a standard mouse cage by a runway and containing  
b) water corners.

The Intellicage software consists of three main divisions; designer, controller and analyzer. The designer defines the desired experimental modules that are then executed individually for each animal by running the experimental file through the controller. Data are then analyzed and plotted into graphs by the analyzer.

The Intellicage hardware contains a group of sensors and actors. Sensors detect and assess the behavior of any individual mouse by: reading the code of the injected transponder (antennae), measuring temperature differential (presence detectors), nose-poking at corner

resulting in interruption of light beams at the opening of the corners (nose-poke sensors) and when the mouse starts licking from the water bottles (lickometer).

Actors execute the actions that shape the animal's behavior and are considered the examiner tools to remotely direct and control all the experimental modules for each animal. Examples for actors are doors, air-puff valves, and LEDs above the water corner. The doors control the access for each mouse by either opening or closing. An air-puff valve is used as a negative reinforcement tool, which blows compressed air onto the back of the mouse.

The Intellicage system recognizes any mouse that visits the corner and selects the stimulus to be presented for each mouse individually. It controls the response events and the subsequent air-puff punishment or water reward based on the settings made by the experimenter, usually depending upon whether there is a nose-poke attempt or not.

All mice were injected with a transponder under anesthesia with isoflurane. Buprenorphine (0.1  $\mu\text{g/g}$ , i.p.) was injected as anesthetic. Transponders were injected subcutaneously on the upper back. Thereafter, the animals were again placed to their home cage and watched until they recovered from anesthesia.

In order to be trained in the Intellicage, each mouse has to pass through the following phases. First, the habituation phase (~ seven days) which takes place directly after the transponder injection where transponder injected mice are placed into the Audiobox. During this phase, the doors giving access to the water corner remain open and no sound is presented during the visits. Second, the default phase (~ four days) comes once the mice learned where to find the water bottles. During this phase the doors are closed and only opened upon nose-poking. At the same time, every visit is coupled, for the whole duration of the visit, with the safe sound stimulus. Then, conditioning phase I, II and III where the standard conditioned stimuli (e.g., 80 dB tone bursts) are presented. In a certain fraction of visits, sounds are played during which the mouse should not nose-poke to access the water bottle. In these visits, the doors stay closed and nose-poking would be punished by an air puff. During this phase the conditioned stimuli are displayed in 5% of the total visits (~ three days), then increase to 7% (~ three days) and then to 12.5% (~ three days). Ideally, this took around nine days. We often prolong this period according to the ability of the mouse to discriminate between the conditioned and the safe stimuli. After the mice learned to discriminate between the conditioned stimuli and safe tones, more stimuli are presented. This phase teaches the mice to generalize their behavior across different conditioned stimuli. For all of these stimuli, nose-pokes are punished by air-puffs and doors remain closed. More different stimuli are

displayed successively in both generalization phases I and II (~ three days each). Finally, all experimental stimuli are displayed in random order in the experimental phase and the performance of each mouse is recorded and saved for further statistical analysis. As shown in the results, it seemed as if better results were obtained when nose-pokes during any experimental stimuli were also punished by air-puffs and doors remain closed. This setting is not ideal, because nose-poking during sub-threshold stimuli may lead to punishment and stress for the mice. However, as the threshold is not known before the experiment and mice might learn to differentiate between stimuli with different rewards/punishments (e.g., loudness discrimination in the threshold experiment), any alternative to this approach were deemed (or previously tested) to be less efficient. Also, only very few visits per day had experimental stimuli.

There was a pre-defined sequence of stimuli (e.g., three safe stimuli, one standard conditioned stimulus, two safe stimuli, one experimental stimulus (randomized), but to exclude the possibility that the mice could “count”, the order and counts were automatically and manually varied.

During the period of my study from 2017 till 2019, I have run six experiments using two Audio-boxes: frequency discrimination, first threshold experiment (in quiet), second threshold detection (in quiet and noise), tone detection in *Otof*<sup>-/-</sup> rescue mice, third threshold experiment (in quiet and noise) and gap detection experiment. Threshold was defined as the value at which the normalized psychometric function crosses 50%.

The first threshold and frequency discrimination experiments were carried out in the following setup:

- a- Two cages, connected with tube, one has a running wheel and the other act as a “home cage”, where mice can hide, sleep or play. Both cages have feeders.
- b- One of the cages was connected to the soundproof box, where mice have access to the water.
- c- Water bottles in the corner with transponder detector.

When comparing our initial data with those of Livia de Hoz, we noted that our mice visited the corner less often than hers (approximately 40 vs 70 visits per day). All of her data was thus shifted towards a higher fraction of visits without nose-pokes. Also, the discrimination performance of her mice was better, possibly because they were less afraid of visiting the corner and thus less stressed.

We thus changed settings before the second threshold experiment, tone detection for *Otof*<sup>-/-</sup> rescue mice, third threshold and gap detection experiment to include the following:

The additional cage with running wheel was removed to reduce the space and to encourage mice to visit water corners more often. In addition, I reduced the strength of the air-puff to 0.75 bar instead of one bar and increased the fraction of punished visits reaching ~ 17-20% instead of 12.5% in the experimental phase. The results of initial conditioning phase were much better afterwards: all mice learned with more than 30% discrimination between safe and punished stimuli.

In the Intellicage, three *Spnb* WT mice were trained in frequency discrimination experiment. Five *Ribeye* mice (three KO and two WT) were trained in the first threshold experiment (in quiet). Seven *Ribeye* mice (two WT, two heterozygotes and three KO mice) were trained in the second threshold experiment (in quiet and noise). Two males and seven female mice with normal hearing, were initially trained in two Audio-boxes as control for *Otof*<sup>-/-</sup> rescue mice in “Click detection” and then in “third threshold in quiet and in noise” experiments. They had the following genotypes: one *Bsn flx.PreCre*<sup>-/-</sup>, two *Bsn flx.PreCre*<sup>+/+</sup>, four *PrCre* - and two *Spnb* WT. Eight *Otof* rescue mice were trained in the “tone detection (click-train)” experiment. Seven *Otof2M* mice (one WT, three heterozygotes and three mutants) were trained in “gap detection” experiment. For each experiment in the Intellicage, data were collected and analyzed twice weekly. Depending on each mouse performance, the new module was chosen individually for each mouse.

### 3 Results

#### 3.1 Shuttle box results

Thirteen mice were trained on tone detection task in shuttle box. Their genotypes were as follows: three *Otit-CBA*<sup>+/-</sup>, four *ATP11a*<sup>+/+</sup>, four *Spnb*<sup>+/+</sup> and two Ribeye (one WT and one KO), divided into four consecutive groups. All those mice but the Ribeye KO mouse had normal hearing and their age was  $\geq$  six weeks in order to reach sufficient weight to be detected by sensors connected to shuttle box metallic grid floor.

**Table 1: Summarized results of mice trained in shuttle box.**

Mice Groups	First group (n = 3)	Second group (n = 4)	Third group (n = 4)	Fourth group (n = 2)
	Mean	Mean	mean	Mean
Age (weeks)	10.6	10.9	7.3	30
Average days in shuttle box	11	19	15	13
Total number of sessions	11	19	30	26
Experimental trials per session	60	60	33	33
Catch trials per session	10	10	6	6
Hit rate	11%	30%	64%	55%
Catch trial crossing rate	0%	12%	30%	21%
Discrimination	11%	18%	34%	34%

At the beginning of my shuttle box trials for mice training, the learning process was not successfully achieved. We realized that this might be due to stress and identified the following modifiable stress factors.

Motion of the mouse and switching sides sometimes was not immediately detected after crossing the hurdle, resulting in wrong or missing punishment. This caused confusion of the mice during training.

Each mouse was initially placed directly in the shuttle box without previous acclimatization period. Starting from group III, I thus introduced an acclimatization period of three to five days. During that period, the examiner just brought the mouse carefully, placed it for 4-5 minutes in the shuttle box and brought it back to the home cage so that mice could get used to the examiner and the testing environment.

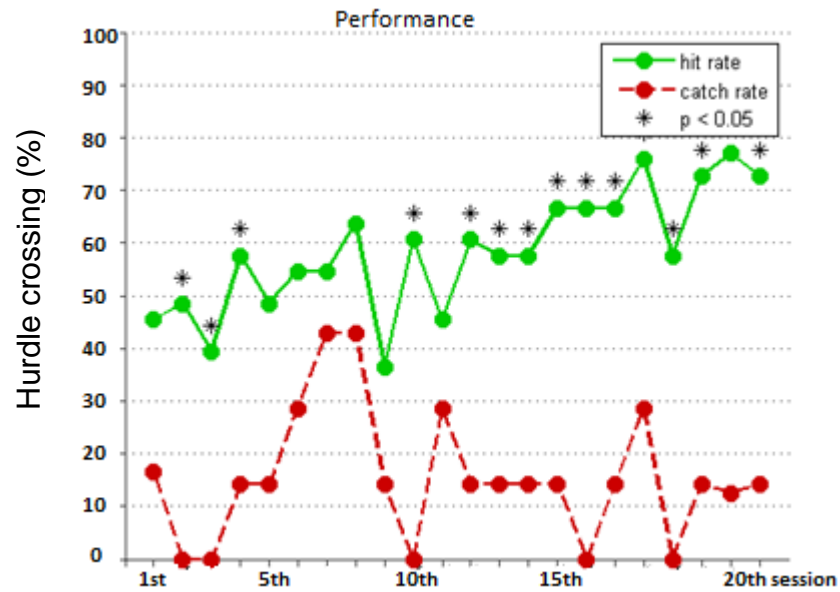
Transporting any mouse from its cage to the soundproof chamber is a stressful process especially when being lifted up by its tail. I decreased this stress by letting mice enter into a small cardboard tube during the initial acclimatization period for a protected transfer to the experimental setup.

Subjecting the mice immediately to pure tones at high intensity level coupled with punishment (electric shock) may have increased the anxiety of the mice and worsened their performance. Some mice occasionally showed freezing behavior, disrupting the learning process. Though we were careful about the foot shock strength from the beginning, from group III we introduced the test stimuli coupled with a very minimal level of electric current applied to the metallic grids on the shuttle box floor even more gradually.

Long sessions of 70 trials were divided into two smaller sessions each of 40 trials as mice usually showed better performance at the beginning of each session than towards the end.

Representative examples of a good and a poor performing mouse are displayed in figure 8. For the good performer (figure 8a), data were collected after the initial acclimatization period. This mouse could successfully discriminate between sound stimulus (12 kHz at 80 dB) and silence across most of the sessions. Data obtained on the day of cage cleaning were discarded since the performance of the mouse usually drops. Figure 8b shows an example of a poor learner mouse. This mouse could not distinguish between stimulus and silence and it showed poor discrimination rates across sessions.

a)



b)

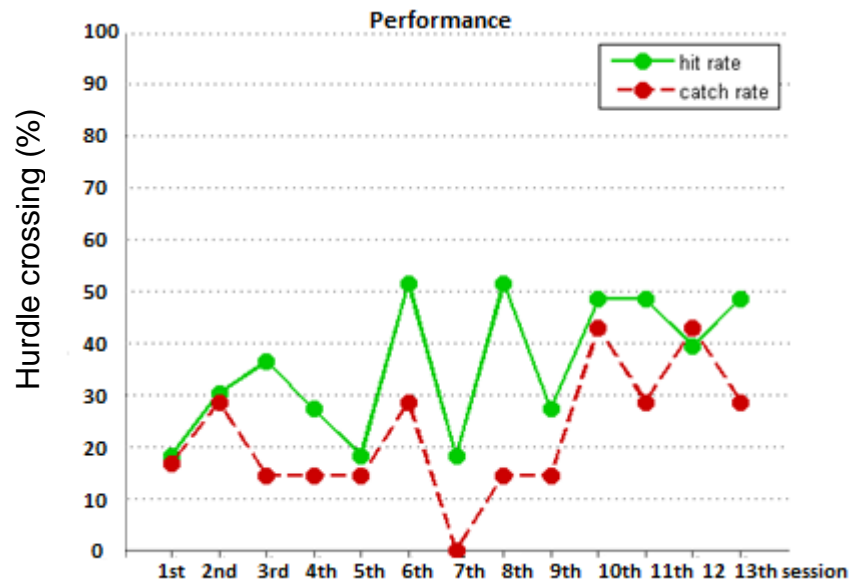


**Figure 8: Examples of good and poor performance in the shuttle box**

Performance through training sessions in a) good learner and b) poor learner, both from group III; Ribeye WT and KO mice. \*p < 0.01; Chi<sup>2</sup>-test.

## 3.2 Intellicage results

### 3.2.1 Frequency discrimination experiment

Three *Spnb* WT female mice, ten weeks old were trained to discriminate between tones of two different frequencies as in (de Hoz und Nelken 2014). Initially, there were two well separated tones (one octave apart). Then, we explored the capacity of mice to discriminate between progressively similar tones, by moving the conditioning tone closer in frequency to the safe tone. 6670 Hz was the safe tone during which mice have free access to

water without punishment. Conditioning tones were 13340, 9433, 8004, 7670, 7337, 7137, 6937 and 6803 Hz. All the tested frequencies were presented at the same intensity (80 dB SPL).

**Table 2: Conditioning paradigm in frequency discrimination experiment.**

Experimental phases	Habituation	Default	Conditioning I	Conditioning II	Conditioning III	Generalization I	Generalization II	Experiment
Average number of days	6	6	10	9	9	9	9	175
Safe visits	100%	100%	95%	93%	87.5%	87.5%	87.5%	93.5%, including 12.5% experimental stimuli
Visits with punishment	-	-	5%	7%	12.5%	12.5%	12.5%	6.5%
Standard safe stimulus	-	6670 Hz	6670 Hz	6670 Hz	6670 Hz	6670 Hz	6670 Hz	6670 Hz
Conditioned stimuli	-	-	13340 Hz	13340 Hz	13340 Hz	13340 & 9433 Hz	13340 & 8003 Hz	13340 Hz
Experimental stimuli without punishment	-	-	-	-	-	-	-	9433, 8003, 7670, 7337, 7137, 6937 & 6893 Hz

The average percentage of visits for each experimental stimulus was 1.5% (12.5 for all stimuli). Punishment was applied only for 13340 Hz tone and not applied for other experimental stimuli. One mouse in the frequency discrimination experiment was not avoiding the conditioned stimuli so it did not proceed to the experimental phase.

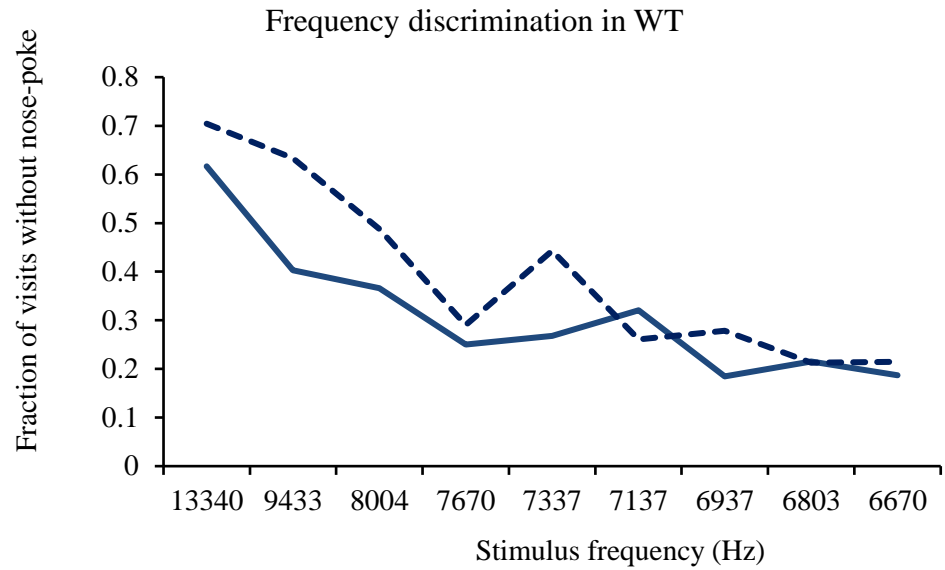


**Figure 9: *Spnb* WT mouse performance in frequency discrimination experiment.** Each line represents one animal.

Two WT mice were capable of distinguishing safe tone (6670 Hz) from conditioned stimuli (13340, 9433, 8004, 7337, 7137, 6937 and 6803 Hz) with a discrimination between 6670 and 13340 Hz of  $35\% \pm 8.2$  (mean  $\pm$  SEM). The closer the proximity between the tested frequencies, the less their ability to discriminate i.e., maximum avoidance was achieved for 13340 Hz (conditioned tone) and discrimination decreased with frequencies of 9433 and 8004 Hz to reach similar values as for the safe visits at around 7670 Hz.

### 3.2.2 First Ribeye threshold experiment

Mice were conditioned to attempt to drink only in silence. When silence was interrupted by 6 kHz, 80 dB SPL tone bursts, access to the water bottles was denied and drink attempts were punished by air-puffs (1 bar air pressure). After reaching a discrimination criterion of more than 30% in the conditioning phases, generalization across variable intensity levels was tested. Then the experimental phase began in which all sound intensities from 80 to 20 dB SPL were evaluated in a total of  $\sim 12\%$  of the trials. The intermediate stimuli (70 to 20 dB SPL) were not punished in the first experiment.

During the first threshold experiment (threshold in quiet), the safe stimulus was silence and the initial conditioned stimulus was a 6 kHz pure tone at 80 dB SPL. The experimental stimuli were 6 kHz pure tones at 80, 70, 60, 50, 40, 30, 20 dB SPL. The average percentage of visits for each experimental stimulus was 1.8% (12 for all stimuli) and punishment was applied only for 80 dB stimulus and not applied for other experimental

stimuli. Tested mice were three Ribeye KO mice (-/-) and two WT (+/+) mice. The average age of mice at the time of introduction to the Intellicage was 16.1 weeks.

**Table 3: Conditioning paradigm in first behavioral threshold experiment.**

Experimental phases	Habituation	Default	Conditioning I	Conditioning II	Conditioning III	Generalization I	Generalization II	Experiment
Average number of days	5	5.4	10	9.6	12.8	7.6	11.6	73.2
Safe visits	100%	100%	95%	93%	87.5%	87.5%	87.5%	93.5%, including 12% experimental stimuli
Visits with punishment	-	-	5%	7%	12.5%	12.5%	12.5%	6.5%
Safe stimulus	-	silence	silence	silence	silence	silence	Silence	Silence
Conditioned stimuli: 6 kHz tone bursts	-	-	80 dB	80 dB	80 dB	80 & 70 dB	80 & 60 dB	80 dB
Experimental stimuli (6 kHz tone bursts) without punishment	-	-	-	-	-	-	-	70 to 20 dB

First threshold experiment (normalized)

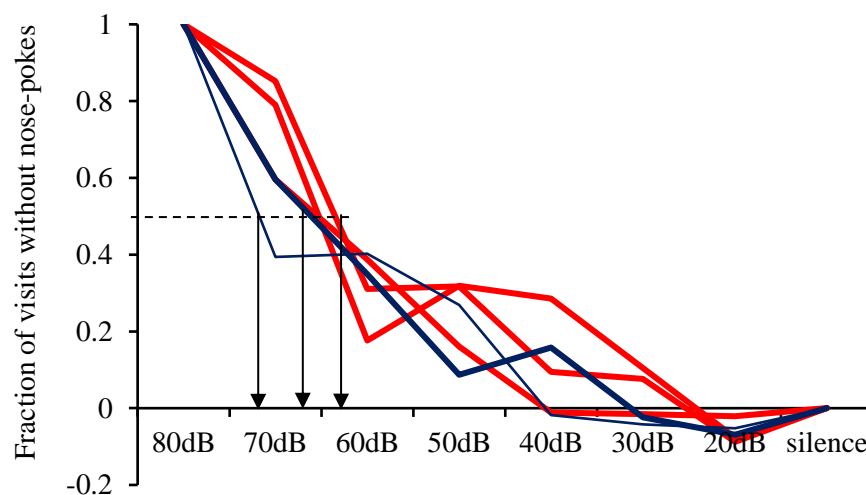


**Figure 10: First threshold experiment in Ribeye mice: thresholds in quiet.**

Each line represents one animal (blue for WT, red for KO). The graph shows the average fraction of visits without nose-poke, normalized to the fraction of visits without nose-poke at 80 dB and silence. Arrows indicate the threshold, interpolated as the intensity at the midpoint between the nose-poke rates for silence and 80 dB stimuli.

Figure 10 shows average fraction of visits in which Ribeye WT ( $n = 2$ , blue lines) and KO ( $n = 3$ , red lines) mice did not attempt to drink normalized to initial conditioned (80 dB) and safe (silence) stimuli. The average percentage of discrimination between safe and 80 dB stimuli was  $50\% \pm 4.9$  (mean  $\pm$  SEM) for all mice. Both Ribeye KO and WT show comparable thresholds between  $\sim 60$  and 70 dB, which was much higher than their recorded ABR threshold (35 dB for Ribeye WT and 45 dB for KO for 6 kHz tone burst). Since normally, ABR thresholds are expected to be slightly worse than subjective thresholds, we figured out that our threshold assessment was incorrect and we had to improve our method. We hypothesized that the mice had learned that punishment would occur only for loud, not for softer sounds.

### 3.2.3 Second Ribeye threshold experiment

In our next attempts, experimental mice were conditioned to attempt to drink only in silence. When the silence was interrupted by 12 kHz 80 dB SPL tone bursts, access to the water bottles was denied and drink attempts were punished by air puffs (0.75 bar air pressure). After reaching discrimination of more than 30% in the conditioning phase, generalization across variable intensity levels was induced. Then the experimental phase began at which all sound intensities from 80 to 20 dB SPL were tested in a total of  $\sim 18$ -20% of the trials. In contrast to the first threshold experiment, all conditioned stimuli were accompanied by punishment.

Silence was always ‘safe’, when there was no sound during a visit, the mice could access the ports and drink water without an associated negative outcome. 12 kHz tone of any intensity (even at 20 dB) was considered a conditioning tone and the mice should avoid drinking, else they were punished by an air-puff and did not get access to water.

Tested mice were three Ribeye KO mice (-/-), two WT (+/+) and two heterozygote littermates (+/-). The average age of the mice at the time of introduction to Intellicage was  $\sim 10.9$  weeks.

In human auditory synaptopathy/neuropathy, patients often complain of poor hearing in noise, thus we wanted to establish a paradigm for threshold testing in noise and apply it to a mouse model of auditory synaptopathy.

While during the first phase (thresholds in quiet), we aimed to have as little background noise in the soundproof box as possible, during the second phase (thresholds in

noise), white noise of 45 or 60 dB was played continuously from two additional loudspeakers placed above the corner. Else, everything was the same as before.

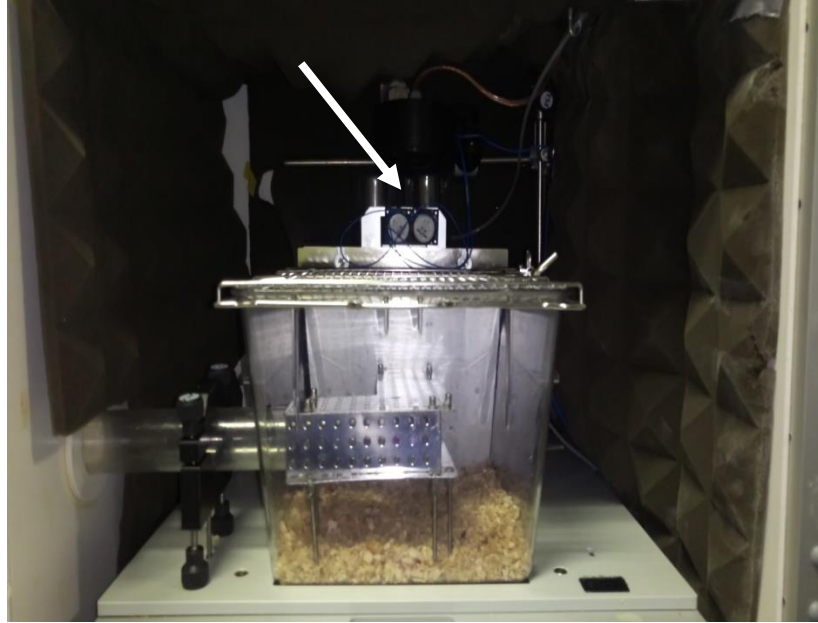


**Figure 11: Photo of the modified Intellicage setup for testing thresholds in noise**  
Two additional miniature loudspeakers (arrow) were placed above the water corner.

**Table 4: Conditioning paradigm in second behavioral threshold experiment (in quiet).**

Experimental phases	Habituation	Default	Conditioning I	Conditioning II	Conditioning III	Generalization I	Generalization II	Experiment
Average number of days	3	6	3	3	3.9	9.8	6.4	43.1
Safe visits	100%	100%	95%	93%	87.5%	87.5%	87.5%	82%
Visits with punishment	-	-	5%	7%	12.5%	12.5%	12.5%	18%
Conditioned stimuli (12 kHz)	-	-	80 dB	80 dB	80 dB	80 & 70 dB	80 & 60 dB	80 to 20 dB

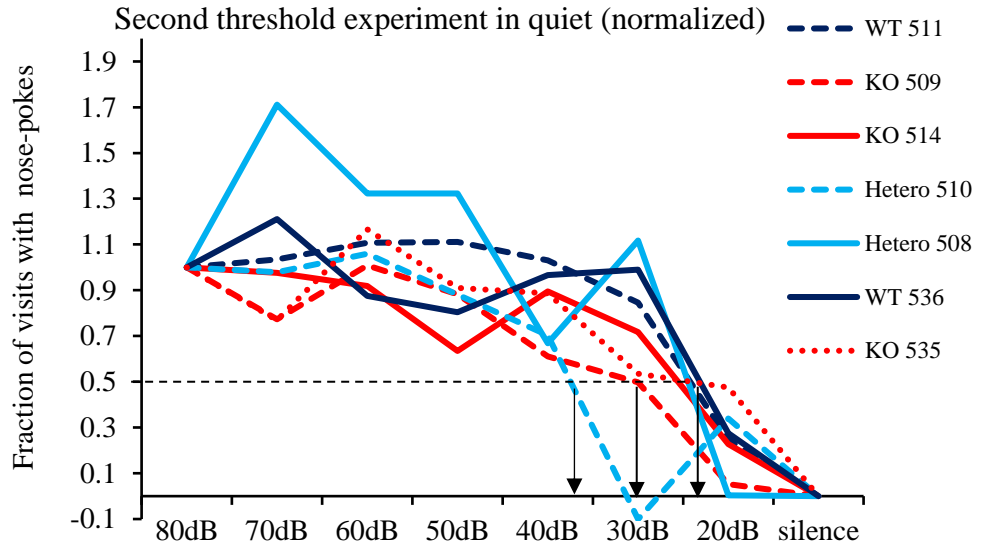


**Figure 12: Second threshold experiment (in quiet) in Ribeye KO mice.**

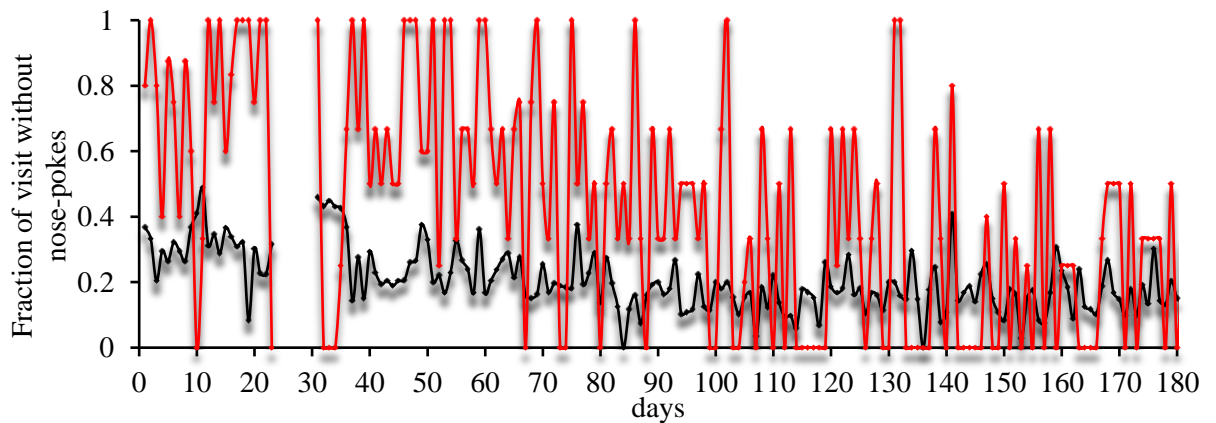
Each line represents one animal. The fraction of visits without nose-pokes was normalized to the values obtained at 80 dB and silence. Each visit can have several nose-pokes. Arrows indicate the threshold, interpolated as the intensity at the midpoint between the nose-poke rates for silence and 80 dB stimuli.

Figure 12 shows the average fraction of visits in which Ribeye KO (red), WT (dark blue) and heterozygous (light blue) mice did not attempt to drink normalized to initial conditioned (80 dB) and safe (silence) stimuli. The average percentage of discrimination between safe and 80 dB conditioning stimuli was  $35\% \pm 8.9$  (mean  $\pm$  SEM) for Ribeye WT and heterozygous and  $39\% \pm 4.7$  for the mutant. KO, WT and heterozygous animals showed similar behavior with interpolated thresholds between 20 and 30 dB, with the exception of one WT mouse having a threshold of  $\sim 40$  dB.

During the second threshold experiment (threshold in noise), a continuous white noise was played independent of visits first at 45 dB for  $\sim 45$  days, then increased to 60 dB SPL for another 45 days. In “safe” visits, no additional stimulus was added. The initial conditioned stimulus was a 12 kHz pure tone at 80 dB SPL. Experimental stimuli were 12 kHz pure tones at 80, 70, 60, 50, 40, 30, 20 dB SPL. The average percentage of visits for each experimental stimulus was 2.6% (18% for all stimuli). Punishment was applied for all experimental stimuli. Tested mice were three Ribeye KO mice (-/-), two WT (+/+) and two heterozygous mice (+/-). Their age was  $\sim 10$  weeks at the time of introduction to the Intellicage.

**Table 5: Conditioning paradigm in second behavioral threshold experiment (in noise).**

Experimental phases	Habituation	Default	Conditioning I	Conditioning II	Conditioning III	Generalization I	Generalization II	Experiment
Average number of days	3	6	3	3	3.9	9.8	6.4	40 days for each noise level, 24 days after noise
Safe visits	100%	100%	95%	93%	87.5%	87.5%	87.5%	82%
Visits with punishment	-	-	5%	7%	12.50%	12.50%	12.50%	18%
Conditioned stimuli (12 kHz) with noise (45, 60 dB)	-	-	80 dB	80 dB	80 dB	80 & 70 dB	80 & 60 dB	80 to 20 dB

**Figure 13: Daily monitoring of the performance of a Ribeye KO mouse.**

The graph shows a representative example of the fraction of visits with no nose-poke in the second threshold experiment for 80dB stimuli (red) and silence (black). At the beginning of the experiment, both curves were well separated. After introduction of background noise on day 80, the red line slowly goes down, approximating the black line from approximately day 120.

The average number of visits without nose-poke decreased slowly and the performance of Ribeye KO mouse declined with introduction of noise on day 80 (45 then 60 dB SPL noise) as shown in Figure 13.

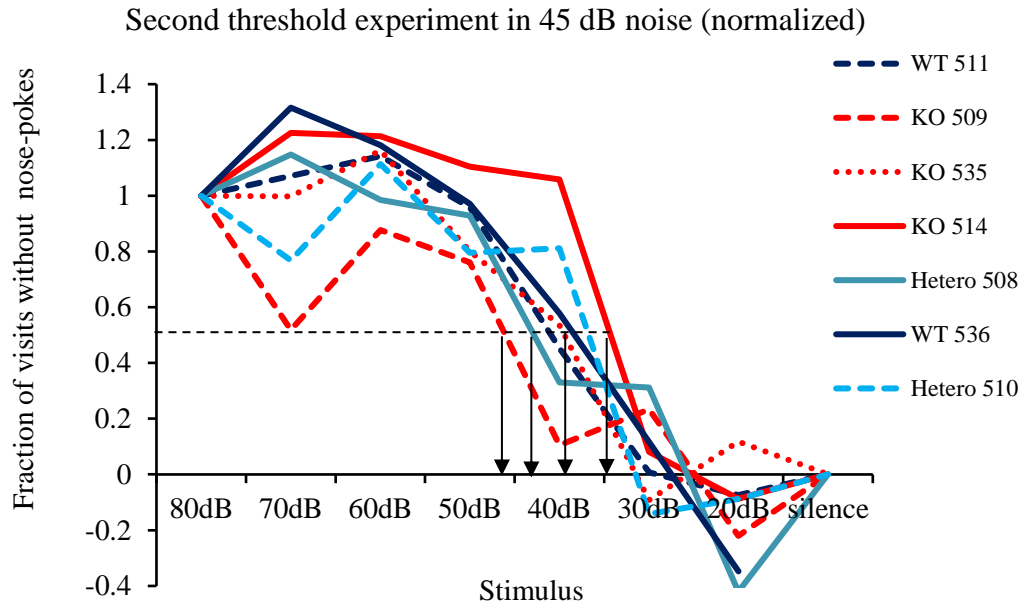


**Figure 14: Second threshold experiment in Ribeye KO mice: 45 dB background noise**

Average fraction of visits without nose-poke (normalized) in second threshold experiment (45 dB noise). Each line represents one animal. The fraction of visits without nose-poke was normalized to the values obtained at 80 dB and silence. Arrows indicate the threshold, interpolated as the intensity at the midpoint between the nose-poke rates for silence and 80 dB stimuli.

Data in figure 14 were collected from Ribeye KO ( $n = 3$ , red lines), WT ( $n = 2$ , dark blue lines) and heterozygous mice ( $n = 2$ , light blue lines). The graph shows data normalized to initial conditioned (80 dB with background noise at 45 dB SPL) and safe (white noise at 45 dB SPL) stimuli.

The average percentage of discrimination between safe and 80 dB conditioned stimuli was  $40\% \pm 2.5$  (mean  $\pm$  SEM) for Ribeye WT and heterozygous mice, and  $35\% \pm 8.2$  for the mutants. Each line represents one animal. All mice exhibited almost the same behavior with interpolated thresholds between 30 and 40 dB, with exception of one KO (509) with a threshold between 40 and 50 dB. There was a threshold shift by 10 dB (masking effect) for all mice except one KO (509) which showed a 20 dB threshold shift.

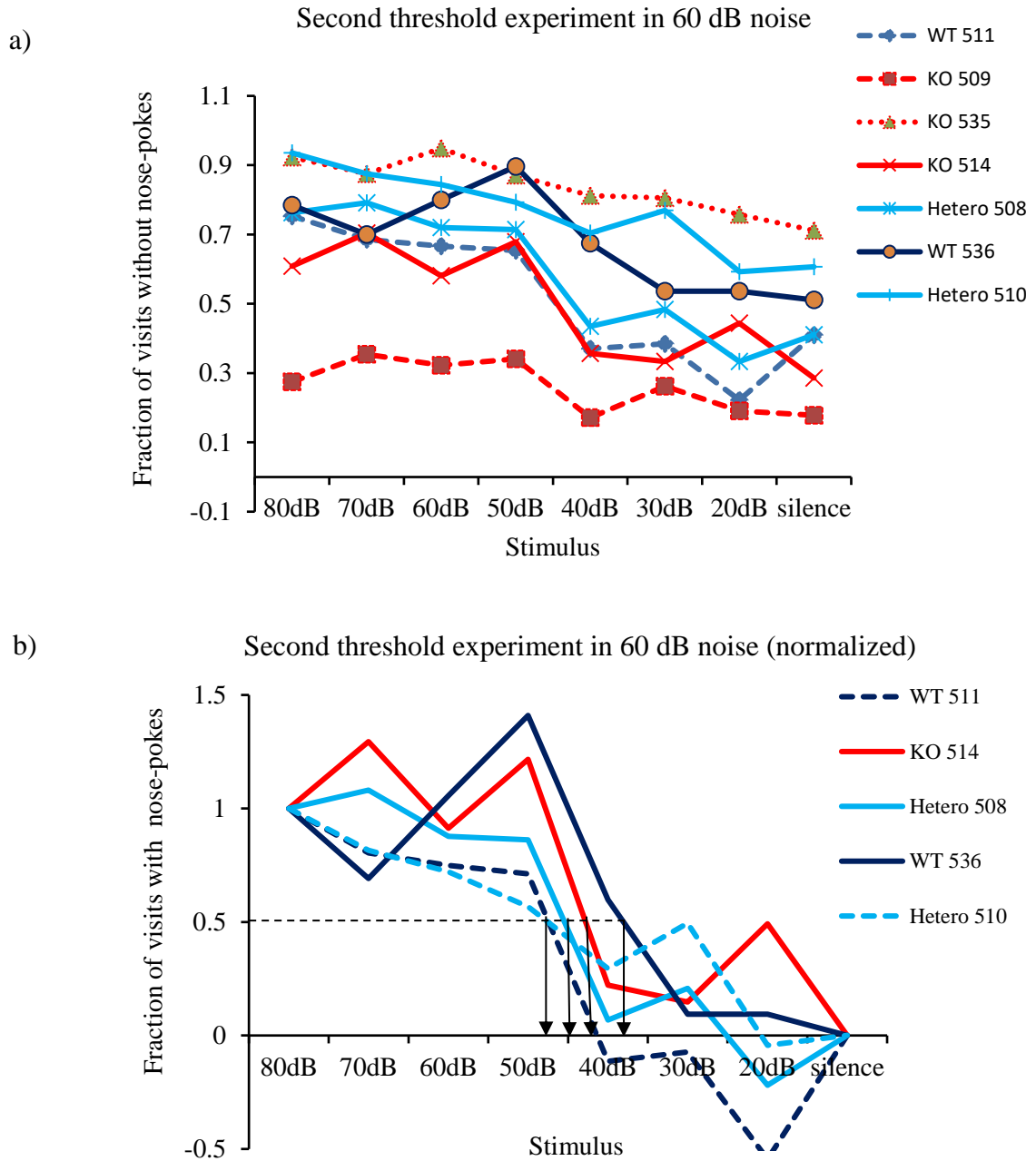


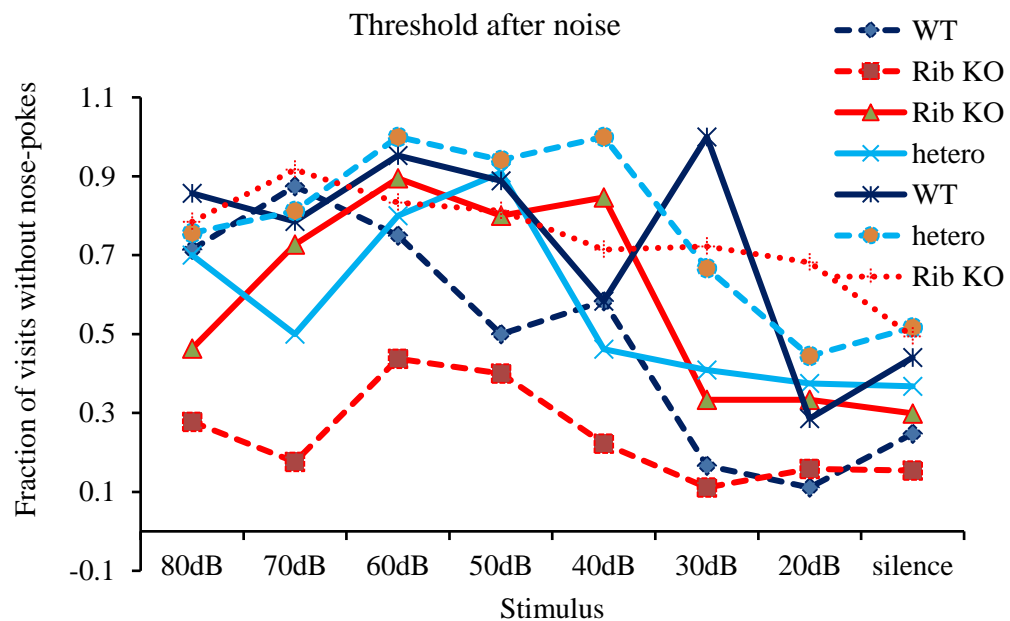
**Figure 15: Second threshold experiment in Ribeye KO mice: 60 dB background noise.**

Each line represents one animal. a) Average fraction of visits without nose-poke for the different stimuli, all presented in 60 dB background noise. b) Same data, but normalized to main conditioned (80 dB tone bursts in 60 dB noise) and safe (60 dB background noise only) stimuli. Arrows indicate the threshold, interpolated as the intensity at the midpoint between the nose-poke rates for background only and 80 dB stimuli.

Data in figure 15 were collected from Ribeye KO ( $n = 1$ , red lines), WT ( $n = 2$ , dark blue lines) and heterozygous mice ( $n = 2$ , light blue lines). WT and heterozygous mice show quite similar interpolated thresholds between 40 and 50, which was consistent with the masking effect (threshold shifts by  $\sim 10$  to 20 dB after the introduction of noise). At 60 dB noise, two Ribeye KO (509 and 535) mice exhibited an alteration in their behavior and they

lost their ability to discriminate between safe and conditioned stimuli (figure 15a), and threshold estimation become not possible so their data were not shown in (figure 15b). The average percentage of discrimination between safe and 80 dB conditioned stimuli was  $41\% \pm 8.7$  (mean  $\pm$  SEM) for Ribeye WT and heterozygous, and dropped to  $22.5\% \pm 8.0$  for the mutant.

a)



b)

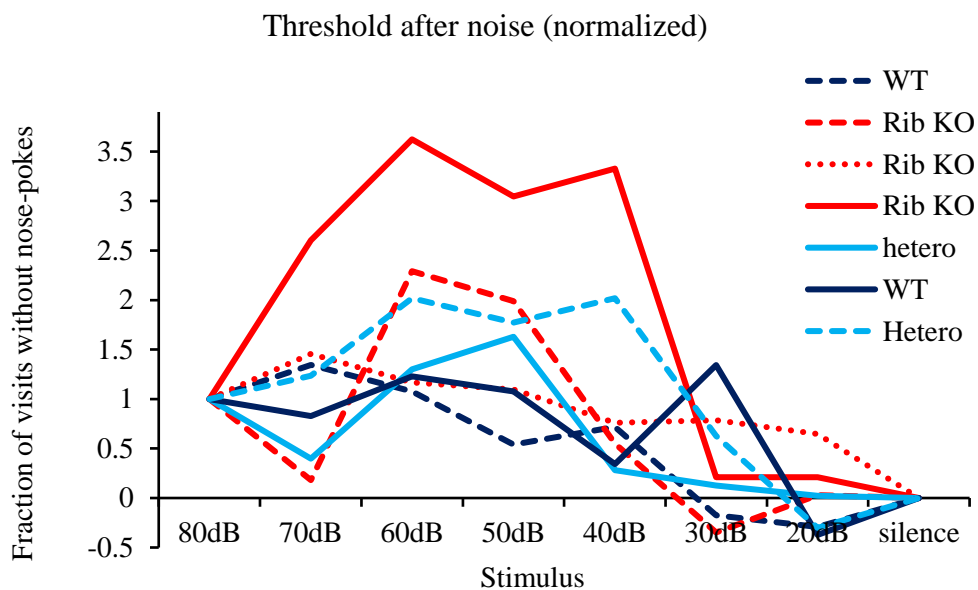


**Figure 16: Second threshold experiment in Ribeye KO mice: after cessation of background noise.**

Each line represents one animal. a) Average fraction of visits without nose-poke for the different stimuli b) Same data, but normalized to main conditioned (80 dB) and safe (silence) stimuli.

Thresholds were re-assessed again after noise cessation for one month, so the total duration of the experiment was almost six months.

Figure 16 shows data collected from WT ( $n = 2$ ), KO ( $n = 3$ ) and heterozygous mice ( $n = 2$ ). The average percentage of discrimination between safe and 80 dB conditioning stimuli was  $41\% \pm 12.8$  (mean  $\pm$  SEM) for Ribeye WT and heterozygous, and  $31\% \pm 5.3$  for the mutants after noise cessation. Ribeye KO mice discrimination percentage showed some improvement after noise cessation. However, the discrimination functions for experimental stimuli did not show a sigmoidal shape anymore (figure 16a) and thus, behavioral threshold estimation was not possible (figure 16b). The steepest increase in discrimination was again between 30 and 40 dB for most mice, in a similar range as in the initial threshold in silence test.

### 3.2.4 Third threshold experiment

The experimental procedures were the same as in the second threshold experiment (in quiet and noise) except that I tested seven mice which had been trained before in the tone detection experiment as control for the *Otof*<sup>-/-</sup> rescue. With the exception of two mice, successful generalization from click trains (tone detection experiment) to 12 kHz tone burst was achieved. These mice were also included in the third threshold experiment (in quiet and noise) as described in table 5 and 6. The intensity of noise used in third threshold experiment was  $\sim 55$  dB SPL. Tested mice were one *Bsn flx.PreCre*<sup>-</sup>, one *Bsn flx.PreCre*<sup>+</sup>, one *PreCre*<sup>-</sup> and two *Spnb*<sup>+/+</sup>. All of those mice are expected to have normal hearing function. The average age of mice at the onset of the experiment was 12.3 weeks.

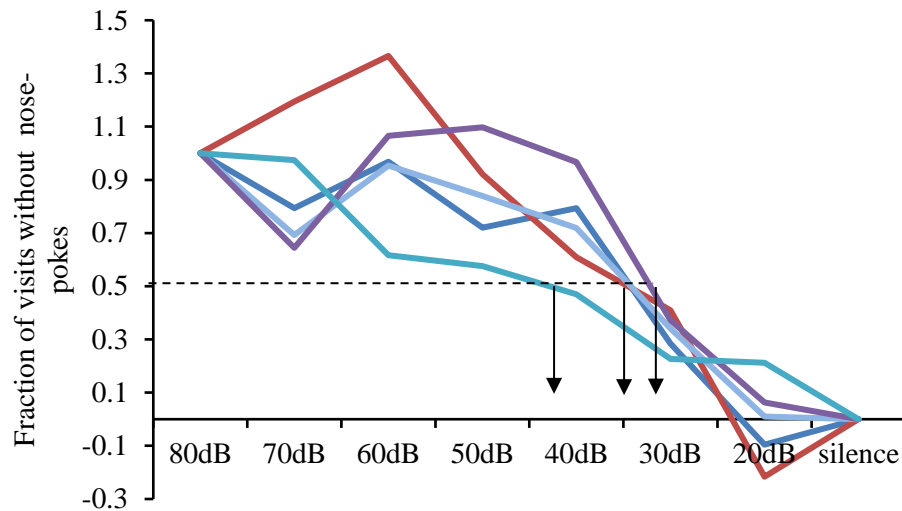


**Figure 17: Average fraction of visits without nose-poke in the third threshold experiment (in quiet).**

Each curve represents data from one animal ( $n = 5$ ). Data were normalized to main conditioned (80 dB) and safe (silence) stimuli. Arrows indicate the threshold, interpolated as the intensity at the midpoint between the nose-poke rates for silence and 80 dB stimuli.

Figure 17 show the number of visits without nose-poke as a fraction of the total number of visits normalized to values for 80 dB and silence. All mice exhibited almost the same behavior with interpolated thresholds between 20 and 30 dB, with exception of one mouse having a threshold at 40 dB. The average percentage of discrimination between safe and 80 dB conditioning stimuli was  $52\% \pm 4.0$  (mean  $\pm$  SEM) for all mice.

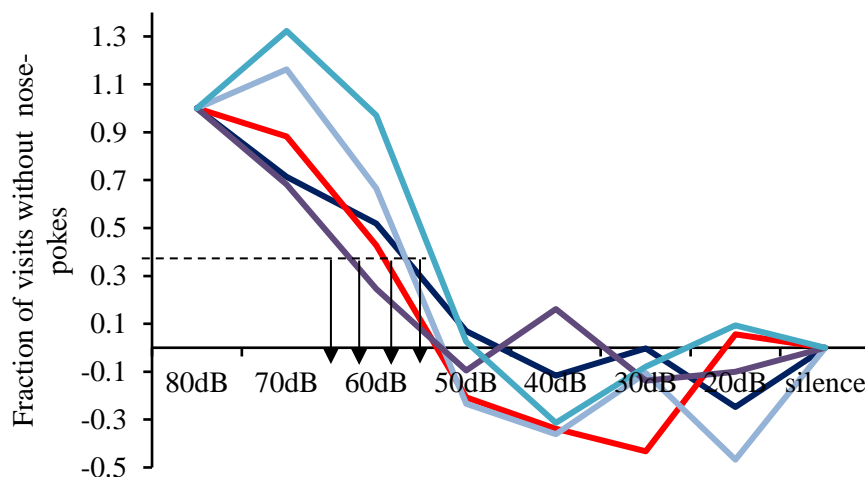


**Figure 18: Average fraction of visits without nose-poke in third threshold experiment (in noise).**

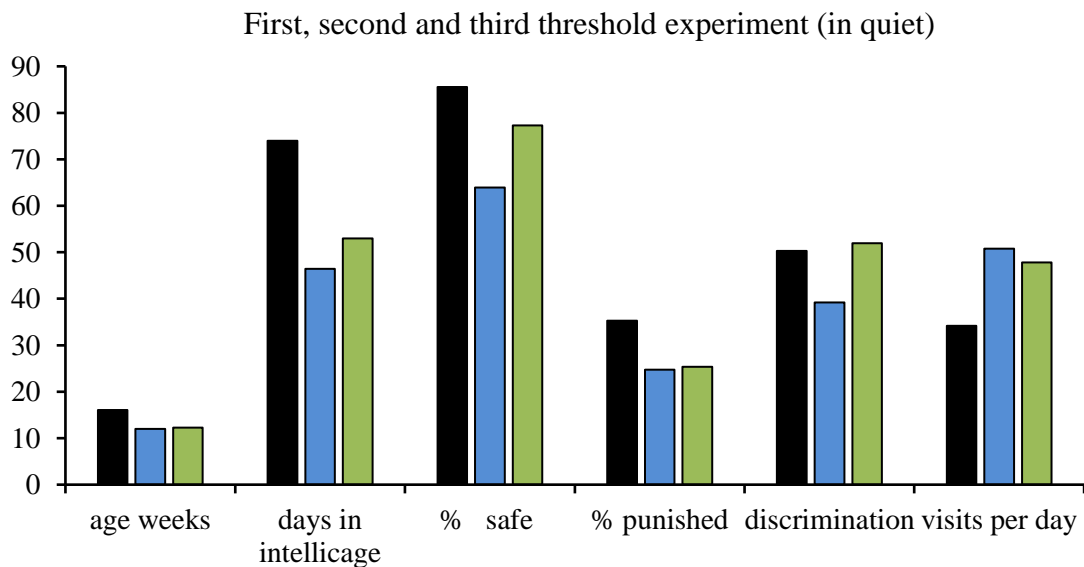
Each curve represents data from one animal ( $n = 5$ ). Data are normalized to main conditioned (80 dB) and safe (silence) stimuli. Arrows indicate the threshold, interpolated as the intensity at the midpoint between the nose-poke rates for silence and 80 dB stimuli.

Figure 18 shows normalized data to initial conditioned (80 dB with background noise at 55 dB SPL) and safe stimulus (white noise at 55 dB SPL). Each line represents one animal. The average percentage of discrimination between safe and conditioned 80 dB stimuli after noise introduction was  $33\% \pm 3.6$  (mean  $\pm$  SEM). All mice exhibited almost the same behavior with interpolated thresholds between 50 and 60 dB, with exception of one mouse having a threshold of  $\sim 65$  dB. There was a threshold shift of about 20 dB SPL for all mice, which likely corresponds to the expected masking effect.

The results of the first, second and third threshold experiment were compared in order to study the test re-test reliability of experiments within Intellicage and to highlight the effects of changes made in the Intellicage as mentioned in the methodology as shown in table 6 and figure 19. They provide a comparison between the first, second and third threshold experiment when comparing data before (first threshold experiment) and after changes (second and third threshold experiment). The main difference was the increase in number of visits made by mice per day, which can be explained by the decrease in air-puff strength and the reduced size of the home cage area. Even though the mice visited the corner more often, they did not nose-poke as often. The fraction of visits with nose-poke attempts both for the safe and for the conditioned stimuli was lower in the second and third experiment. The discrimination ability was more than 30% in all experiments although the initial training modules were shorter in second and third experiment. All mice in the third experiment were capable of generalization between click trains and 12 kHz tone burst and they achieved a slightly better discrimination ability ( $52\% \pm 0.04$ ) than those in the first ( $\sim 50\%$ ) and second threshold experiment ( $\sim 40\%$ ). Importantly, in the experimental phase, the discrimination curves were more homogenous, steeper and shifted towards lower sound intensities, close to the expected behavioral thresholds as estimated from published ABR and single ANF recording data.

**Table 6: Comparison between first, second and third threshold experiment.**

Intellicage	First threshold experiment		Second threshold experiment		Third threshold experiment	
Mice in each group (n = 5)	Mean	SEM	Mean	SEM	mean	SEM
Age in weeks	16.1	0.3	12	0	12.3	1.9
Days in Intellicage	74	6.6	46.4	4.4	53	4.3
% Safe	85.6	1.1	63.9	5.0	77.3	0.7
% Punished	35.3	4.9	24.7	6.7	25.3	3.3
Discrimination	50.3	4.9	39.9	3.8	51.9	4.0
Visits per day	34.2	2.6	50.8	1.5	47.8	3.5
Total number of visits	2612.6	359.6	2343.2	205.8	2572.2	332.9

**Figure 19 Summary of results for the three Intellicage threshold experiments**

Comparison between the first (black bars), second (blue) and third (green) threshold experiments. The legend “age weeks” refers to the age of mice at time of introduction to the Intellicage, “days in Intellicage” refers to duration of the experimental phase,” % safe”: means the average percentage of attempts to nose-poke during visits with standard safe stimuli (no tone), “% punished”: means the percentage of averaged mice attempts to nose-poke when the conditioned tone is displayed, “visits per day”: means the average number of visits made by each mouse per day.

### 3.3 *OtofQX* and *Otof2M* mice: electrophysiological and behavioral assessment

#### 3.3.1 *OtofQX* ABR

*OtofQX* mutant mice underwent auditory characterization as they were planned for trial attempts of gene-therapy.

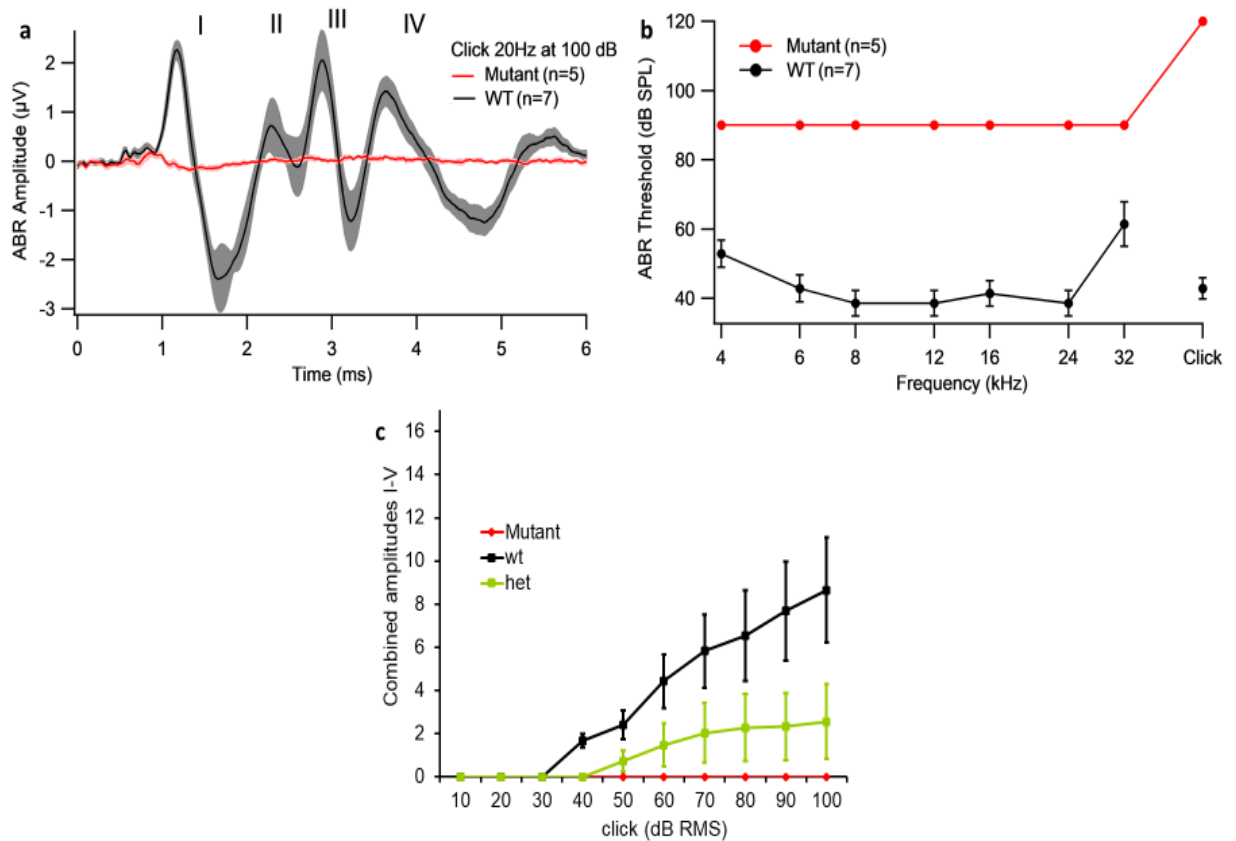


**Figure 20: *OtofQX* mice auditory phenotype**

a) Grand averages of ABR waveforms evoked by 100 dB SPL click sound stimuli recorded from *OtofQX* mutant and WT mice, b) ABR click sound and tone burst threshold. Where no ABR was present at sound intensity of 80 dB (tone bursts) or 100 dB (clicks), 90 or 100 dB were entered as thresholds. c) Summed ABR wave I-V amplitude growth function.

Figure 20 shows data which were collected from mutant *OtofQX* (n = 5), WT control mice (n = 7) and heterozygous mice (n = 2) at age 7-15 weeks. ABR of *OtofQX* mutants showed no ABR waves in response to click 20 Hz and tone burst (figure 20 a, b and c) up to intensities of 100 dB or 80 dB respectively. Only the summing potentials (small positive peak at a latency of 1 ms) still existed.

### 3.3.2 *Otof2M* ABR

Data were collected from *OtofQX* mutant ( $n = 9$ ) and WT control mice ( $n = 9$ ) at an age of 3 to 20 weeks.

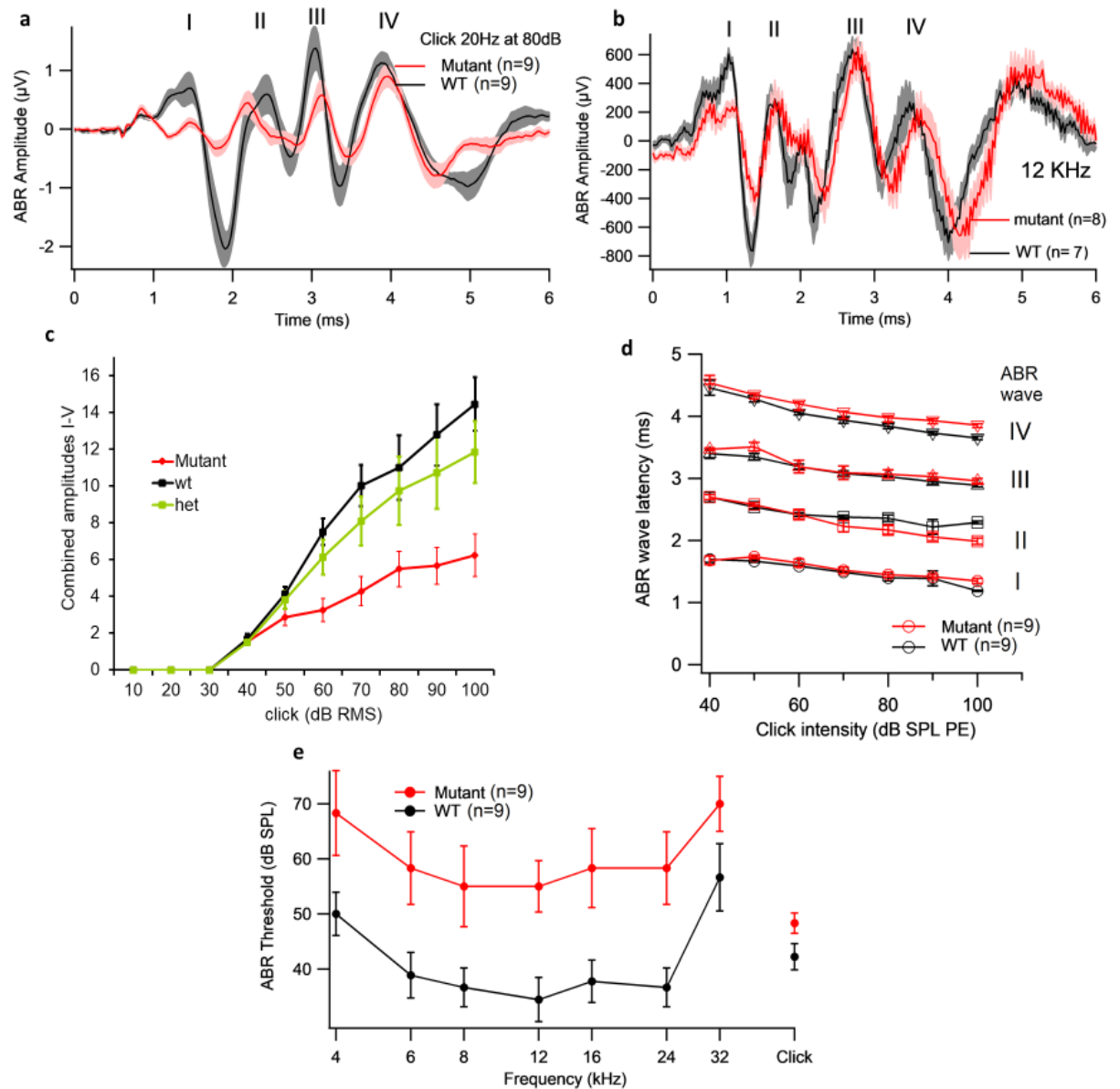


**Figure 21: *Otof2M* mice auditory phenotype**

a) *Otof2M* mutant and WT average ABRs evoked by 80 dB SPL click sound stimuli, b) *Otof2M* mutant and WT average ABRs evoked by 80 dB SPL 12 kHz tone burst stimuli, c) Summed ABR wave I-V amplitude growth function, d) ABR wave I-IV latencies e) ABR tone burst and click thresholds.

*Otof2M* mutants exhibit a moderate reduction in ABR amplitudes to click (figure 21a) and tone burst (figure 21b) stimulation. ABR latencies were normal (figure 21c). ABR thresholds were increased by 20 dB for tone bursts and 8 dB for clicks (figure 21d).

*Otof2M* mutant mice showed a reduction in the amplitudes of wave I and wave III. Wave II and IV were comparable to the WT (figure 21c). There was no latency shift for the ABR waves (figure 21d).

Since otoferlin is essential for vesicle exocytosis and replenishment, we measured the ABR response at different stimulus repetition rates in an attempt to modify synaptic turnover rates. So, click stimuli at 80 dB SPL were presented at three different repetition rates (1 Hz, 20 Hz and 100 Hz) and averaged for 7 WT (figure 22a) and 8 *Otof2M* mutant mice (figure 22b).

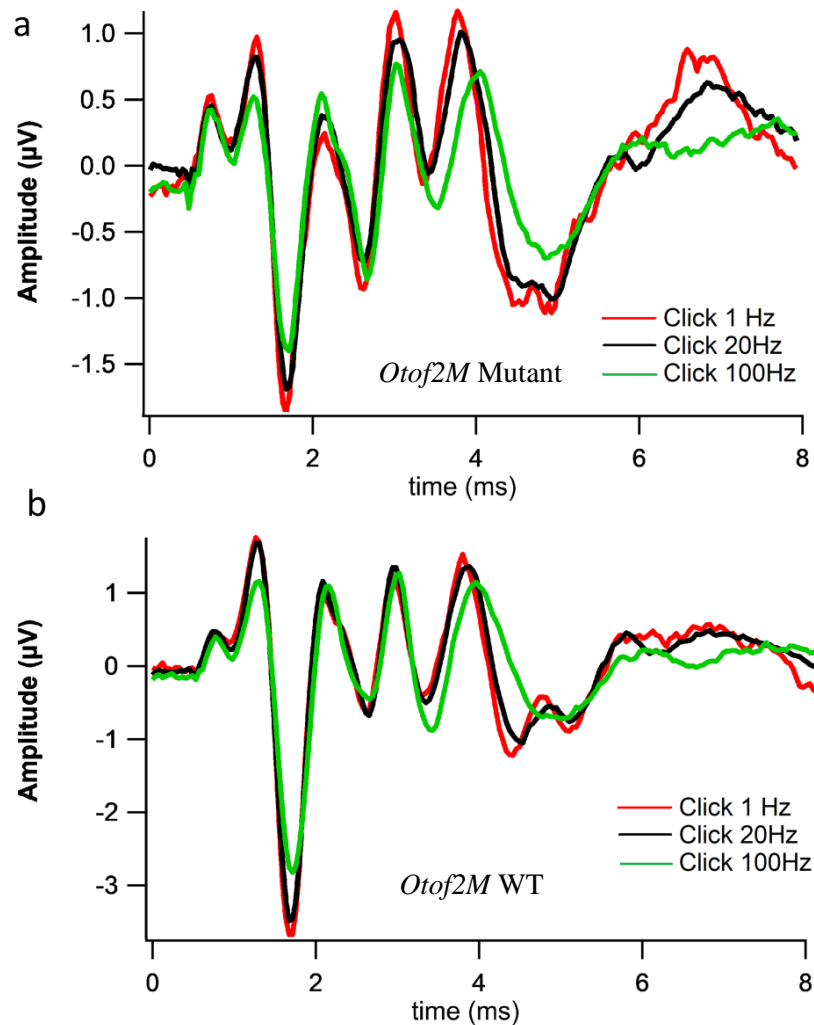


**Figure 22: *Otof2M* ABRs to 1, 20, and 100 Hz click stimulation**

a) *Otof2M* mutant (n = 8) and b) *Otof2M* WT (n = 7), age 3-4 weeks. Grand averages of the waveform to 80 dB Click stimuli.

In both genotypes, wave I amplitude was slightly lower at 100 Hz compared to 1 and 20 Hz. In mutants, wave I amplitude tended to slightly increase (9.2%) when the click rate was reduced from 20 to 1 Hz ( $p = 0.89$ , paired t test).

### 3.3.3 *Otof2M* behavioral auditory assessment

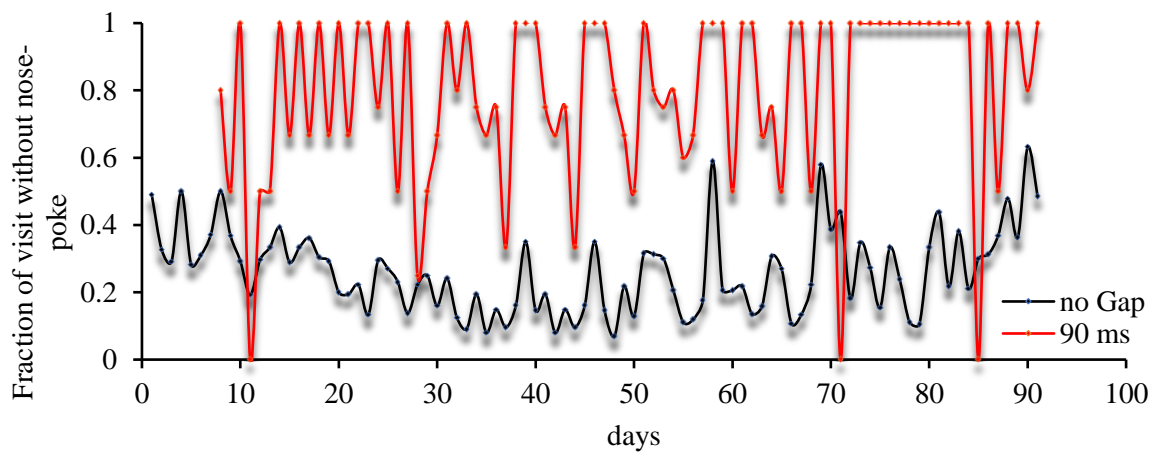
I used the gap detection paradigm in order to assess the temporal precision of synaptic transmission of auditory stimuli in *Otof2M* mutant mice in comparison to WT.

**Experiment overview:** The safe stimulus was continuous broadband noise (safe tone) at 65 dB SPL. The initial conditioned stimulus was the same broadband noise interrupted by 90 ms gaps. Experimental stimuli were broadband noise with 90 ms, 80 ms, 70 ms, 50 ms, 30 ms, 10 ms, 5 ms, 3 ms, 1 ms gaps. The average percentage of visits for each experimental stimulus was 2% (18% for all stimuli). Punishment was applied for all experimental stimuli. Mice were three *Otof2M* mutants, one WT and three heterozygous mice with an age of five to six weeks at the time of introduction to the Intellicage.

**Table 7: Conditioning paradigm during the gap detection experiment.**

Experiment: Gap detection	Habituation	Default	Conditioning I	Conditioning II	Conditioning III	Generalization I	Generalization II	Experiment
Safe stimulus	continuous broad band noise (safe tone)							
Safe, fraction of visits	100%	100%	95%	93%	87.50%	87.50%	87.50%	82%
Conditioned stimuli (Noise with gaps)	-	-	90 ms gap	90 ms gap	90 ms gap	90 & 80 ms gap	90 & 70 ms gap	90 to 2 ms gaps
Conditioned stimuli, fraction of visits	-	-	5%	7%	12.50%	12.50%	12.50%	18%

a)



b)

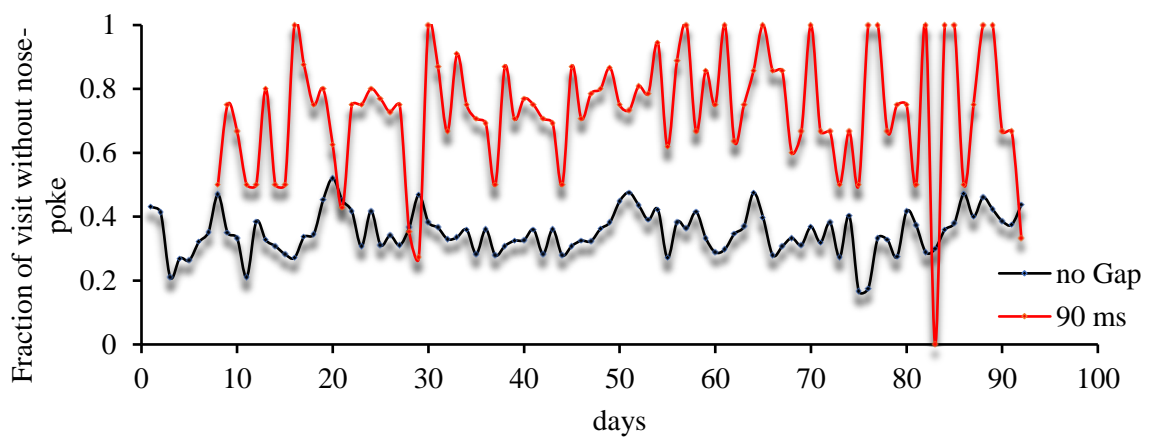


**Figure 23: Examples of a) *Otof2M* WT and b) mutant performance on daily monitoring during training in the Intellicage.**

Representative examples of fraction of visits without nose-poke for safe (black curve) and conditioned (red curve) stimuli are shown in figure 23a and b.

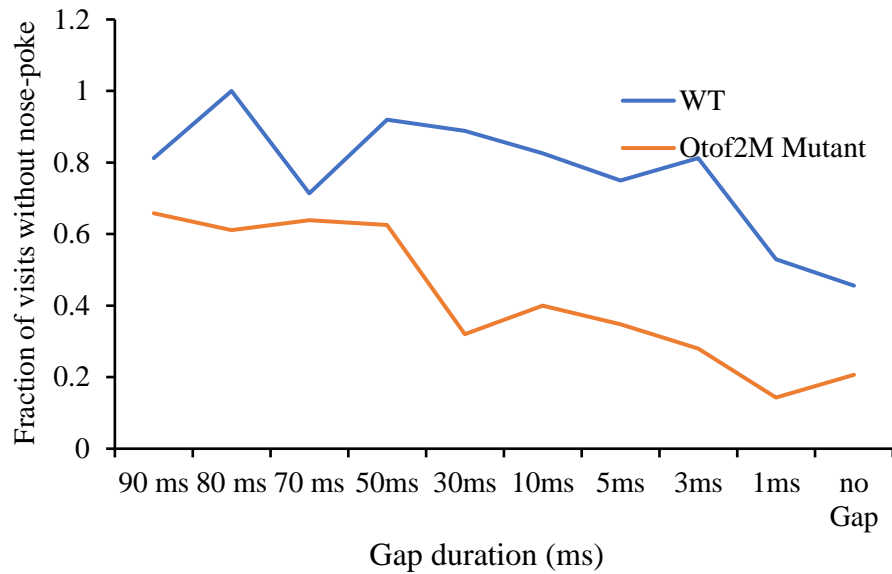


**Figure 24: Example of *Otof2M* WT and mutant mouse performance in a gap detection experiment.**

Figure 24 shows that both *Otof2M* WT and mutant were successfully trained to discriminate between continuous noise and noise interrupted by gaps of different length (90, 80, 70, 50, 30, 10, 5, 3, 1 ms).

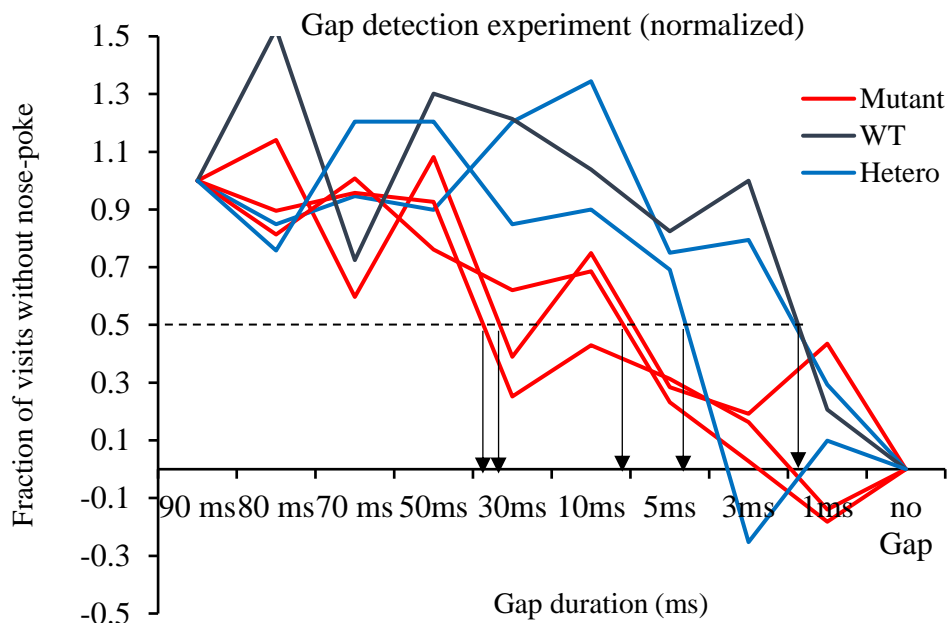


**Figure 25: *Otof2M* mutants in gap detection experiment.**

Each curve represents data from one animal, *Otof2M* mutant (red,  $n = 3$ ), WT (dark blue,  $n = 1$ ) and heterozygous mice (light blue,  $n = 2$ ). Data were normalized to main conditioned (90 ms gap) and safe (no gap) stimuli. Arrows indicate the threshold, interpolated as the intensity at the midpoint between the nose-poke rates for the no gap and 90 ms gap conditions.

The average discrimination between 90 ms gaps and continuous noise was  $31\% \pm 2.7$  (mean  $\pm$  SEM) for *Otof2M* WT/heterozygous mice and  $42\% \pm 3.0$  for the mutants. However, *Otof2M* mutant mice showed lower discrimination abilities for conditioned stimuli with shorter gap length. Figure 25 shows that WT and heterozygous animals show a similar behavior and were able to recognize short gaps with thresholds between 1 and 5 ms. Meanwhile, *Otof2M* mutants had more difficulty recognizing shorter gaps, resulting in thresholds between  $\sim 10$  and 30 ms.

### 3.4 Viral rescue in *Otof*<sup>-/-</sup> mice

Mice used for rescue in this study had either (CD1B6F1) *Otof*<sup>-/-</sup> or (CD1) *Otof*<sup>-/-</sup> background. Animals of both genders were used. AVV viral vectors overloaded with otoferlin were injected through the round window membrane (RWM) at P5. My role in the *Otof* rescue project was to perform ABR measurements in the injected *Otof*<sup>-/-</sup> mice, followed by behavioral hearing assessment in mice that showed successful rescue in ABR. Before I joined the project, ABR was recorded by Nadine Dietrich. I completed and analyzed these datasets.

#### 3.4.1 *Otof*<sup>-/-</sup> rescue assessed by ABR

ABR recorded from mice with two different backgrounds as observed in figure 26. ABR was done at both ipsilateral then the contralateral side of the injection. The injected ear was plugged during contralateral recordings to avoid acoustic cross-talk.

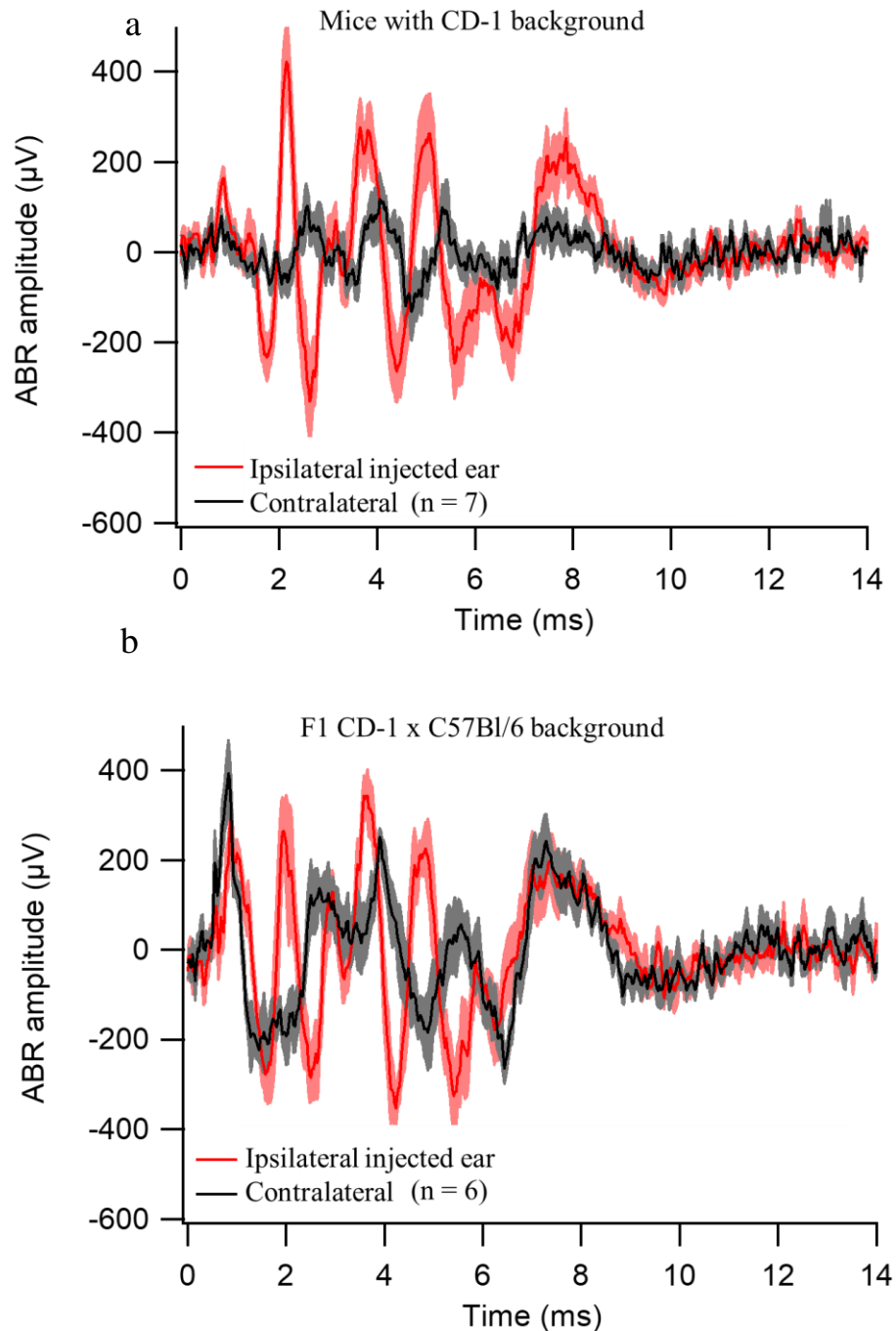


**Figure 26: *Otof*<sup>-/-</sup> rescue: averaged waveforms of ABRs**

*Otof*<sup>-/-</sup> rescue mice with a) CD-1 and b) CD-1 x C57Bl/6 background injected with AAV virus overloaded with otoferlin. Stimulus: 100 dB clicks. Red: injected ears; black: non-injected contralateral ears. Shaded areas indicate the SEM.

ABR were recorded at an age of 5 weeks. In both background strains, viral injection rescued hearing function as assessed by ABRs with average click threshold of 60 dB in ~ 66% of injected mice. Non-injected contralateral ears also showed a partial recovery of ABRs which was likely explained by viral spread as demonstrated by immunohistochemistry

(not shown). It could also be caused by acoustic cross-talk, as our ear plugging method only attenuates the sound by about 30 dB (personal communication, Nadine Dietrich).

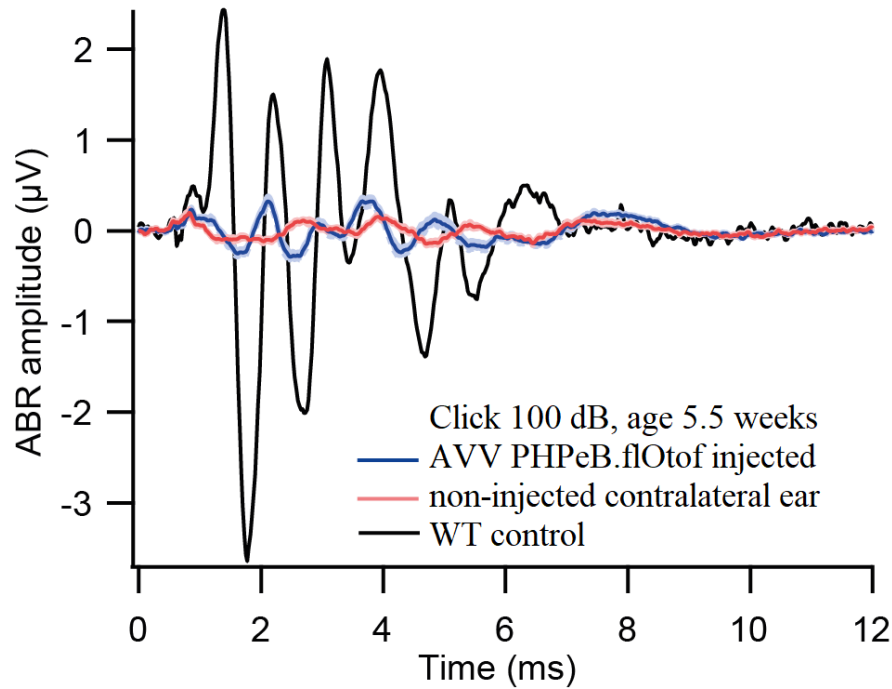


**Figure 27: *Otof*<sup>-/-</sup> rescue mice: comparison to WT**

Grand averages of ABRs evoked by 100 dB click stimulation at 20 Hz as recorded from WT and *Otof*<sup>-/-</sup> rescue mice injected at P5 with AVV PHPeB viral vector overloaded with full-length otoferlin.

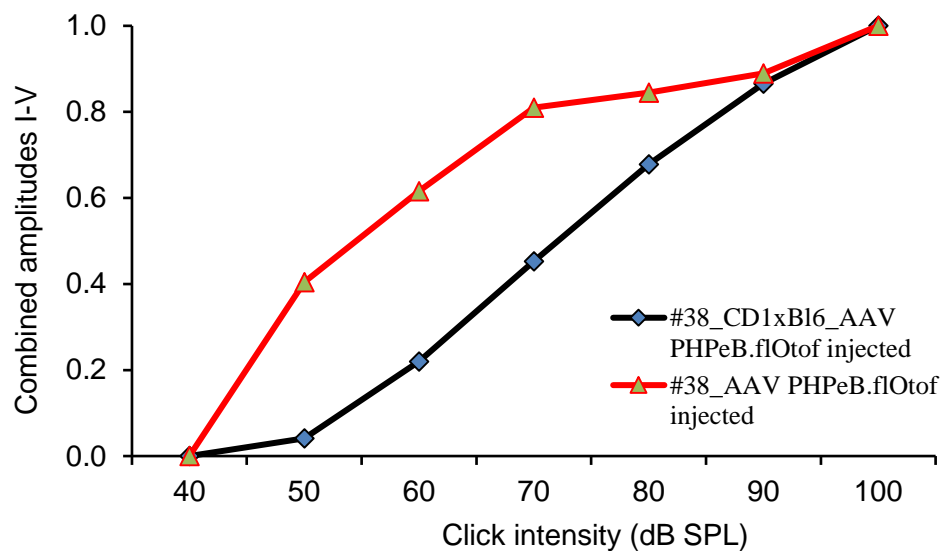
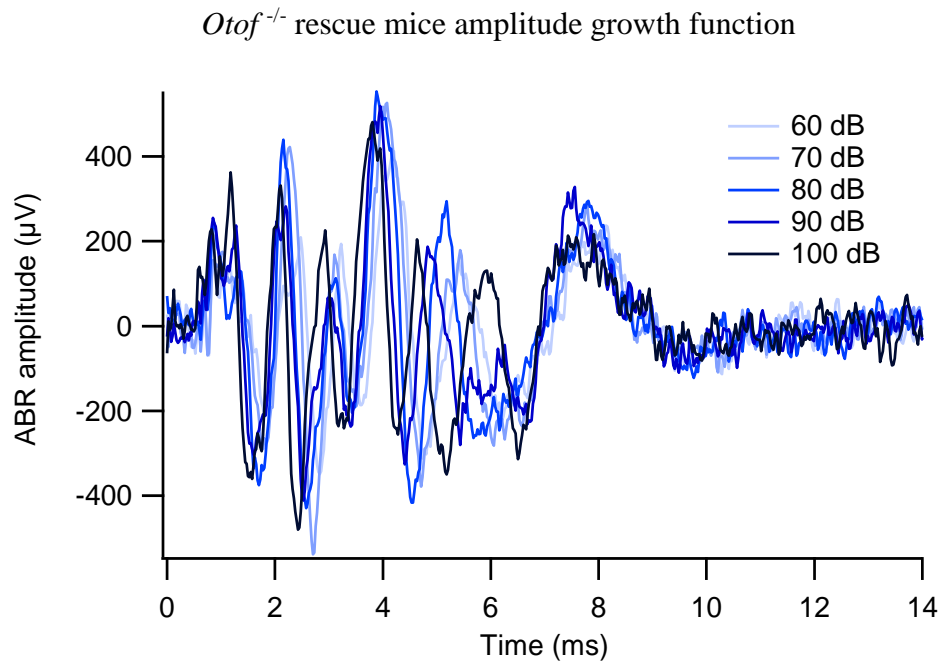


**Figure 28: *Otof*<sup>-/-</sup> rescue: ABR amplitude growth functions**

Normalized summed ABR wave I-V amplitudes to maximum intensity value recorded from ipsilateral injected ears of *Otof*<sup>-/-</sup> rescue (red) and C57Bl6 (black) mice.

*Otof*<sup>-/-</sup> rescue mice showed a partial recovery of ABR waves. Waves I and III remained at a low amplitude, whereas ABR waves II and IV were relatively well-preserved. Compared to WT, ABR latencies were similar, but amplitudes were smaller. Amplitudes were much lower in *Otof*<sup>-/-</sup> rescue mice and exhibited shallower growth functions (figure 28).

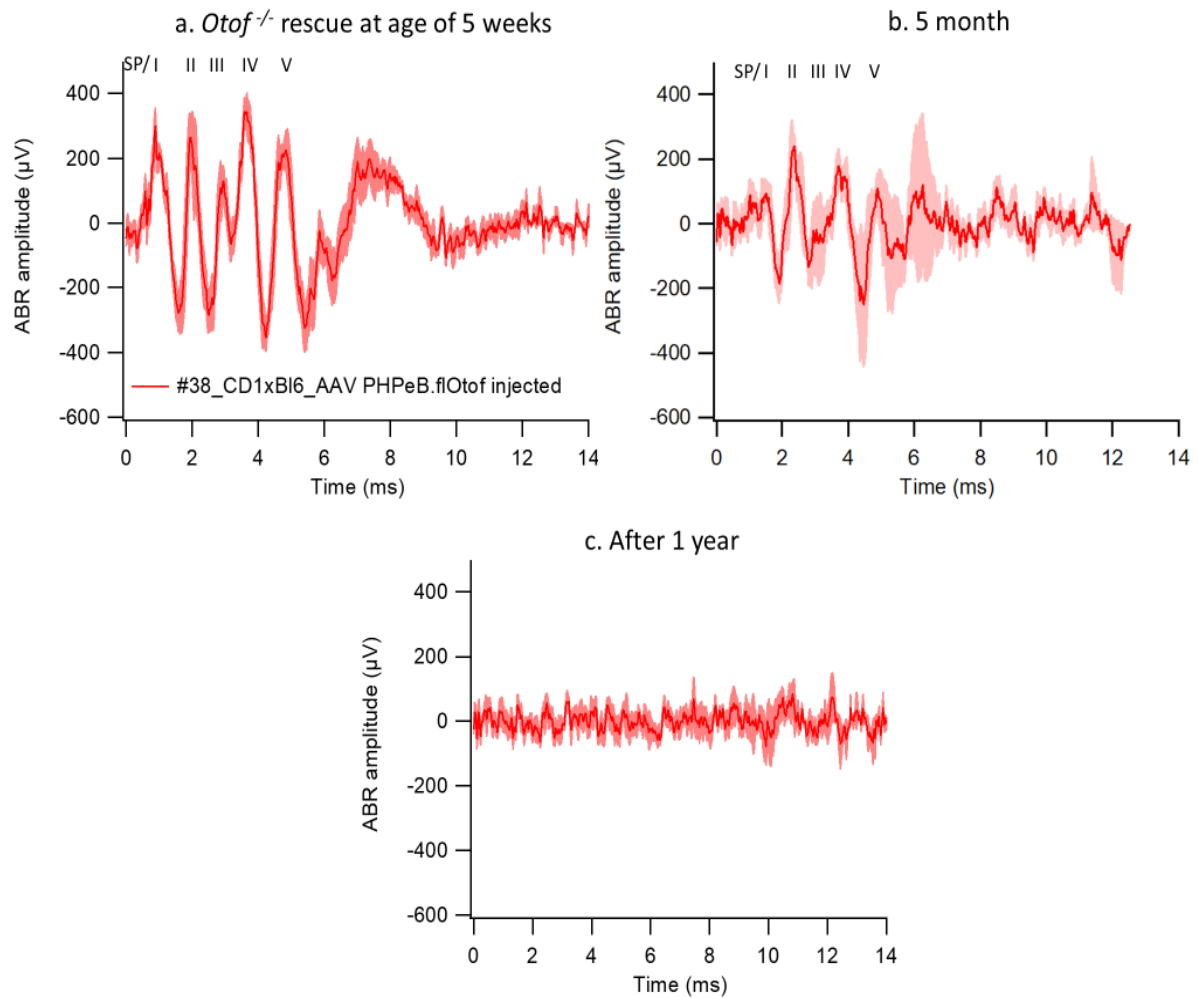
In both genotypes, amplitude growth functions had a more or less sigmoidal shape with saturation starting at 70 dB (figure 28 and 29).



**Figure 29: *Otof*<sup>-/-</sup> rescue: suprathreshold growth of ABR amplitudes.**

Grand averages of ABR waveforms to click stimulation at varying intensities from four *Otof*<sup>-/-</sup> rescue mice.

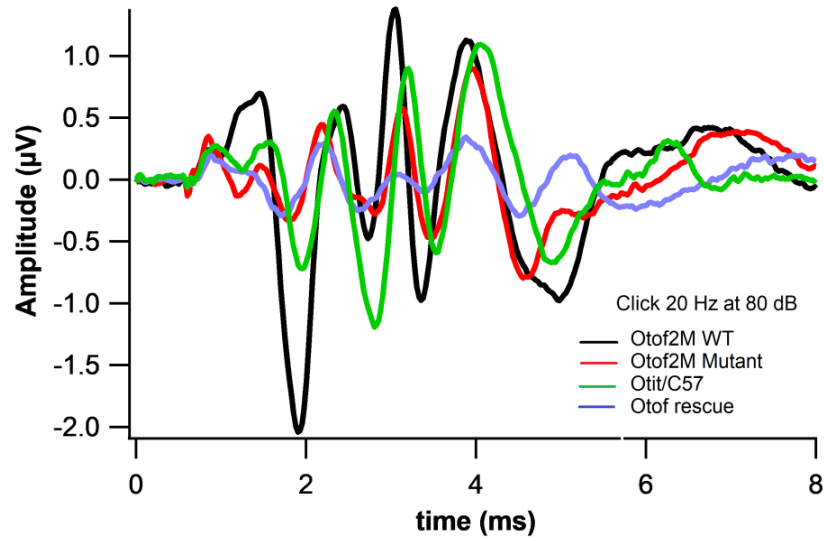
To study whether the otoferlin expression in *Otof*<sup>-/-</sup> rescue mice is transient or long lasting (injected with AAV\_PHP/B #30 or AAV\_PHP/eB.flOtof #38), I also performed ABR recordings after 5 months and 1 year.



**Figure 30: *Otof*<sup>-/-</sup> rescue: duration of ABR rescue.**

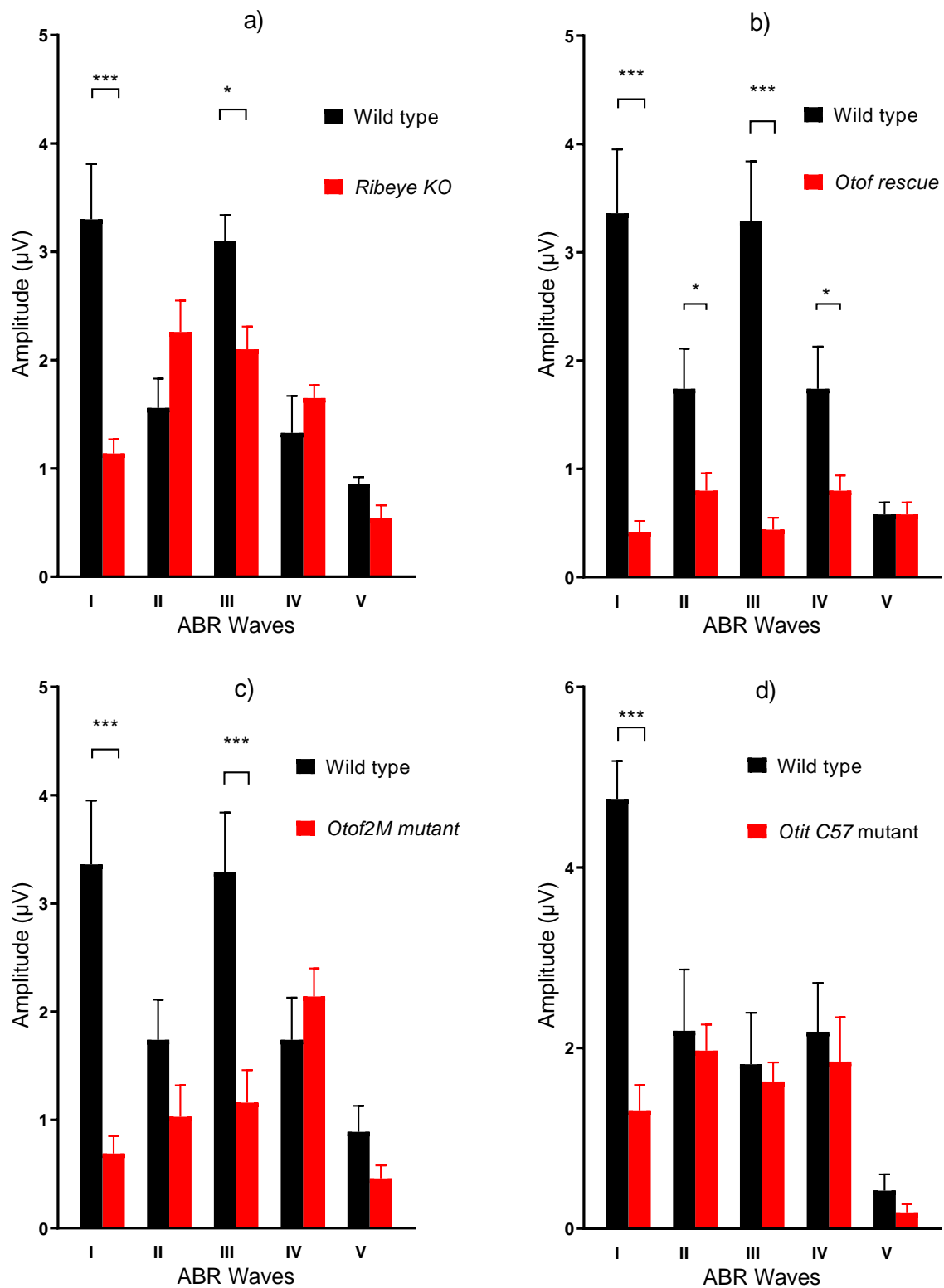
Grand averages  $\pm$  SEM of ABR waveforms evoked by 100 dB SPL click stimuli at 20 clicks/s for *Otof*<sup>-/-</sup> rescue mice at ages of a) 5 weeks ( $n = 10$ ), b) 5 months ( $n = 5$ ) and c) after 1 year ( $n = 5$ ).

Figure 30 shows grand averages of ABRs recorded from *Otof*<sup>-/-</sup> rescue mice at the age of 5-6 weeks (figure 30a) with clearly identifiable ABR waves in response to click stimulation at 100 dB. By age of 5-6 month the amplitude of ABR waves decreased and their threshold increased to  $74 \pm 2.45$  dB (mean  $\pm$  SEM) (figure 30b). After 1 year from injection, there was a complete absence of any reproducible ABR wave (figure 30c) even in two animals, which had previously been tested and showed ABRs. Even the summing potential was absent, suggesting hair cell degeneration.



**Figure 31: Grand averages of ABR waveforms evoked by 80 dB click 20 Hz from WT mice, *Otof2M* mutant, *Otit/C57* and *Otof*<sup>-/-</sup> rescue mice.**

Figure 31 shows ABR waveforms evoked by 80 dB click 20 Hz from *Otof2M* (n = 9), WT (n = 9), *Otof*<sup>I515T/I515T</sup> (*Otit/C57*, n = 5) and *Otof*<sup>-/-</sup> rescue mice (n = 10). The comparison between ABR waveform morphology, latencies and amplitudes across different *Otof* mutant mouse lines, shares similarity in amplitude reduction in ABR wave I and III with well-preserved ABR wave II and IV amplitudes as shown in figure 32.



Asterisks indicate significant amplitude differences (t-test): \* p > 0.05, \*\*\* p > 0.0005.

**Figure 32: Comparison of ABR wave amplitudes in different mutant mouse strains**

a) Ribeye KO, b) Otof rescue mice, c) Otof2M and d) *Otof*<sup>1515T/1515T</sup> (Otit/C57) mutants in comparison to their respective WT littermates.

### 3.4.2 *Otof*<sup>-/-</sup> rescue assessed by behavioral testing

To assess whether the ABR recovery yielded behaviorally relevant recovery of auditory function, I measured acoustic startle responses in subsets of *Otof*<sup>-/-</sup> mice injected with AAV-PHP.B or AAV-PHP.eB AAV with DNA coding full-length otoferlin.

#### Startle reflex

Thirteen *Otof*<sup>-/-</sup> rescue mice were tested in the startle setup at an average age of 2 months. *Otof*<sup>-/-</sup> rescue mice must achieve ABR thresholds at 50 to 60 dB SPL. The chosen stimuli were 12 kHz tone bursts and noise bursts at intensities ranging from 70 to 115 dB with 10 repetitions per intensity. None of the *Otof*<sup>-/-</sup> rescue showed reproducible startle responses.

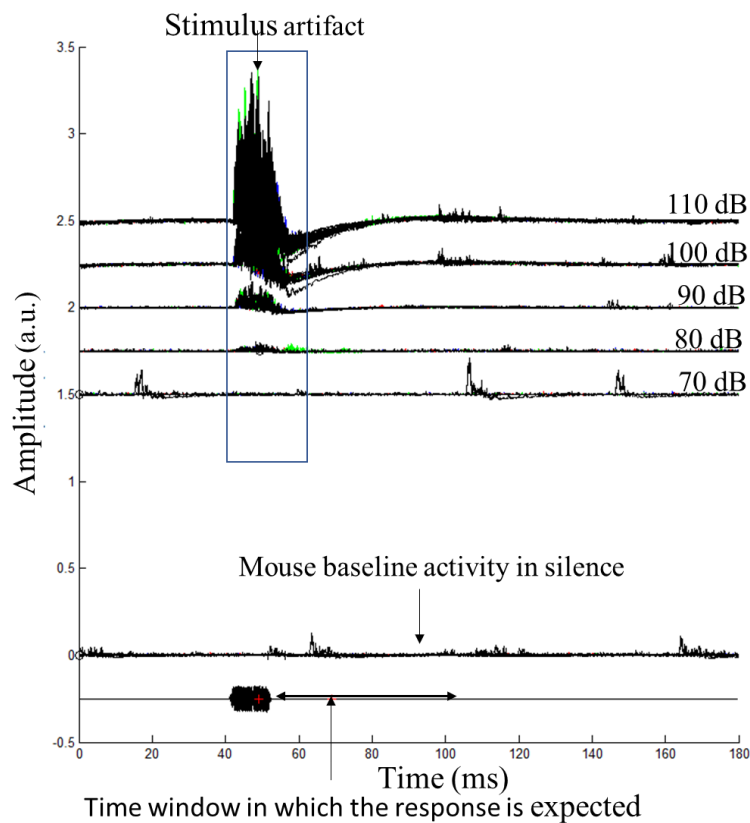


**Figure 33: Representative example of startle response recordings from an *Otof*<sup>-/-</sup> rescue mouse.**

The stimulus used to elicit startle reflexes was white noise of variable intensity levels (110 to 70 dB) which is higher than their ABR threshold. Figure 33 shows the absence of startle responses in an *Otof*<sup>-/-</sup> rescue mouse, although it had an ABR threshold at 50 dB SPL.

**Tone detection experiment (Intellicage):**

The main target of this experiment was to study whether the *Otof*<sup>-/-</sup> rescue mice injected with AAV-PHP.B and/or AAV-PHP.eB AAV loaded with otoferlin can behaviorally perceive sound stimuli. The experiment was designed to run for a short period since ABR rescue tended to decline with time as previously demonstrated in the ABR section. Click trains at 100 dB SPL were used as a conditioning stimulus and silence was the safe stimulus. Clicks were chosen because the acoustic response to these stimuli was clear as concluded from ABR data. WT mice (n = 6) showed high discrimination ability (~ 50%) (figure 34). Five out of six female *Otof*<sup>-/-</sup> rescue were capable of discriminating between sound and silence with 30% discrimination (figure 34).

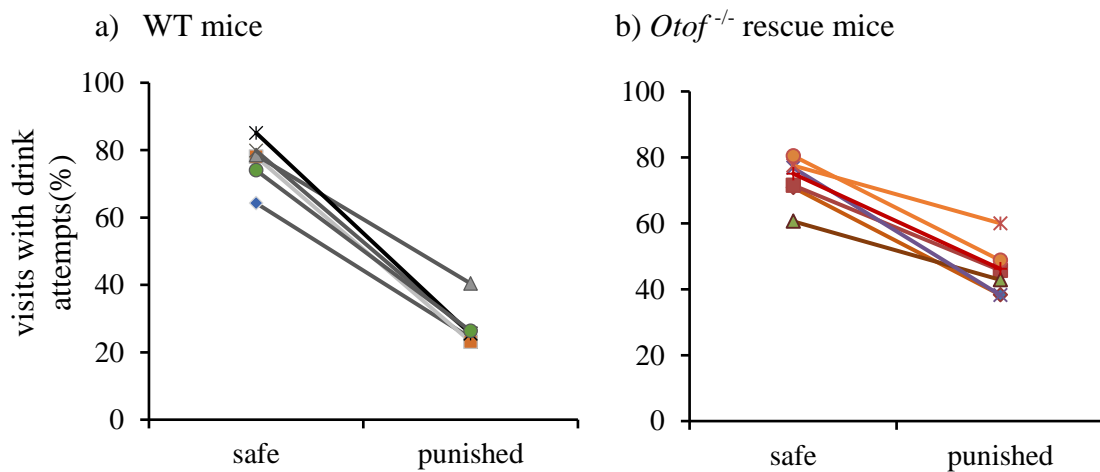
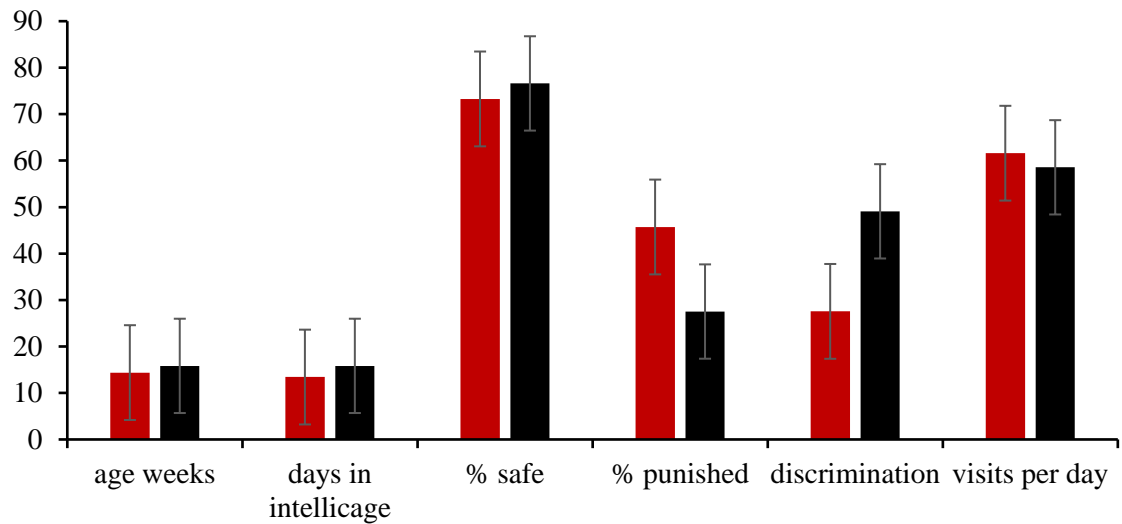


**Figure 34: *Otof*<sup>-/-</sup> rescue: sound detection in the Intellicage**

Percentage of visits with attempt to drink water during safe (silence) and conditioning stimuli in tone detection experiment in: a) WT mice and b) *Otof*<sup>-/-</sup> rescue mice.

**Table 8: Comparison between *Otof*<sup>-/-</sup> rescue with age and sex matched WT mice.**

	<i>Otof</i> <sup>-/-</sup> Rescue		WT Control	
	Mean	SEM	mean	SEM
Age (weeks)	14.4	2.4	16	2.6
Days in Intellicage	13.4	3.8	15.8	0.2
% Safe	73.3	2.5	76.6	2.9
% Punished	45.7	2.8	27.5	2.6
Discrimination	27.6	3.0	49.1	3.5
Visits per day	61.6	7.1	58.6	7.3
Total number of visits	804.9	222.6	860.5	120.4

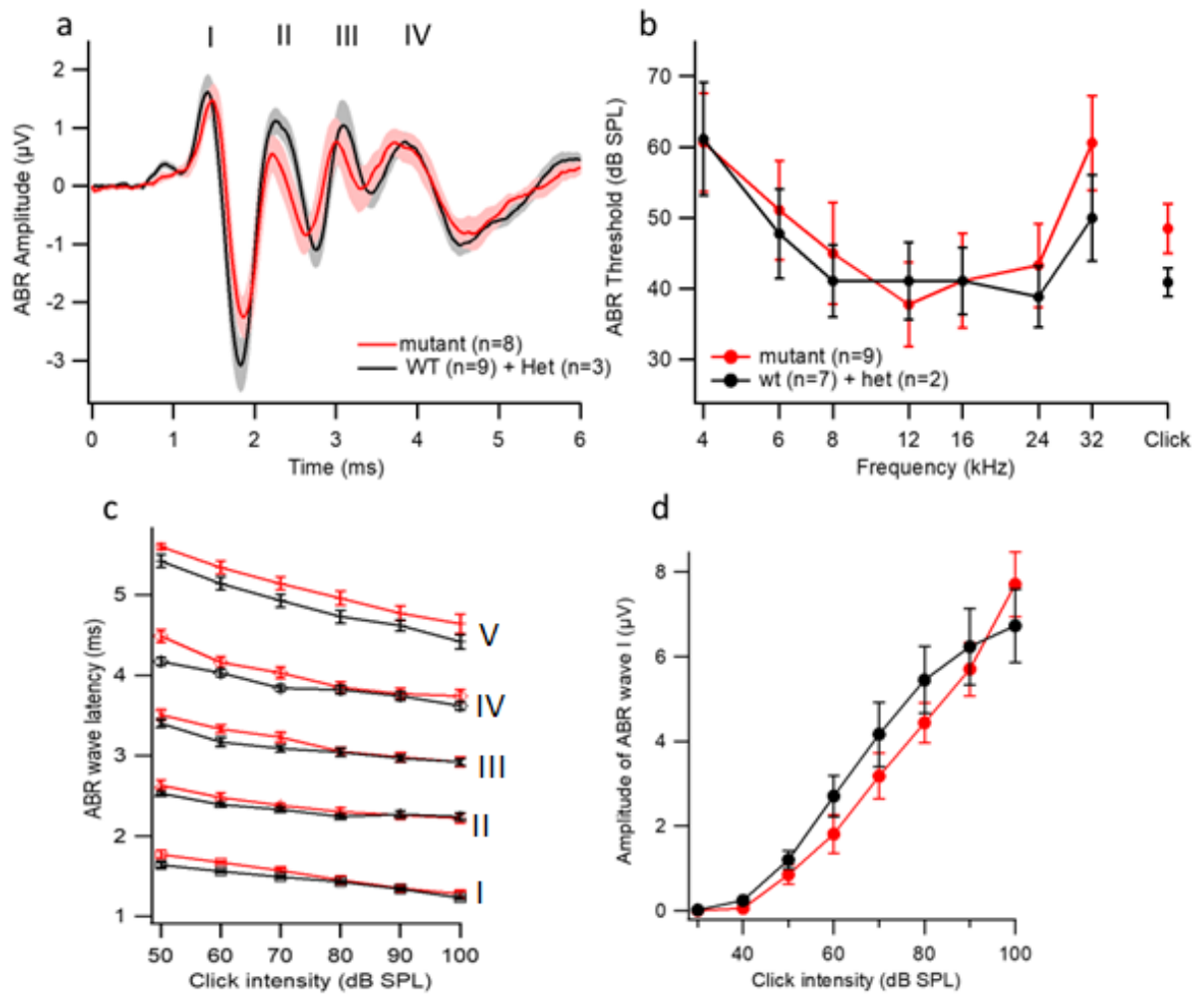


**Figure 35: Comparison between WT (black) and *Otof*<sup>-/-</sup> rescue mice (red).**

Both the WT and *Otof*<sup>-/-</sup> rescue mice had a comparable age, duration of training in Intellicage, and almost the same number of visits per day. However, WT mice had better discrimination (~ 50%) than *Otof*<sup>-/-</sup> rescue mice (~ 30%) as also shown in table 8 and figures 34 and 35.

### 3.5 Auditory phenotype of *CAPS* mutant mice

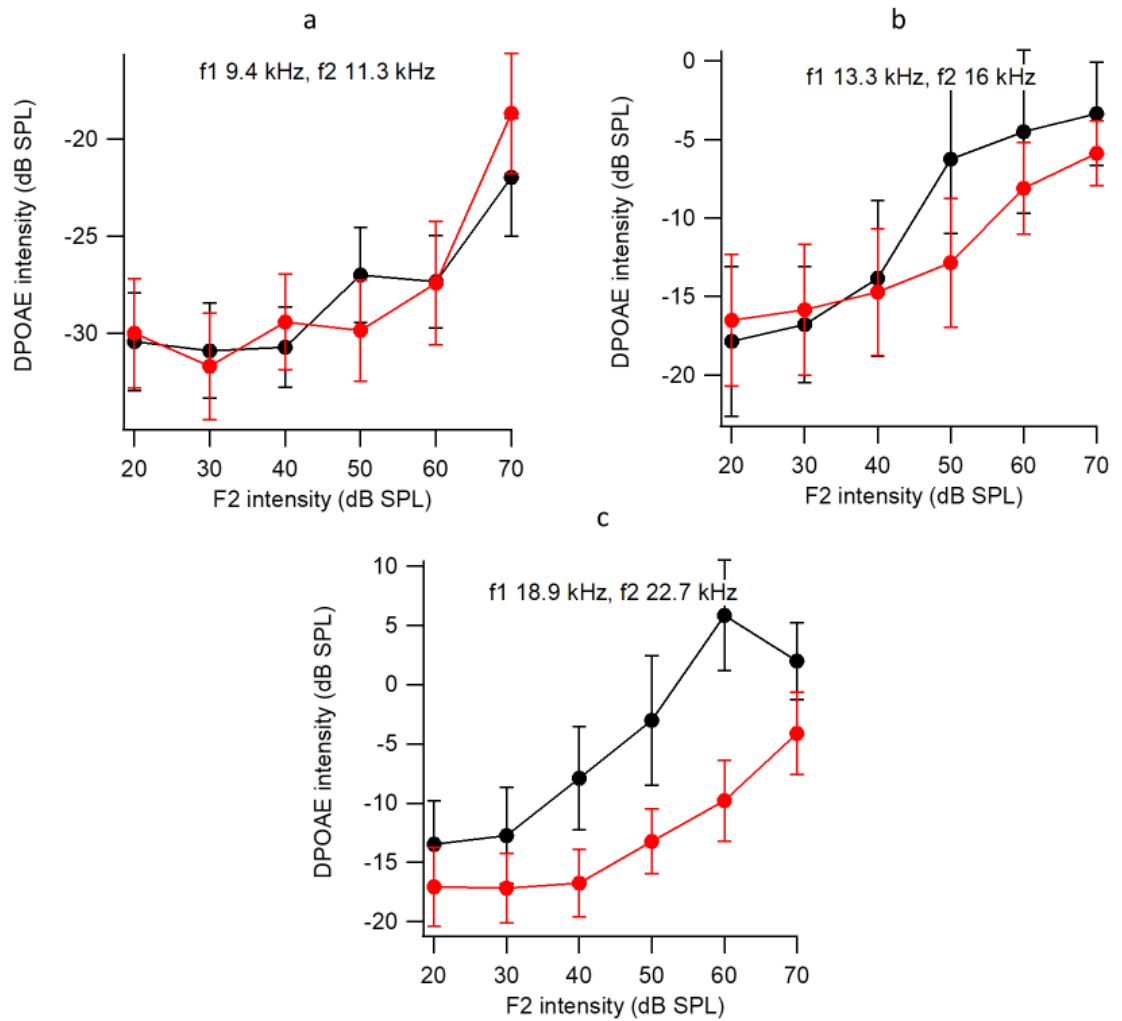
*CAPS* mutation (deletion of Exon 2) was identified in a female patient suffering from bipolar disorder. A mouse model carrying the same mutation was generated. Those mice showed abnormal startle reflex with acoustic stimuli so they were referred to our auditory physiology group for auditory assessment. ABR, DPOAE and ASSR were done for those mutants as shown in figure 36, 37 and 38.

3.5.1 *CAPS* ABR

**Figure 36: *CAPS* mice have normal ABRs:**

a) *CAPS* mutant (red) and WT (black) grand averages of ABR waveforms to 80 dB SPL clicks, b) ABR threshold, c) ABR wave I-V latency and d) wave I amplitude growth function. Shaded areas/error bars indicate the SEM.

Figure 36a shows well preserved ABR wave morphology in *CAPS* mutant as compared to their WT control littermates. Figure 36b shows no alteration in ABR threshold in *CAPS* mutant mice. Figure 36c illustrates a slight latency shift in *CAPS* mutant for all ABR waves at lower intensities, however, a slight delay of waves I, III, IV, V ( $p < 0.05$ , two-way ANOVA for 50-100 dB). Figure 36d shows a comparable ABR wave I amplitude growth function in *CAPS* mutant mice.

3.5.2 *CAPS* DPOAE

**Figure 37: DPOAE elicited in *CAPS* mutant mice and WT littermates.**

DPOAE test is a direct measure of cochlear amplification. As expected, different frequency stimulation showed no significant difference between *CAPS* mutant and their WT littermates as shown in figure 38 (a, b and c) i.e., outer hair cell function and cochlear amplification are spared in the *CAPS* mutant mice arguing against a role for *CAPS* protein in the outer hair cells ( $p > 0.05$  for all frequency combinations, two-way ANOVA; Figure 37).

### 3.5.3 CAPS auditory steady state responses (ASSR)

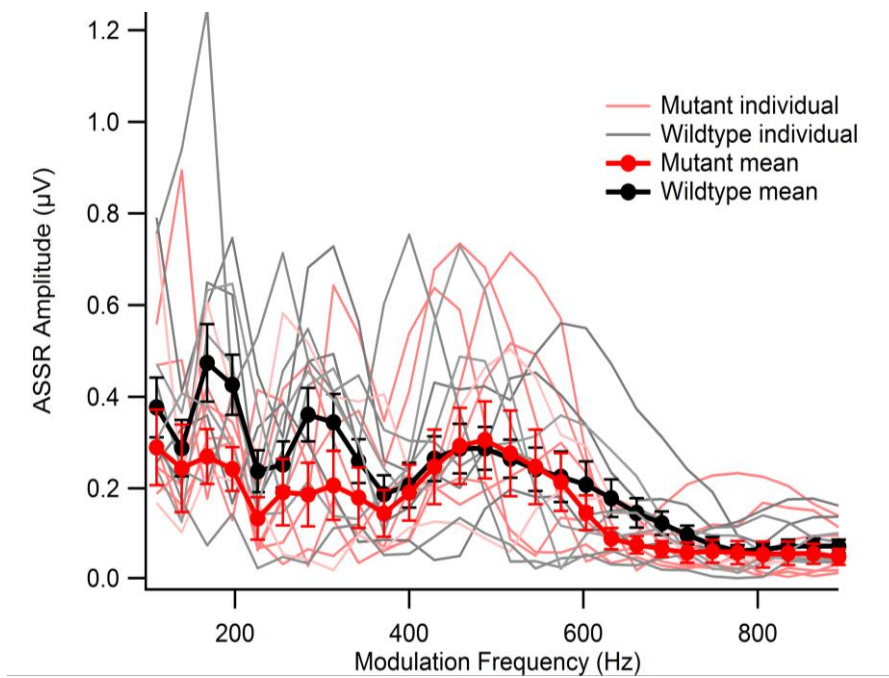


**Figure 38: ASSR in CAPS mice**

Individual (grey/pink) and mean (black/red,  $\pm$  SEM) modulation transfer functions (ASSR amplitudes for varying modulation frequencies) for CAPS mutant and WT mice.

ASSR data were collected from WT/Het ( $n = 13$ , black) and CAPS mutant mice ( $n = 8$ , red). They were recorded in response to an amplitude-modulated sine wave with a carrier frequency of 12 kHz and a stimulus intensity of 80 dB SPL.

ASSR were present in all genotypes with no obvious differences. ASSR amplitudes were slightly lower for modulation frequencies between 110 and 400, which might be related to abnormal pulse train responses from central neurons (unpublished data by Dennis Nestvogel). The reduction in ASSR amplitudes over all frequencies in mutants was significant ( $p = 0.0001$ , 2way ANOVA). Post hoc Sidac test showed no significant reduction for individual modulation frequencies. ASSR apparent latencies calculated from phase information of modulation transfer function were not significantly different ( $4.7 \pm 0.6$  ms in 7 KO vs  $4.5 \pm 0.5$  ms in 9 Het/WT,  $p = 0.8635$ , unpaired student's t-test).

## 4 Discussion

Human auditory synapto-/neuropathy or auditory neuropathy spectrum disorder (ANSD) are terms that refer to a disease condition in which sound perception is compromised even though active cochlear amplification is functioning normally. In routine audiometric testing, speech perception is typically much worse than what is expected from pure tone thresholds. ABR and auditory reflexes are usually absent (Starr 1996; Strenzke 2009). Outer hair cell functions, as measured by otoacoustic emissions or cochlear microphonic potentials are at least initially preserved. However, there is abnormal signal transmission from the IHC synapse to the brainstem as detected by the altered ABR response and difficulty in speech perception especially in the presence of noise (Moser und Starr 2016).

ANSD includes lesions that may impair auditory synapses (auditory synaptopathy) or the auditory nerve (auditory neuropathy). ANSD may be due to pre-synaptic causes affecting the release of glutamate in hair cells, synaptic causes or postsynaptic causes affecting action potential generation in ANFs (Shearer und Hansen 2019).

Auditory synaptopathy cannot be distinguished clinically from auditory neuropathy except by confirmation of its underlying pathological mechanism, e.g., by genetic testing. In humans, synaptopathy could be related to several factors like noise exposure or degenerative processes during aging. In routine pure tone audiometry, synaptopathy may not be detected, thus many patients might suffer from synaptopathy without being diagnosed (Kujawa und Liberman 2015). In rodents, a reduction in ABR wave I can reflect a reduced number of functioning synapses (Kujawa und Liberman 2009) or a reduced synchronicity of ANF firing (Buran et al. 2010; Strenzke et al. 2016; Jean et al. 2018). In humans, the absolute ABR wave I amplitude is small and highly variable. It is thus not optimal to be used in clinics as an indicator for synaptopathy (Trune et al. 1988). Behavioral auditory assessment may be an alternative diagnostic tool for detection and proper management of patients with ANSD but needs to be better established. Individuals with ANSD typically have deficits in the temporal precision of the encoding of acoustic signals resulting in an impairment of speech comprehension and sound localization. Notably, deficits in ANSD are more prominent in tests for temporal precision of coding for instance low frequency pitch perception, gap detection and interaural time differences (Zeng et al. 2005).

ABR is driven by synchronous neural activity in the auditory pathway elicited by the onset of short acoustic stimuli. However, this process is not necessarily identical to the actual perception of sound stimuli. In case of malfunctioning temporal precision of action potential generation in individual auditory nerve fibers, the ABR thresholds can appear worse than the perceived threshold (Buran et al. 2010). On the other hand, ABRs may be better than sound perception when the defect does not involve the onset response but only the encoding of continuous sounds. When the ABR amplitudes or latencies are affected but still measurable, both the mechanism and the actual extent of hearing impairment remain unclear. This applies in particular to disorders of synaptic transmission from the hair cell to the auditory nerve fibers leading to disruption of sound encoding (Chambers et al. 2016).

## 4.1 Auditory phenotype of Ribeye KO mice

Ribbons support synaptic vesicle replenishment, promote a greater availability of synaptic vesicle release sites, and allow the clustering of calcium channels at the AZ (Moser et al. 2019). Ribeye protein is the main constituent of ribbon synapse in cochlear IHCs. IHCs of the Ribeye KO mouse line have no ribbon structure, allowing us to study the function of ribbon and its role in sound encoding of the IHC synapse. Ribeye KO mice displayed normal OHC amplification as shown by normal DPOAEs. Interestingly, they form and maintain a normal number of synapses although they are devoid of ribeye. There is no evidence of any compensatory proteins that take over ribeye function (Becker et al. 2018). Unexpectedly, Ribeye KO mice have a milder hearing deficit phenotype than the Bassoon mutant mice. Ribeye KO mice exhibited a 10 dB threshold shift in ABR recordings with a significant reduction in Wave I and III amplitude but no latency shift. SGNs of Ribeye KO mice have slightly elevated ABR thresholds (Jean et al. 2018) despite intact cochlear amplification. Thus, the ABR wave I amplitude reduction reflects an impairment in SGN activation.

The analysis of ABR traces recorded from Ribeye KO revealed a significant reduction in wave I and III (Figure 32), reflecting an impairment in signal transduction at the primary auditory synapse and SOC. The results from the behavioral threshold experiment in quiet for the Ribeye KO mice were very comparable to their WT littermates and revealed consistent threshold shifts that are mild (Figure 12). Remarkably, noise had a masking effect for the WTs and heterozygotes: behavioral threshold in noise increased slightly in parallel with the noise level. On the contrary, Ribeye KO mouse showed a severe deterioration in discrimination performance when noise was introduced as illustrated in Figure 14 and Figure 15. Ribeye KO mice were unable to discriminate between safe (noise) and conditioned

stimuli (pure tone against noise) even at high sound intensities exceeding the noise level. Thus, sound perception in Ribeye KO mice seemed to be severely impaired by the introduction of background noise. This can likely be attributed to the spiral ganglion neurons in mice lacking ribeye exhibiting reduced EPSCs in response to sustained stimulation (Jean et al. 2018). Noise as a state of continuous stimulation of the inner hair cell ribbon synapse increases the rate of vesicle release and replenishment, which causes exacerbation of deficits in synapses devoid of ribeye.

## 4.2 Auditory phenotype of *OtofQX* mice and *Otof2M* mutant mice

The multi-C2 domain protein otoferlin is essentially required for exocytosis at the inner hair cell ribbon synapse (Roux et al. 2006; Pangršič et al. 2010; Strenzke et al. 2016). Several mutations have been identified in the *OTOF* gene which in most cases leads to profound prelingual deafness DFNB9 (Varga et al. 2003). However, some patients have residual hearing with an auditory synaptopathy phenotype. To find out whether *OtofQX* and *Otof2M* mutant mice have an auditory phenotype, the first step was to record and study their ABR, which reflects the synchronized response activity across the auditory pathway.

### 4.2.1 Electrophysiological auditory assessment

*OtofQX*<sup>-/-</sup> mice showed an absence of ABR waves even to high intensity sounds (100 dB SPL) with preservation of summing potentials (SP) which usually start to appear at high intensities, i.e. 70 to 80 dB SPL and probably reflect inner hair cell receptor potential (Zheng et al. 1997). In case of the otoferlin mutation, summing potentials are intact since the main impairment affects synaptic transmission (Figure 20). The hearing disorder in *OtofQX* mutant mice resembles the phenotype described in human patients and in *Otof* KO mice (Roux et al. 2006). This mouse line was generated for preclinical trials of gene therapy.

*Otof2M*<sup>-/-</sup> mice exhibited reproducible and repeatable ABR waves with a moderate to severe hearing deficit. *Otof2M* exhibited poor ABR morphology and reduced ABR wave I and III amplitudes whereas waves II and IV were mostly normal. Reduction of wave I amplitude across different sound intensity levels might be related to deficit in sound encoding at SGNs with central compensatory mechanisms occurring at the higher order neuron regions in brainstem to the cortex. In contrast, all ABR wave latencies appeared to be unaltered in *Otof2M* mutants (Figure 21).

#### 4.2.2 *Otof2M* behavioral auditory assessment

*Otof2M* mice were successfully trained for a gap detection experiment carried out in Intellicage (Figure 23). In agreement with documented gap thresholds in CBA/J WT mice of 2 ms (Radziwon et al. 2009), our WT mice were capable of identifying gaps as small as 2 ms (Figure 24 and Figure 25Figure 24). In contrast, *Otof2M* mutant mice could not recognize gaps shorter than 3-30 ms. *Otof2M* mutant mice displayed similar results to *Otof*<sup>I515T/I515T</sup> mice whose gap detection thresholds were also poor (Strenzke et al. 2016). Patients with the I515T point mutation have a mild degree of hearing loss affecting the lower frequency region and poor speech comprehension especially in noisy places. Their hearing loss profile deteriorates and reaches severe to profound loss upon elevation of their basal body temperature above 38.1 °C (Varga 2006). *Otof*<sup>I515T/I515T</sup> mutant mice exhibited a strong reduction in sustained exocytosis during prolonged stimulation, supporting the essential role of otoferlin for RRP replenishment at IHC ribbon synapse. This explains why patients with *Otof* mutation have auditory fatigue (Wynne et al. 2013).

Such weakening of gap detection ability in *Otof*<sup>I515T/I515T</sup> mice was explained by the reduction in spike rate adaptation together with slower recovery of the onset response (Strenzke et al. 2016) which was explained by reduced expression of otoferlin leading to delayed replenishment of the synaptic vesicle pool. Further studies are required to determine the otoferlin expression level in *Otof2M* mutant IHCs and/or other possible functional details specific to the *Otof2M* point mutation.

### 4.3 Partial *Otof*<sup>-/-</sup> rescue

Otoferlin-related auditory synaptopathy DFNB9 is an important candidate disorder for gene replacement therapy. The process of gene delivery can utilize viral or non-viral vectors (nanoparticles or exosomes). Viral vectors can include adeno-associated viruses (AAVs), adenoviruses (AdVs) and retroviruses (Pietola et al. 2008). However undesired immune responses against the virus can occur which could affect long-term transgene expression.

Currently, numerous studies are attempting to improve the percentage of otoferlin expression into the IHCs. The choice of virus vector (packaging size, safety profile, cloning capacity of the vector), route of delivery, injection procedures and the age at the time of injection are all important factors which could immensely affect the outcome of the rescue (Ren et al. 2019). In our project, we used a single adeno-associated viral vector, which was overloaded with full-length otoferlin.

I studied the ABR of *Otof*<sup>-/-</sup> mice after they have been injected by AAV-PHP.B or AAV-PHP.eB viruses carrying DNA coding full-length otoferlin. *Otof*<sup>-/-</sup> mice were injected through the round window at early postnatal days (P5). ABR results (illustrated in Figure 26 and Figure 27) show partial restoration of hearing function in *Otof*<sup>-/-</sup> rescue mice. The AAVs drove specific expression of otoferlin in IHCs as proven by immunofluorescence labeling and by polymerase chain reaction. ABR recordings showed reproducible and repeatable ABR waves with clear distinguishability of the ABR waves II and IV and partial restoration of wave I and III achieving a click ABR threshold of ~ 60 dB SPL in 66 % of *Otof*<sup>-/-</sup> injected mice. However, all ABR waves in *Otof*<sup>-/-</sup> rescue mice showed significant amplitude reductions (Figure 32).

Even though the virus injection was executed unilaterally, ABR waves were detected upon recording from the contralateral side of injection as shown in Figure 26 and Figure 27. ABR waves recorded from the contralateral side of injection have a higher threshold and poor morphology when compared to the ipsilateral side. They may either be attributed to crossing of virus to the opposite side of injection or to acoustic cross-talk. Sounds delivered to the ear in the free field reach the contralateral ear, and as ear plugging during recordings yields only about 30 dB attenuation. ABR generated in the virus-injected contralateral ear may be larger than those from the deaf non-injected ear. Further manual destruction of the middle/inner ear has a high morbidity and the cochlea cannot be used for in vitro studies afterwards.

Similar partial rescue results were also achieved in Al-Moyed et al. (2019) at the ipsilateral side of injection, but here, crossing of the viral vector was excluded by absence of otoferlin expression in the contralateral side of injection.

Despite partial rescue, ABR amplitudes in rescued *Otof*<sup>-/-</sup> mice were much lower than in WT controls and amplitude growth functions were much shallower. In both genotypes, saturation of the ABR amplitudes occurred at similar intensities (Figure 28 and Figure 29).

*Otof*<sup>-/-</sup> rescue mice were successfully conditioned in Intellicage for tone detection task where five out of six rescued mice were capable of detecting click-trains at 100 dB with ~ 30% discrimination as shown in Table 8 and Figure 34 and Figure 35.

In contrast, none of the virus-rescued mice showed reproducible startle responses (Figure 33), a finding which was not completely unexpected as the otoferlin expression was not uniformly distributed across all IHCs (~ only 30% of the IHCs were transduced by the

viral vector showing otoferlin expression after immunofluorescence labelling). In addition, the rescue was done only unilaterally and not in both ears. Startle reflex results agreed with (Akil et al. 2012) who stated that KO mice lacking the vesicular glutamate transporter 3 vGlut3 with successful viral rescue did not show startle responses after unilateral rescue but startled only when the rescue was performed bilaterally.

ABR recordings from *Otof*<sup>-/-</sup> rescue mice showed that gene therapy of DFNB9 using a single overloaded AAV vector is feasible. This might reduce the complexity of gene transfer when compared to dual-AAV approaches. However, ABR amplitudes tend to decline with age. Possible reasons might include a decline in virus expression, decline in otoferlin expression independent of the virus, degenerative changes in *Otof*<sup>-/-</sup> mutant or age-dependent decline in ABR amplitudes independent of otoferlin or virus treatment.

#### 4.4 Auditory phenotype of *CAPS* mutant mice

CAPS1 promotes the priming process, which is essential for vesicle fusion at conventional CNS synapses (Farina et al. 2015). However, at inner hair cell ribbon synapse, vesicle exocytosis is SNARE-independent with no indication of CAPS expression or function (Vogl et al. 2015). *CAPS1 exon2* deletions serve as a novel mouse model for a complex human phenotype in patients suffering from bipolar disorder. The mutation does not affect the normal ABR morphology, thresholds and amplitudes when compared to their WT littermates. This suggests no affection of synchronized spiking in response to sound onset recorded from the auditory nerve (wave I) and auditory brainstem (Figure 36).

As expected, analysis of the DPOAE revealed no significant changes in *CAPS1* mutant mice reflecting preserved active cochlear amplification in mice lacking CAPS1 (Figure 37). Still, there was a reduction in ASSR amplitudes at lower modulation frequencies (110-400) (Figure 38). Since ASSR is a response to continuous stimulation, such an ASSR phenotype might be related to the reduction in tonic release or to stronger adaptation in central neuron as shown in hippocampal neurons *in vivo*. Nestvogel recorded that phasic release (correlating to vesicle release) is not altered, but the tonic release (correlating to vesicle replenishment) is impaired (Nestvogel 2017) in the same mutants. He also noted that the first pulse response was not altered, which is consistent with our normal ABR data in *CAPS* mutant mice. However, the stronger fatigue is consistent with our ASSR data. The significant delay for ABR waves I, II, III and V when pooling 50 to 100 dB together with the reduction in the ASSR amplitude raise the question of possible existence of CAPS protein in certain neurons

in brainstem across the auditory pathway. Further immunostaining of AVCN and olivary complex would be required to check if CAPS is expressed there or not.

## 4.5 ABR waveform morphologies in mouse models of auditory synaptopathy

ABR includes five main waves. The origin of each single ABR wave cannot be clearly demarcated. There is no definite one to one correlation between each ABR wave and the click evoked activity in either station of the auditory trajectory. ABR waves could originate from parallel distributed independent anatomical sources sharing the same temporal onset of firing (Land et al. 2016). This is brought by the complex interconnected afferent and efferent projections of the ascending and descending auditory pathways. (Buchwald und Huang 1975)) suggested that the main ABR generator for wave I is the auditory nerve, for wave II the cochlear nucleus, for wave III the region of the superior olivary complex, for waves IV and V the region of lateral lemniscus and/or inferior colliculus. They also suggested that the first two ABR waves are produced before any crossing or decussation occurs in the central auditory pathways.

Amplitudes of wave I and III were reduced in several mutant mouse lines suffering from auditory synaptopathy (*Ribeye*, *Otof2M*, *Otof*<sup>1515T/1515T</sup> and *Otof* rescue) as seen in (Figure 32). Wave I reflects rapid (fraction of milliseconds) and extremely precise synaptic release at inner hair cells ribbon synapses (Jean et al. 2018). Meanwhile, wave III reflects transmission at the superior olivary complex, which is an important station for coincidence detection that transmits acoustic temporal and intensity information from both sides allowing accurate sound localization through inter-aural time difference and inter-aural correlation (Franken et al. 2014).

Wave II and wave IV reflect transmission at cochlear nucleus and inferior colliculus, which show large heterogeneity in their neuronal composition. Here, every neuronal subtype may have different neuronal response properties and receive inputs from several stations, which allows for central compensatory mechanisms augmenting their response and sparing significant visible alterations in wave II and IV as recorded externally with ABR.

## 4.6 Behavioural assessment of hearing function in mice

Rodents are commonly the preferred animal model in auditory research as their ears show close resemblance to human inner ear structure and function. Genetic modifications

can be achieved easily, breeding is relatively fast and cost-effective, and they can be readily used for pre-clinical testing of new treatment methods.

It is relatively easy to obtain a behavioral pure tone audiogram in humans; however, this is a challenging and time-consuming process in animal models. Therefore, hearing in mice is preferentially assessed by electrophysiological methods such as ABR rather than by psychophysical methods.

A subjective hearing threshold is always required for auditory assessment of human patients in parallel to objective electrophysiological methods as it completes the auditory information required for diagnosis of certain auditory pathologies such as synaptopathies. Behavioral hearing threshold can differ markedly from the ABR threshold in ANSD. Chambers and colleagues showed that even in mice with 90% loss of the auditory nerve that lead to absent ABR and startle responses, the hearing thresholds determined by behavioral measurement remained normal (Chambers et al. 2016).

It is fundamental to establish standard operating procedures to be used as tools for characterizing the behavioral auditory phenotype in the newly selectively generated transgenic mouse models. Those tests should be designed to provide reliable, reproducible and replicable results of the process under investigation. Behavioral auditory testing can provide us with a broader scope for studying different auditory functions, which could not be assessed by electrophysiological methods. Moreover, behavioral methods can improve our understanding for the role of different proteins involved in the process of hearing.

During my studies, the main goal was to optimize and improve the methods used for behavioural assessment of hearing in mice in our lab, aiming to have a standard method that can be used for behavioural characterisation auditory phenotypes for existing or newly generated mouse lines. This would then improve our understanding for the behavioural auditory role of various proteins involved in sound transmission at the inner hair cell ribbon synapse.

Regarding the Intellicage system, I made some modifications in Intellicage housing environment; increasing the proximity of cage to water corner which facilitated mice access to the water corner; decreasing the strength of punishment (air-puffs) from 1 to 0.75 bar, and increasing the percentage of the total punished visits from 12.5 to ~ 20%. These changes encouraged more visits to the water corner improving discrimination performance. My first threshold experiment revealed relatively good results and almost all mice were successfully

trained to avoid conditioned stimuli. In the second and third threshold experiment, performance of the mice became better and the obtained behavioral threshold data became more comparable to the recorded ABR results (Table 6 and Figure 19)

Our Intellicage data became comparable to those of Prof. Livia de Hoz in terms of the percentage of total number of daily visits to the water corner and the percentage of discrimination between the conditioned and safe stimuli together with the duration of each phase to achieve successful training. I carried out the threshold experiment three times and each time the results were fairly comparable and repeatable with the best results obtained in the third threshold experiment, which yielded the best discrimination performance (Figure 17, Figure 18, Figure 19)

With each experiment, I gained more experience on how to better adjust the design, duration of each phase, when and how often to apply punishment. I introduced the threshold in noise experiment and repeated it with good reproducibility of the results. I combined the threshold in noise with the threshold in quiet experiment taking advantage of the already trained mice and making use of their generalization ability, which was also obvious in the tone detection experiment (Figure 34). This reduced the time and decreased the required number of mice. I was also able to train *Otof2M* mice to discriminate between continuous noise and noise with gaps of different length, which showed promising and relevant results as was expected from the underlying genetic mutation (Figure 23 and Figure 25) with close resemblance to the *Otof<sup>1515T/1515T</sup>* mutant mice both with regards to their ABR data and their behavioral data.

After performing several experiments using different operant conditioning methods, I proposed that the results obtained from mice trained in Intellicage were the most reliable and replicable. Intellicage allows remote continuous (24 hours) monitoring of mice performance without requiring attendance of the experimenter in the testing environment. With the exception of the weekly cleaning day, Intellicage allows no interference in the mice living arena decreasing the stress exerted on mice due to handling before each experiment that affects the learning process during training. Those advantages were obvious when comparing the Intellicage to Shuttle box system, which is another method used for animal training.

The shuttle box allows live monitoring (through a USB camera) of how each mouse reacts with each stimulus, giving a rapid estimation of the auditory behavioral phenotype for the tested mouse line. Even though the Shuttle box yields replicable results in training larger,

more resilient species like gerbil and rats, the Shuttle box requires attendance of the examiner and transport of the mice from their cages to the testing environment for each training session. This exerts stress on the mice and lowers the success rates. In addition, the nature of punishment in the Shuttle box (electric shock adjusted at minimal levels  $\sim 0.05\mu\text{V}$ ) is more stressful for the mice in comparison to the Intellicage (air-puffs) which is another factor affecting the mouse behavior and the reliability of the obtained results as displayed in Table 1 and Figure 8.

My results from the Shuttle box experiment with mice were not very consistent. We think that this due to greater stress induced by handling and the stronger negative reinforcement by foot shock punishment. When the latter was too strong, mice showed “freezing” behavior and could not be successfully used for further testing. If the shuttle box should be used again for mouse experiments, it should be done in a quiet room in which only mice are tested, and the setup should be modified to better accommodate their light body weight to exclude the possibility that hurdle crossings pass undetected.

The performance of mice during training in the shuttle box showed some improvement after adding a period of 3 to 5 days before the initiation of training in order to allow mice to get used to the examiner and the testing environment (acclimatization period). In addition, titrating the punishment percentage (10% of trials are punished then 20%, 30%, and so on) and its amount (starting from zero level up to  $0.1\mu\text{V}$ ) were two other factors that decreased the stress exerted on mice in the shuttle box and improved their discrimination performance.

## 5 Summary

Auditory synaptopathy in humans is characterized by poor speech perception especially in noisy environments despite of preserved active cochlear amplification. The ABR of affected patients is absent or shows a significant reduction of wave I amplitude caused by abnormal function of inner hair cell ribbon synapses. Here, I characterized auditory function in mouse models of auditory synaptopathy by comparing electrophysiological (ABR, ASSR, and DPOAE) and behavioral experiments (acoustic startle reflexes, operant conditioning in the shuttle box and Intellicage). The best behavioral results were obtained in the Intellicage, which produced consistent repeatable results in thresholds, gap detection, and frequency discrimination experiments. The subsequent testing of the same mice in the threshold and threshold in noise experiment was possible and demonstrated the expected masking effect in WT animals. In contrast, in Ribeye mutants, the introduction of background noise resulted in a decrease in discrimination ability.

Ribeye KO mice: Analysis of ABR traces recorded from Ribeye KO revealed a significant reduction in wave I and III amplitudes, suggesting impaired activation of the auditory nerve and superior olivary complex. The behavioral threshold estimation in quiet for the Ribeye KO mice was comparable to the mild threshold shift seen in their ABRs. Introduction of noise had the expected masking effect in WT and heterozygous mice, while Ribeye KO mice showed a severe deterioration in discrimination performance when noise was introduced.

Auditory phenotype of *OtofQX* mice and *Otof2M* mutant mice: *OtofQX*<sup>-/-</sup> mice showed absence of ABR waves with preservation of the summing potential. The hearing deficits in *OtofQX*<sup>-/-</sup> mice resembled the auditory phenotype described in human patients with the same mutation, making this mouse model a good candidate for gene therapy trials. *Otof2M* mutants exhibited a moderate hearing deficit with a significant amplitude reduction in ABR waves I and III. *Otof2M* mutants showed an impaired gap detection ability in comparison to their WT littermates. Such pathology could explain the deficient speech perception in patients with *OTOF* mutations.

*Otof*<sup>-/-</sup> rescue: Viral gene therapy partially restored hearing function in *Otof*<sup>-/-</sup> mice with clearly distinguishable ABR waves II, IV and V and partial restoration of wave I and III, achieving click thresholds of ~ 60 dB SPL in 66% of *Otof*<sup>-/-</sup> mice injected with AAV-PHP.B or AAV-PHP.eB carrying DNA coding full-length otoferlin. Rescued *Otof*<sup>-/-</sup> mice were

capable of detecting sound stimuli in the Intellicage. Results suggested that viral gene therapy of DFNB9 using a single overloaded AAV vector is feasible and might reduce the complexity of gene transfer when compared to dual-AAV approaches.

*CAPS exon 2* deletion mice: Deletion of *CAPS1 exon2* was detected in a complex human phenotype in patients suffering from bipolar disorder. In mice, this mutation caused no obvious hearing impairment as evidenced by DPOAE and ABR findings; preserved ABR thresholds and comparable amplitude to their WT littermates. Interestingly, there was a reduction in ASSR amplitudes at lower modulation frequencies (110-400). Those findings suggest a role for CAPS1 protein in auditory brainstem neurons.

In summary, ABR results for mutants with an auditory synaptopathy phenotype showed a reduction in the amplitude of ABR waves I and III in several mutant mouse lines (*Ribeye*, *Otof2M*, *Otit CBA* and *Otof rescue*). The reduction was less obvious for waves II and IV which might be explained by central compensatory mechanisms augmenting their response.

## 6 References

- Akil O, Seal RP, Burke K, Wang C, Alemi A, During M, Edwards RH, Lustig LR (2012): Restoration of hearing in the VGLUT3 knockout mouse using virally mediated gene therapy. *Neuron* 75, 283–293
- Akil O, Dyka F, Calvet C, Emptoz A, Lahlou G, Nouaille S, Monvel JB de, Hardelin J-P, Hauswirth WW, Avan P, et al. (2019): Dual AAV-mediated gene therapy restores hearing in a DFNB9 mouse model. *Proc Natl Acad Sci* 116, 4496–4501
- Al-Moyed H, Cepeda AP, Jung S, Moser T, Kügler S, Reisinger E (2019): A dual-AAV approach restores fast exocytosis and partially rescues auditory function in deaf otoferlin knock-out mice. *EMBO Mol Med* 11, e9396
- Ashmore J, Avan P, Brownell WE, Dallos P, Dierkes K, Fettiplace R, Grosh K, Hackney CM, Hudspeth AJ, Jülicher F, et al. (2010): The remarkable cochlear amplifier. *Hear Res* 266, 1–17
- Becker L, Schnee ME, Niwa M, Sun W, Maxeiner S, Talaei S, Kachar B, Rutherford MA, Ricci AJ (2018): The presynaptic ribbon maintains vesicle populations at the hair cell afferent fiber synapse. *eLife* 7, e30241
- Buchwald JS, Huang C (1975): Far-field acoustic response: origins in the cat. *Science* 189, 382–384
- Buran BN, Strenzke N, Neef A, Gundelfinger ED, Moser T, Liberman MC (2010): Onset coding is degraded in auditory nerve fibers from mutant mice lacking synaptic ribbons. *J Neurosci Off J Soc Neurosci* 30, 7587–7597
- Cao X-J, Oertel D (2010): Auditory nerve fibers excite targets through synapses that vary in convergence, strength, and short-term plasticity. *J Neurophysiol* 104, 2308–2320
- Chambers AR, Salazar JJ, Polley DB (2016): Persistent Thalamic Sound Processing Despite Profound Cochlear Denervation. *Front Neural Circuits* 10, 1-13
- Dallos P (1992): The active cochlea. *J Neurosci* 12, 4575–4585
- Dallos P, Fakler B (2002): Prestin, a new type of motor protein. *Nat Rev Mol Cell Biol* 3, 104–111
- de Hoz L, Nelken I (2014): Frequency Tuning in the Behaving Mouse: Different Bandwidths for Discrimination and Generalization. *PLoS ONE* 9, e91676
- de Siati RD, Rosenzweig F, Gersdorff G, Gregoire A, Rombaux P, Deggouj N (2020): Auditory Neuropathy Spectrum Disorders: From Diagnosis to Treatment: Literature Review and Case Reports. *J Clin Med* 9, 1074
- Farina M, van de Bospoort R, He E, Persoon CM, van Weering JR, Broeke JH, Verhage M, Toonen RF (2015): CAPS-1 promotes fusion competence of stationary dense-core vesicles in presynaptic terminals of mammalian neurons. *eLife* 4, e05438

- Fettiplace R, Hackney CM (2006): The sensory and motor roles of auditory hair cells. *Nat Rev Neurosci* 7, 19–29
- Franken TP, Bremen P, Joris PX (2014): Coincidence detection in the medial superior olive: mechanistic implications of an analysis of input spiking patterns. *Front Neural Circuits* 8, 42
- Furman AC, Kujawa SG, Liberman MC (2013): Noise-induced cochlear neuropathy is selective for fibers with low spontaneous rates. *J Neurophysiol* 110, 577–586
- Godfrey DA, Lee AC, Hamilton WD, Benjamin LC, Vishwanath S, Simo H, Godfrey LM, Mustapha AIAA, Heffner RS (2016): Volumes of Cochlear Nucleus Regions in Rodents. *Hear Res* 339, 161–174
- Grieger JC, Samulski RJ (2005): Packaging capacity of adeno-associated virus serotypes: impact of larger genomes on infectivity and postentry steps. *J Virol* 79, 9933–9944
- Gruters KG, Groh JM (2012): Sounds and beyond: multisensory and other non-auditory signals in the inferior colliculus. *Front Neural Circuits* 6, 96
- Heffner HE, Koay G, Heffner RS (2006): Behavioral assessment of hearing in mice--conditioned suppression. *Curr Protoc Neurosci* Chapter 8, Unit 8.21D
- Jean P, Lopez de la Morena D, Michanski S, Jaime Tobón LM, Chakrabarti R, Picher MM, Neef J, Jung S, Gültas M, Maxeiner S, et al. (2018): The synaptic ribbon is critical for sound encoding at high rates and with temporal precision. *eLife* 7, e29275
- Jockusch WJ (2007): CAPS-1 and CAPS-2 are essential synaptic vesicle priming proteins. *Cell* 131, 796–808
- Kujawa SG, Liberman MC (2009): Adding Insult to Injury: Cochlear Nerve Degeneration after “Temporary” Noise-Induced Hearing Loss. *J Neurosci* 29, 14077–14085
- Kujawa SG, Liberman MC (2015): Synaptopathy in the noise-exposed and aging cochlea: primary neural degeneration in acquired sensorineural hearing loss. *Hear Res* 330, 191–199
- Kurt S, Ehret G (2010): Auditory discrimination learning and knowledge transfer in mice depends on task difficulty. *Proc Natl Acad Sci* 107, 8481–8485
- Land R, Burghard A, Kral A (2016): The contribution of inferior colliculus activity to the auditory brainstem response (ABR) in mice. *Hear Res* 341, 109–118
- Liberman MC (1978): Auditory-nerve response from cats raised in a low-noise chamber. *J Acoust Soc Am* 63, 442–455
- Marlin S (2010): Temperature-sensitive auditory neuropathy associated with an otoferlin mutation: deafening fever! *Biochem Biophys Res Commun* 394, 737–742
- Martin TFJ (2015): PI(4,5)P<sub>2</sub>-binding effector proteins for vesicle exocytosis. *Biochim Biophys Acta* 1851, 785–793

- Matsunaga T (2009): Value of genetic testing in the otological approach for sensorineural hearing loss. *Keio J Med* 58, 216–222
- Møller AR, Jannetta PJ, Møller MB (1981): Neural generators of brainstem evoked potentials. Results from human intracranial recordings. *Ann Otol Rhinol Laryngol* 90, 591–596
- Moser T, Starr A (2016): Auditory neuropathy--neural and synaptic mechanisms. *Nat Rev Neurol* 12, 135–149
- Moser T, Grabner CP, Schmitz F (2019): Sensory Processing at Ribbon Synapses in the Retina and the Cochlea. *Physiol Rev* 100, 103–144
- Nayagam BA, Muniak MA, Ryugo DK (2011): The spiral ganglion: connecting the peripheral and central auditory systems. *Hear Res* 278, 2–20
- Nestvogel DB (2017): Electrophysiological Analysis of the Synaptic Vesicle Priming Process. (Doctoral thesis). Dissertations at Georg-August-Universität Göttingen, 109
- Nouvian R, Neef J, Bulankina AV, Reisinger E, Pangršič T, Frank T, Sikorra S, Brose N, Binz T, Moser T (2011): Exocytosis at the hair cell ribbon synapse apparently operates without neuronal SNARE proteins. *Nat Neurosci* 14, 411–413
- Palmer AR, Russell IJ (1986): Phase-locking in the cochlear nerve of the guinea-pig and its relation to the receptor potential of inner hair-cells. *Hear Res* 24, 1–15
- Pangršič T, Lasarow L, Reuter K, Takago H, Schwander M, Riedel D, Frank T, Tarantino LM, Bailey JS, Strenzke N, et al. (2010): Hearing requires otoferlin-dependent efficient replenishment of synaptic vesicles in hair cells. *Nat Neurosci* 13, 869–876
- Pangršič T, Reisinger E, Moser T (2012): Otoferlin: a multi-C2 domain protein essential for hearing. *Trends Neurosci* 35, 671–680
- Pauli-Magnus D, Hoch G, Strenzke N, Anderson S, Jentsch TJ, Moser T (2007): Detection and differentiation of sensorineural hearing loss in mice using auditory steady-state responses and transient auditory brainstem responses. *Neuroscience* 149, 673–684
- Peng AW, Salles FT, Pan B, Ricci AJ (2011): Integrating the biophysical and molecular mechanisms of auditory hair cell mechanotransduction. *Nat Commun* 2, 523
- Pickles JO: Auditory pathways. In: *Handbook of Clinical Neurology*. Band 129; Elsevier 2015, 3–25
- Pietola L, Aarnisalo AA, Joensuu J, Pellinen R, Wahlfors J, Jero J (2008): HOX-GFP and WOX-GFP lentivirus vectors for inner ear gene transfer. *Acta Otolaryngol (Stockh)* 128, 613–620
- Radziwon KE, June KM, Stolzberg DJ, Xu-Friedman M, Salvi RJ, Dent ML (2009): Behaviorally Measured Audiograms and Gap Detection Thresholds in CBA/Cal Mice. *J Comp Physiol A Neuroethol Sens Neural Behav Physiol* 195, 961
- Rance G (2005): Auditory neuropathy/dys-synchrony and its perceptual consequences. *Trends Amplif* 9, 1–43

- Regus-Leidig H, Fuchs M, Löhner M, Leist SR, Leal-Ortiz S, Chiodo VA, Hauswirth WW, Garner CC, Brandstätter JH (2014): In vivo knockdown of Piccolino disrupts presynaptic ribbon morphology in mouse photoreceptor synapses. *Front Cell Neurosci* 8, 259
- Ren Y, Landegger LD, Stankovic KM (2019): Gene Therapy for Human Sensorineural Hearing Loss. *Front Cell Neurosci* 13, 323
- Rodríguez-Ballesteros M, del Castillo FJ, Martín Y, Moreno-Pelayo MA, Morera C, Prieto F, Marco J, Morant A, Gallo-Terán J, Morales-Angulo C, et al. (2003): Auditory neuropathy in patients carrying mutations in the otoferlin gene (OTOF). *Hum Mutat* 22, 451–456
- Rodríguez-Ballesteros M, Reynoso R, Olarte M, Villamar M, Morera C, Santarelli R, Arslan E, Medá C, Curet C, Völter C, et al. (2008): A multicenter study on the prevalence and spectrum of mutations in the otoferlin gene (OTOF) in subjects with nonsyndromic hearing impairment and auditory neuropathy. *Hum Mutat* 29, 823–831
- Rodríguez-Ballesteros M (2008): A multicenter study on the prevalence and spectrum of mutations in the otoferlin gene (OTOF) in subjects with nonsyndromic hearing impairment and auditory neuropathy. et al 29, 823–831
- Roux I, Safieddine S, Nouvian R, Grati M, Simmler MC, Bahloul A, Perfettini I, Le Gall M, Rostaing P, Hamard G, et al. (2006): Otoferlin, defective in a human deafness form, is essential for exocytosis at the auditory ribbon synapse. *Cell* 127, 277–289
- Sadakata T, Itakura M, Kozaki S, Sekine Y, Takahashi M, Furuichi T (2006): Differential distributions of the Ca<sup>2+</sup>-dependent activator protein for secretion family proteins (CAPS2 and CAPS1) in the mouse brain. *J Comp Neurol* 495, 735–753
- Safieddine S, Wenthold RJ (1999): SNARE complex at the ribbon synapses of cochlear hair cells: analysis of synaptic vesicle and synaptic membrane-associated proteins. *Eur J Neurosci* 11, 803–812
- Schmitz F, Königstorfer A, Südhof TC (2000): RIBEYE, a Component of Synaptic Ribbons: A Protein's Journey through Evolution Provides Insight into Synaptic Ribbon Function. *Neuron* 28, 857–872
- Schug N, Braig C, Zimmermann U, Engel J, Winter H, Ruth P, Blin N, Pfister M, Kalbacher H, Knipper M (2006): Differential expression of otoferlin in brain, vestibular system, immature and mature cochlea of the rat. *Eur J Neurosci* 24, 3372–3380
- Schwander M, Kachar B, Müller U (2010): The cell biology of hearing. *J Cell Biol* 190, 9–20
- Shearer AE, Hansen MR (2019): Auditory synaptopathy, auditory neuropathy, and cochlear implantation. *Laryngoscope Investig Otolaryngol* 4, 429–440
- Shearer AE, Hildebrand MS, Smith RJ: Hereditary Hearing Loss and Deafness Overview. In: Adam MP, Ardinger HH, Pagon RA, Wallace SE, Bean LJ, Stephens K, Amemiya A (Hrsg.): *GeneReviews®*. University of Washington, Seattle, Seattle (WA) 1993; NBK1434

- Spitzer MW, Semple MN (1995): Neurons sensitive to interaural phase disparity in gerbil superior olive: diverse monaural and temporal response properties. *J Neurophysiol* 73, 1668–1690
- Starr A (1996): Auditory neuropathy. *Brain* 119, 741–753
- Sterling P, Matthews G (2005): Structure and function of ribbon synapses. *Trends Neurosci* 28, 20–29
- Strenzke N (2009): Complexin-I is required for highfidelity transmission at the endbulb of held auditory synapse. *J Neurosci* 29, 7991–8004
- Strenzke N, Chakrabarti R, Al-Moyed H, Müller A, Hoch G, Pangrsic T, Yamanbaeva G, Lenz C, Pan K-T, Auge E, et al. (2016): Hair cell synaptic dysfunction, auditory fatigue and thermal sensitivity in otoferlin Ile515Thr mutants. *EMBO J* 35, e201694564
- Südhof TC (2004): The synaptic vesicle cycle. *Annu Rev Neurosci* 27, 509–547
- Südhof TC (2012): The presynaptic active zone. *Neuron* 75, 11–25
- Takeuchi S, Ando M, Kakigi A (2000): Mechanism Generating Endocochlear Potential: Role Played by Intermediate Cells in Stria Vascularis. *Biophys J* 79, 2572–2582
- Trune DR, Mitchell C, Phillips DS (1988): The relative importance of head size, gender and age on the auditory brainstem response. *Hear Res* 32, 165–174
- Uthaiiah RC, Hudspeth AJ (2010): Molecular anatomy of the hair cell's ribbon synapse. *J Neurosci* 30, 12387–12399
- Varga R (2006): OTOF mutations revealed by genetic analysis of hearing loss families including a potential temperature sensitive auditory neuropathy allele. *J Med Genet* 43, 576–581
- Varga R, Kelley PM, Keats BJ, Starr A, Leal SM, Cohn E, Kimberling WJ (2003): Non-syndromic recessive auditory neuropathy is the result of mutations in the otoferlin (OTOF) gene. *J Med Genet* 40, 45–50
- Vogl C, Cooper BH, Neef J, Wojcik SM, Reim K, Reisinger E, Brose N, Rhee J-S, Moser T, Wichmann C (2015): Unconventional molecular regulation of synaptic vesicle replenishment in cochlear inner hair cells. *J Cell Sci* 128, 638–644
- Wichmann C, Moser T (2015): Relating structure and function of inner hair cell ribbon synapses. *Cell Tissue Res* 361, 95–114
- Wynne DP, Zeng F-G, Bhatt S, Michalewski HJ, Dimitrijevic A, Starr A (2013): Loudness adaptation accompanying ribbon synapse and auditory nerve disorders. *Brain* 136, 1626–1638
- Yasunaga S, Grati M, Cohen-Salmon M, El-Amraoui A, Mustapha M, Salem N, El-Zir E, Loiselet J, Petit C (1999): A mutation in OTOF, encoding otoferlin, a FER-1-like protein, causes DFNB9, a nonsyndromic form of deafness. *Nat Genet* 21, 363–369

- Zeng F-G, Kong Y-Y, Michalewski HJ, Starr A (2005): Perceptual Consequences of Disrupted Auditory Nerve Activity. *J Neurophysiol* 93, 3050–3063
- Zheng XY, Ding DL, McFadden SL, Henderson D (1997): Evidence that inner hair cells are the major source of cochlear summing potentials. *Hear Res* 113, 76–88

## Acknowledgment

Firstly, I am deeply thankful to my supervisor, Prof. Nicola Strenzke for her acceptance, care, guidance and appreciated input. This thesis would not be possible without her continuous support, comprehension and interest in advances in managing hearing deficits. I am grateful for her extended support and help not only in the scientific field but also in its clinical applications.

I would also like to thank Prof. Tobias Moser that he gave me the opportunity of pursuing my MD in the Inner Ear lab and for his support.

I also thank Prof. Michael Müller, my second thesis advisor, for accompanying this work's advance, supporting and helping to guide it.

I would like to extend my thanks to Dr. Ellen Reisinger, Dr Vladan Ranković and Dr Christian Vogl for giving me the chance of contribution and collaboration in their projects and for their discussions, help and guidance.

I am thankful to Alexander Dieter, Hanan Al-Moyed, Gulnara Yamanbaeva and Maike Pelgrim and to all my colleagues in inner ear lab for their help and discussions on science and on scientific methods.

Special thanks go to Dr. Astrid Klinge-Strahl and the audiology team in the otolaryngology department under oversight of Prof. Dr. med. Dirk Beutner for teaching and supporting me.

My gratitude goes also to Prof. Dr. Jeong Seop Rhee in Max Planck Institute of Experimental Medicine for his collaboration and chance of my contribution in the CAPS project.

## Curriculum Vitae

My name is Iman Adel Youssef Bahader. I was born on 29 November 1982 in Cairo, Egypt. I received my MBBCh, Bachelor of internal Medicine and Surgery with honors in the year 2008, Kasr Elainy Cairo University of Medicine, Egypt. Afterwards, I fulfilled my residency in the Otolaryngology department at Kasr El-Ainy Teaching Hospital Cairo University 2008-2013 where I obtained my masters in clinical audiology from the same department. I worked as an ENT specialist and Clinical audiology researcher at Child health department in the National Research Centre in Cairo from 2013 until 2016. Afterwards, I travelled with my family to Germany where I started my medical doctorate at Universitätmedizin in Göttingen. I worked as auditory system physiologist researcher and performed the aforementioned studies in Inner Ear Lab during the time from 2016-2020 under supervision of Prof. Dr. med. N. Strenzke.